Utah State University

DigitalCommons@USU

All Graduate Theses and Dissertations   Graduate Studies

5-2011

Comparative Studies on Scale-Up Methods of Single-Use Bioreactors

Emily B. Stoker
Utah State University

Follow this and additional works at: https://digitalcommons.usu.edu/etd

Part of the Engineering Commons

Recommended Citation

Utah State University
MERRILL-CAZIER LIBRARY

COMPARATIVE STUDIES ON SCALE-UP METHODS OF SINGLE-USE BIOREACTORS

by

Emily B. Stoker

A thesis submitted in partial fulfillment
of the requirements for the degree

of

MASTER OF SCIENCE

in

Biological Engineering

Approved:

_____   _____
Dr. Timothy Taylor   Dr. Ronald Sims
Committee Chairman   Committee Member

_____   _____
Dr. Heng Ban   Dr. Robert Spall
Committee Member   Committee Member

_____
Dr. Byron Burnham
Dean of Graduate Studies

UTAH STATE UNIVERSITY
Logan, Utah

2011

ABSTRACT

Comparative Studies on Scale-Up Methods in Single-Use Bioreactors

by

Emily Stoker, Master of Science

Utah State University, 2011

Major Professor: Dr. Timothy Taylor
Department: Biological Engineering

This study was performed to increase knowledge of oxygen mass transfer ($k_L a$) and

mixing times in the scale-up of disposable bioreactors.   Results of oxygen mass transfer studies

showed $k_L a$ to increase with increasing agitation and aeration rates. By maintaining a scale-up

constant including gassed power to volume or shear, an almost constant $k_L a$ was achieved

during scale-up from 50 to 2000 L. Using the scale-up constant P_g/V resulted in statistically

higher $k_L a$ values at greater reactor volumes.   Mixing times were revealed to be significantly

affected by agitation, but not by the aeration rates tested. No pattern was recognized in the

mixing time data over an increase in volume.

Commonly used methods for predicting $k_L a$ upon scale-up were compared to

experimental data. New coefficients were determined in order to fit the historic models to the

parameters of this study, namely the unique geometry and low agitation and aeration rates

used in the single-use systems. Each of the resulting four models was found to have average

error rates from 16-23%. Although the error rates are not statistically different, the Moresi and

Patete model was determined to be most conceptually accurate when comparing the

theoretical concepts behind the models. The Moresi and Patete model found $k_L a$ to be more

dependent on aeration than on the power input. This finding was consistent with the results of the experimental studies.

The results of this study were for aeration rates (0.02-0.04 vvm) and agitation rates (P_g/V range of 2-20 W/m^3) that are commonly used in single-use bioreactor systems.

(112 pages)

ACKNOWLEDGMENTS

CONTENTS

LIST OF TABLES

LIST OF FIGURES

LIST OF SYMBOLS

a	=	gas-liquid interfacial area per unit liquid volume (m^2)
b	=	constant of the dependence of k_La on agitation
c	=	constant of the level of dependence of k_La on sparging rate
C	=	actual oxygen concentration of the liquid phase (%)
C_m	=	measured oxygen concentration
C_o	=	initial oxygen concentration
C(t)	=	oxygen concentration in tank at specified time
C*	=	oxygen concentration in a saturated liquid (%)
D_i	=	impeller diameter
D_t	=	tank diameter
Fl_G	=	gas flow number, ratio of gas to idealized liquid flow
Fr	=	Froude number
g	=	acceleration due to gravity
g_c	=	dimensional constant (1 kg-m/N-s^2)
H	=	tank height = $1.5D_t$
h	=	time step
I	=	95% homogeneity
k	=	the deflection constant
k_L	=	volumetric liquid phase mass transfer coefficient (1/m^2s)
N	=	agitation rate
N_p	=	impeller power number
P_g	=	mean power input(W)
Q	=	volumetric gas flow rate (m^3/s)
Re_i	=	Reynold's number

s	=	displacement (m)
S_i	=	material parameters which describe coalescence behavior of solution
t	=	time
U	=	uncertainty
Θ_m	=	mixing time required to reach 95% oxygen saturation
W	=	height of impeller blade (m)
V	=	liquid volume (L)
V_d	=	volume of liquid dispersed by impeller (L)
V(t)	=	volume of gas in tank at specified time
v_g	=	superficial gas velocity (m/s)
z	=	z-distribution
α	=	volume rate coefficient
β	=	surface area rate coefficient
δ	=	diffusivity of gas in liquid
ε	=	rate of energy dissipation per unit mass
ε_G	=	gas void fraction (%)
ε_{ijk}	=	the statistical residual or random error term
η	=	Kolmogoroff's eddy size
ζ	=	ratio of first and second time constants
μ	=	viscosity
ρ	=	liquid density
σ	=	surface tension
Ω	=	shear stress
τ	=	time constant
υ	=	kinematic viscosity

CHAPTER 1

INTRODUCTION

1.1   Purpose

Over the past decade the biotechnology industry has seen an increase in the production

of protein therapeutics (Chu and Robinson, 2001). This growth is due in part to the increase in

reliable scale-up culturing technologies for mammalian cells. The development of bioreactors

has provided a scale-up method which is dependable and which reduces some of the cost and

labor associated with large-scale cell cultures. For example, studies have shown that a 5 L

bioreactor is capable of producing an equivalent amount of hybridoma cells as 150, 250 mL T-

flasks (Julien, 1998). Nonetheless, in the biotechnology industry cultures must be maintained at

much larger volumes in order to produce the desired amount of product. Scaling up to

industrial volumes requires changes in the geometric and physical conditions of the culture.

Such changes can lead to decreased yields and reduce batch-to-batch consistency (Schmidt,

2005). The purpose of this study was to provide oxygen mass transfer and mixing data for

single-use systems at seven different volumes, as well as to determine a reliable scale-up

method for disposable bioreactors.

Industrial bioreactors are typically stainless steel units, which initially require large

capital investments. The cost of running the equipment is increased by the need for continual

re-sterilization of each reactor. Required cleaning times reduce overall production, and the risk

of contamination is still prevalent. These issues have led to the increased use of disposable

systems over the past few years. The development of single-use technologies can reduce initial

capital investments and contamination, in addition to eliminating cleaning requirements

(Forgione and Van Trier, 2006). Thus, to optimize the production of mammalian cells in

industry, new reactor designs, which will allow for easier scale up as well as reduce costs and risks associated with cleaning requirements and contamination are needed (Langer, 2008).

The need for reliable scale up methods and reduced contamination are common themes in industry which will be addressed in this study (Dhanasekharan, 2006; Flores et al., 1997; Gill et al., 2008; Ju and Chase, 1992; Schmidt, 2005; Votruba and Sobotka, 1992; Vrabel et al., 1999). While temperature, dissolved oxygen (DO), and pH requirements are independent of volume, parameters such as mixing time and agitation rate need to be determined specifically for each volume (Yang et al., 2007). The power input and agitation rates required at larger scales do not linearly correlate with those used at the lab scale. In order to reduce the risk of failure in large batches, it is suggested to perform step-wise scale-up runs. Performing these runs can be costly and time consuming, hence a reliable method for estimating requisite power and mixing requirements would be valuable to the industry.

To eliminate cleaning requirements, as well as to decrease the risk of product cross-contamination, more companies are increasing their use of disposable systems. The availability of such systems allows companies to change cell lines and target proteins in a production process quickly and inexpensively (Genetic Engineering and Biotechnology News, 2006). Polyethylene bags have been developed which act as inserts into stainless steel casings to serve as a bioreactor. After each batch, the bag can be removed and replaced with a new pre-sterilized bag. A development manager at Sartorius said "Benefits of flexible bag containers include faster facility set-up, reduction of down time, simplified validation, and more efficient use of plant floor space. Disposable bags greatly reduce the risk of cross contamination" (Genetic Engineering and Biotechnology News, 2006). This study was focused on providing reliable scale-up methods in single-use bioreactors.

The single-use bioreactors used in this study are not only unique from the disposable aspect, but in their geometry as well. Unlike typical fermentation systems, bioreactors do not have baffles. Baffles are normally used to disrupt the swirling of the liquid which in turn creates desirable flow patterns for mixing. However, due to the fragility of animal cells, baffles are removed from bioreactors to lessen the amount of shear in the reactor. Fermentors also typically use multiple impellers to provide both axial and radial mixing. These single-use systems on the other hand, use a single down-pumping impeller despite studies which show radial impellers to provide better conditions for mass transfer (Sorenson, 2010). Again, this design is to limit the amount of shear stress in the system. To avoid the formation of vortices, the impeller shaft in single-use systems is set at a 19.6˚ angle instead of the typical vertical shaft. While all these factors do provide a low shear environment, they also create unique mixing zones within the reactors. In this study those mixing zones will be characterized through mixing studies and computational fluid dynamics (CFD) modeling.

To address scale-up methods in disposable bioreactors, changes in mixing time and oxygen transfer as working volume increases was studied. A 3 L glass stir-tank reactor was geometrically modified to resemble single-use reactors. Mixing times were determined using both a colorimetric method and a conductance tracer method. Oxygen transfer was monitored using the unsteady-state method. The same methods employed to test mixing times and oxygen transfer were then used in larger disposable reactors at volumes of 50, 100, 250, 500, 1000 and 2000 L. Mixing patterns and velocities were calculated by a mechanical engineering team using CFD. The trends found during the experimental studies were then compared with the empirical results of the CFD models. The comparison of these two studies allowed for the calculation of equations for scale-up in disposable bioreactors. It was hoped that the unique

opportunity to work with several bioreactor volumes were better able to reveal the accuracy of the studied model equations.

1.2   Objectives

The main objective for this study was to provide scale up strategies in single-use bioreactors. Parameters for comparison include: mixing time and oxygen mass transfer (k_La). A mechanical engineering team used computational fluid dynamics (CFD) to model mixing patterns and velocities in various disposable reactors. Their work was then compared to the obtained experimental results to produce theoretical models and empirical data for scale up to a 2000 L disposable stir-tank reactor. The specific aims of this study are as follows:

- Modify glass reactor to mimic geometry found in single-use reactors

  - Build adaptor for head-plate to provide the 19.6° angle found in the shafts of single-use models.

  - Scale-down and machine the 3-blade pitched elephant-ear impeller used in the single-use systems for the 3 L reactor.

  - Machine an insert to act as a false bottom to adjust for proper height to diameter (H/D_T) ratio.

- Method verification studies in lab-scale bioreactor

  - Determine mixing times in the stir-tank using a colorimetric method. Compare results to times found using pH and conductance tracers.

  - Calculate oxygen transfer rates (k_La) using the unsteady-state method in the modified stir-tank unit.

- Scale-up from 3 L to 2000 L single-use bioreactor

- o At each level of scale-up (50, 100, 250, 500, 1000 and 2000 L), perform studies to determine k_La trends while maintaining constant P_g/V, Q_G/V and N. K_La will be calculated using the unsteady-state method.

- o Use determined k_La trends to estimate the best procedures for maintaining constant k_La during scale-up.

- o Determine mixing times at each scale under equal conditions using the conductance tracer method.

- o Establish differences in mixing times upon scale-up using constant k_La.

- o Use experimental results to derive models that can be used for successful scale-up of single-use bioreactors.

CHAPTER 2

LITERATURE REVIEW

2.1   Scale-up

2.1.1   Scale-up Studies

The biotechnology industry has continued to grow as new protein therapeutics are

approved to enter the market (Chu, 2001). With the increase in production comes a need for

successful scale-up strategies in order to more quickly and efficiently convert laboratory results

to the industrial scale. Scale-up is difficult as large vessels are much more heterogeneous than

small tanks (Shuler and Kargi, 2002). Even if geometrically similar tanks are used, it seems

impossible to maintain the level of shear, mixing time, and mass transfer from the small system

to the larger tank as power and aeration requirements usually fail to scale linearly. The

industrial bioreactor must be able to maintain the correct physiological environment as culture

conditions can affect product quality (Anderson et al., 2000). However, determining the

optimum conditions at production scale can be costly and time-consuming. This work aims to

review past methods of scale-up in order to determine the best means to predict oxygen mass

transfer in single-use bioreactors.

In biochemical engineering, there are certain "rules of thumb" that are applied to the

scale-up of bioreactors (Catapano et al., 2009). By applying these rules, one assumes that

certain criteria, which are optimal on the small scale, can also be considered optimal at the large

scale. These criteria are divided into two groups which focus on 1) mass transfer and mixing and

2) mechanical cell damage (impeller tip speed, mean power input per volume, impeller

Reynold's number, and volumetric gas flow rate). By maintaining a specific set of parameters

constant, the other parameters will change and can thus produce undesired effects on the yield

of the culture (Ju and Chase, 1992). Process characteristics that have been suggested to be maintained constant during scale-up include:

1. Reactor geometry

2. Volumetric oxygen transfer coefficient, $k_L a$

3. Maximum shear

4. Power input per unit volume of liquid, P_g/V

5. Volumetric gas flow rate per unit volume of liquid, Q_G/V

6. Superficial gas velocity

7. Mixing time

8. Impeller Reynolds number

9. Momentum factor

Criterion 1 was based on known empirical correlations for scale-up that have been developed experimentally for reactors with similar geometries. Reactor geometry consists of the height to diameter ratio as well as the ratio of the impeller to vessel diameters. The second criterion is most often used as the performance of aerobic fermentations is usually oxygen limited. Constant $k_L a$ ensures equal oxygen transfer rates at the various scales of operation. As previously discussed, mammalian cells are very shear sensitive, thus maintaining a non-lethal level of shear will make sure the cells will not undergo excessive damage. The fourth criterion is closely related as P_g/V correlates with the shear in the system. Equal P_g/V has been used in several fermentation studies as a scale-up parameter in shear-sensitive operations. Criteria 5 and 6 relate to the aeration rate used in aerobic fermentations. Both provide for the oxygen transfer in bioreactors, but also can negatively affect cells in respect to shear damage. Finally, criteria 7, 8 and 9 address issues of mass transfer in the system and how they relate to shear sensitivities (Ju and Chase, 1992).

Conventional scale-up strategies use combinations of the basic criteria (Ju and Chase, 1992). One method is to use geometric similarity, and maintain constant k_La and Q_G/V. This method focuses on the oxygen transfer needs of the reactor but ignores the effects of shear and mixing rates. Another strategy again involves geometric similarity and constant k_La, but pairs them with a constant maximum shear or impeller tip speed. In this way, the oxygen needs of the culture are met without risk of intense cell damage. A third approach is to maintain constant k_La, impeller tip speed and Q_G/V. Again, this allows for oxygen needs to be met, as well as constant mixing time (Ju and Chase, 1992). The most used criteria for scale-up are based on the empirical relationships that correlate P_g/V and k_La (Vilaca et al., 2000). This relationship accounts for agitation and aeration parameters, which directly influence gas-liquid mass transport (Yawalkar et al., 2002).

Gill et al. (2008) studied the effect of constant power per unit volume, P_g/V, on scale-up in stirred-tank fermentors. In the study, a miniature (0.1 L) and a conventional (2 L) laboratory fermentor were compared. The system requirements needed for maintaining similar conditions between the 0.1 L to the 2 L fermentor were based on the Hughmark correlation (Hughmark, 1980). Rushton impellers were used, and the 2 L was fitted with two impellers. To account for the use of multiple impellers, with spacing $<D_i$, a dual Power number of 10.5 (Hudcova et al., 1989) was used to determine the operating parameters of the 2 L vessel at three P_g/V values (657, 1487, 2960 W/m^3). The dual power number is designed to account for differences in power requirements when multiple impellers are used (Gogate et al., 2000). The runs were operated without control of dissolved oxygen tension (DOT) in order to determine when the cultures became oxygen limited (DOT ≤ 0). At the lowest P_g/V value of 657 W/m^3, the conventional fermentor only produced a final biomass concentration of about 50% that of the miniature reactor. This is likely the result of inadequate mixing at low agitation rates. At the

higher P_g/V, the performance of the conventional vessel improved, achieving similar cell growth and biomass. However, it was shown that oxygen limitation occurred earlier in the conventional fermentor than in the miniature vessel (Gill et al., 2008).

The volumetric mass transfer coefficient is the most often applied physical scale-up variable. It includes relevant parameters that influence oxygen supply such as agitation and aeration (Alam et al., 2005; Marks, 2003; Schmidt, 2005; Yawalkar et al., 2002). Alam et al. performed scale-up of stirred and aerated fermentors based on constant k_La. Their protocol applied the rule of thumb, trial and error, interpolation and extrapolation. Scale-up experiments relied on the correlation developed by Cooper et al. (1944), in which k_La is empirically linked with power consumption and superficial air velocity (Equation 1). Constant α represents the level of dependence of k_La on agitation, and constant β represents the level of dependence of k_La on the sparging rate.

$$k_La = K'\left(\frac{P_g}{V}\right)^{\alpha} v_g{}^{\beta} \qquad\qquad (1)$$

Studies were performed which maintained constant P_g/V, constant superficial velocity, v_g, and constant impeller tip speed, πND_i, upon scale-up. They used the gassing out method to determine k_La and then used scale-up equations to determine the minimum and maximum operating variables for impeller speeds and air flow rates in order to achieve similar k_La values at the larger scale. By changing the power input and air velocity, common k_La values were obtained. Their work helped to illustrate the dependence of k_La on power input, air velocity and agitation (Figure 1). Hence, manipulation of these variables is useful in maintaining a constant k_La upon scale-up (Alam et al., 2005).
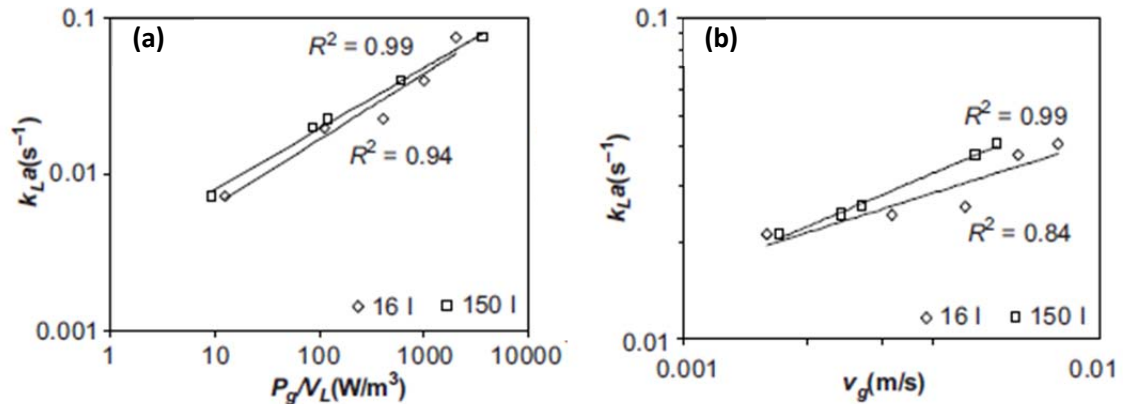
Figure 1. Dependence of kLa on a) volumetric power consumption and b) superficial velocity, in distilled water T=30˚C (Alam et al., 2005).

While maintaining constant $k_L a$ is a common theme in scale-up strategies, another approach by Votruba and Sobotka (1992) was to preserve physiological similarity. They state that:

> The transfer of microbial technology from the laboratory to the industrial production level is critically affected, in contrast to chemical reactors, by the physiology of growth and production, *i.e.* by the relationship between the potential production ability of selected microorganisms and the external condition in the bioreactor. (Votruba and Sobotka, 1992)

They suggest that failure to retain the physiological conditions experienced at the laboratory scale is a frequent cause of failure in scale-up. Deviations from physiological homogeneity caused by environmental changes can cause stress reactions. These reactions can lower the cells' physiological functions, resulting in a lower product yield. Physical factors including pressure, temperature, pH, agitation and viscosity can affect the kinetics of growth and production. The criteria for scale-up based on physiological similarity can be split into two methods.

The first approach is to use dimensional analysis while the second uses mathematical models to simulate the fluid flow and biochemical reactions. In the first method, the volumetric gas flow rate was determined by assuming a constant gas superficial velocity. The impeller

rotation speed was also calculated from the power correlation. Method II assumed rotation speed and impeller diameter to be constant and calculated the gas flow rate from the power correlation and aeration capacity of the vessel. Their results showed that increasing volume resulted in decreasing specific power input per unit volume and an increase in mixing time. The impeller tip velocity was constant over the increasing volume (Votruba and Sobotka, 1992).

Shear stress is an important physiological condition to consider when working with bioreactors. As shear can have a negative effect on cell viability and yield, constant shear has been used as a criterion for scale-up. The shear sensitivity of a culture is influenced by the cell line, availability of key nutrients, concentration of inhibitory metabolites and batch age (Marks, 2003). Due to the extreme sensitivity of insect cells to shear, Maranga et al. (2004) used constant shear methods to scale-up from 2 to 25 L cultures of *Spodopetera frugiperda*. To define the operation conditions of the 25 L fermentor, hydrodynamic parameters were computed, including: the impeller Reynolds number (Re_i), the Kolmogoroff's eddy size (η), the rate of energy dissipation per unit of mass (ε) and the shear stress (Ω). These parameters were calculated using the following equations.

$$\text{Re}_i = \frac{\rho N D_i^2}{\mu} \tag{2}$$

where ρ is the medium density, *N* is the agitation rate and μ is the viscosity of the medium.

$$\eta = \left(\frac{v^3}{\varepsilon}\right)^{1/4} \tag{3}$$

in which v is the kinematic viscosity (μ/ρ).

$$\varepsilon = (Np)N^3 D_i^2 \tag{4}$$

in which Np is the power number and D_i^3 is the volume into which the energy is dissipated.

$$\Omega = \left(\frac{\varepsilon_s}{v}\right)^{1/2} \mu \tag{5}$$

The impeller rate and air flow were adjusted during scale-up to maintain the maximum shear

level calculated by Equation 5. By retaining constant shear, a successful scale-up was performed

and there were no detectable differences in the growth cycles of cells cultured in the 2 L

fermentors versus the 25 L vessels (Maranga et al., 2004).

2.1.2   Increasing Volume or Vessel Numbers

Issues to scale-up include the argument on whether it's best to increase the size or the

number of reactors used. Rouf et al*. (*2000) performed studies to determine whether using

single versus multiple reactors upon scale-up is more economically favorable. Simulations, using

BioProcessSimulator^TM (Aspen Technology Inc., MA), were performed to compare the

performance of a 6000 L reactor with six 1000 L bioreactors of equal size. Results showed that

the costs for the 6000 L reactor only contributed 14% to the total cost compared to 37% for

multiple reactors. However, when downstream processing was considered, the multiple

reactors proved to be more cost efficient. The multiple reactors were able to share the same

downstream equipment when inoculated at least five hours apart. The equipment was much

smaller in size and thus cheaper. Overall, the use of multiple units appeared to provide more

flexibility, ease of startup and reduced costs (Rouf et al., 2000). The return of investment for the

multiple bioreactor system was 144% compared to 65% for the single reactor (Table 1).

Table 1.Comparative economic analysis in millions of dollars (Rouf et al., 2000).

	Multiple Reactors	6000 L Reactor
Purchased equipment cost	1.5	2.84
Fixed capital	6.9	13.06
Total capital	8.25	15.62
Revenue	34.2	35.2
Annual operating cost	15.45	20.2
Gross profit	18.75	15
Net profit	11.25	9
Net cash flow	11.85	10.2
Return on investment (%)	144	65
Gross margin (%)	55	43

As the scale-up of reactors can be quite complicated, simplified deterministic models with lumped parameters are often used (Aiba et al., 1973; Biryukov and Kantere 1985; Marks, 2003; Rouf et al., 2000; Takamatsu et al., 1981; Votruba and Sobotka, 1992). Kinetic models can be formulated to describe the physiology of the culture within the reactor, including substrate consumption and rate of product formation (Schmidt, 2005). However, the known mathematical methods used in scale-up are not able to completely define the complex interactions of the physical conditions (Liden, 2002). Thus, in most cases, successful scale-up relies on the outcome of independent optimization at each scale (Schmidt, 2005).

Dhanasekharan (2006) used computational fluid dynamics (CFD) to simulate mixing, gas hold-up and mass transfer coefficients within bioreactors to aid in scale-up. CFD uses numerical methods to solve fundamental transport equations for heat and mass transfer, as well as fluid flow. This type of modeling is thought to increase process understanding, which reduces risks associated with scale-up. In his study, a dual-impeller stirred-tank bioreactor with a diameter of 96 inches was simulated using CFD. The produced velocity vectors portrayed a downward flow

produced by the Lightnin A320 impellers (SPX Process Equipment). Smaller bubbles were shown

near the impellers where the shear was high. Larger bubbles then formed due to coalescence,

as they would rise along the reactor's outer wall. The variation of the turbulence and bubble-

size in the reactor caused a non-uniform mass-transfer coefficient distribution. However, the

CFD results were able to offer a spatially dependent function derived from flow variables to

determine a single mass-transfer coefficient. This coefficient was compared with an

experimentally determined value and found to be within the same order of magnitude. Thus

Dhanasekharan (2006) concluded that CFD is a useful approach to scale-up as it could manage

risk and reduce downtime by determining the proper bioreactor design.

2.2   Comparison Studies of Different Volumes

2.2.1   Mixing Time

Mixing performances of agitated bioreactors are most often characterized by mixing

times. Mixing time, θ_m, is defined as the time it takes to achieve a specified degree of

homogeneity following a perturbation. Mixing studies will be performed at seven volumes of

scale in single-use reactors to reveal any changes in mixing conditions upon scale-up. Although

there is no universally accepted technique, methods for determining mixing time can be

classified into two groups, namely those that use local measurements, and those that perform

global measurements.

Local measurements rely on physical measurements of changes in thermal, conductive,

fluorimetric, or pH within the system. Such methods require the use of probes, which are

intrusive to the system and can only measure the homogeneity at a given location. To

circumvent this restriction, several probes placed in varied locations can be used, but this is

thought to disrupt the flow within the vessel. In contrast, global measurements are either

chemically based, involving a reaction which causes a color change, or optically based like in the Schlieren method (Cabaret et al., 2007).

Global measurements can be advantageous, as they allow the identification of unmixed zones and are nonintrusive to the system. However, chemically based global methods are often subject to the interpretation of the results. Color changes are often determined with the naked eye and can thus lead to differing results if performed by different individuals or repeated several times (Cabaret et al., 2007). Table 2 gives a summary of the advantages and drawbacks of the use of local and global methods.

Although both local and global methods will obtain differing values for θ_m, they do follow similar trends. Mixing time has been found to be inversely proportional to the impeller tip speed or agitation rate, and it is also influenced by the ratio of the diameter of the impeller to the diameter of the vessel. These relationships aid in determining mixing times upon scale-up.

Table 2. Comparison of Local and Global Measurement Methods (Cabaret et al., 2007).

	Local Methods	Global Methods
Examples	Thermal method Conductometric method pH method	Decolorization methods Schlieren method
Advantages	Accurate Can be used in industrial tank	Non-intrusive Can identify unmixed zones Give the end point of the mixing
Drawbacks	Intrusive Do not quantify segregated regions and dead zones Do not give the end point of the mixing	Inaccurate (subjective) Transparent vessel needed

2.2.2   Oxygen Transfer

Aerobic bioprocesses require a continuous oxygen supply. Oxygen is a key nutrient used by microorganisms for growth as well as maintenance and metabolite production. Oxygen is

often a rate-limiting substrate due to its low solubility in cell mediums, and is often a concern

upon scale-up. Before being utilized by the cells, oxygen must overcome a series of transport

resistances as shown in Figure 2. The oxygen must first be transferred from the interior of the

bubble through the gas-liquid interface. Once through the interface, the oxygen must diffuse

through the liquid film surrounding the bubble before entering the bulk liquid. After entering

the bulk liquid, the oxygen will diffuse through the medium into the liquid film that surrounds

the cells. The oxygen must then pass through the liquid-cell interface before finally reaching the

cell. The rate at which these steps occur is known as the oxygen transfer rate, or OTR (Doran,

1995).

　　　　To optimize culture conditions, the oxygen transfer rate within a culture needs to be

determined to identify the oxygen requirements of the system. The concentration gradient

between the air and bulk liquid acts as the driving force behind this transfer, and is affected by
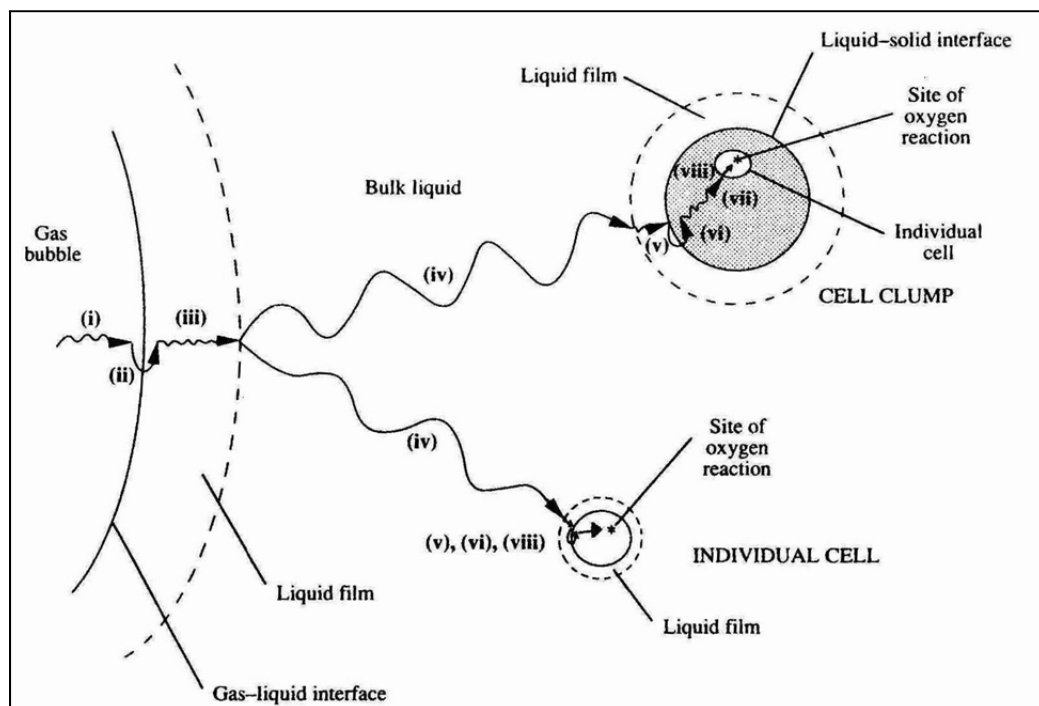
Figure 2. Steps for the transfer of oxygen from a gas bubble to a cell and cell clump (Doran, 1995).

the solubility, which in turn is dependent on temperature, pressure, concentration as well as other factors. Thus, the OTR is a function of the solubility of oxygen in the culture medium, diffusivity and the oxygen concentration gradient. Oosterhuis and Kossen (1984) used Equation 6 to define OTR:

$$OTR = k_L a(C * - C) \qquad (6)$$

where k_L is the volumetric liquid phase mass transfer coefficient, a is the gas-liquid interfacial area, C^* is the saturation concentration of oxygen in the liquid, and C is the actual oxygen concentration.

There are currently two approaches that can be used to determine k_L and a: experimental measurement or calculation using empirical equations. However, for either method, it is extremely difficult to determine k_L and a separately (Doran, 1995). Therefore, the two variables are most often combined to form $k_L a$, referred to as the overall liquid phase mass transfer coefficient, which is used to ascertain the amount of dissolved oxygen present in the culture. Determination of $k_L a$ is required to verify aeration efficiency and to test the effect of the operating parameters on dissolved oxygen availability (Garcia-Ochoa and Gomez, 2008).

During aerobic fermentations, $k_L a$ is dependent on the hydrodynamic conditions surrounding the gas bubbles. Parameters including bubble diameter, liquid velocity, density, viscosity and oxygen diffusivity have been investigated in order to derive empirical correlations for the prediction of $k_L a$. In theory, such correlations would allow one to predetermine the expected $k_L a$ of a system. However, the high variability of the culture conditions makes the accuracy of this practice rather low. A further explanation of predictive modeling of $k_L a$ will be discussed in a later section.

Literature is available on a number of empirical equations used to determine $k_L a$. These methods are based on the differences between the aeration systems used, the bioreactor type,

the composition of the culture medium, as well as if a microorganism is present during the measuring (Garcia-Ochoa and Gomez, 2008). Four common approaches used to measure k_La are the unsteady state, steady state, dynamic and sulfite methods (Shuler and Kargi, 2002).

In the unsteady-state method, the reactor is filled with water or a medium void of cells. The oxygen is then removed from the system by sparging with nitrogen. Air is then reintroduced to the system and the level of dissolved oxygen is monitored until it has reached saturation. The log of changes in concentration can then be plotted versus time resulting in a slope equal to k_La (Shuler and Kargi, 2002). This method is often used due to its ease of execution and simplicity, as it only requires the use of a dissolved oxygen probe. However, this method is not without limitations.

Problems may arise when using the unsteady-state method if rapid changes in dissolved oxygen concentration occur or if the probe has a slow response time. Such a response lag is mainly due to the diffusion through the probe membrane. Corrections for the time lapse need to be made in order to obtain accurate data. However, if the probe response time is smaller than the mass transfer response time of the system, $1/k_La$, no correction needs to be made (Van't Riet, 1979). Van't Riet demonstrated this concept using Van de Sande's model in which the ultimate error in $k_La < 6\%$ for a probe response time $< 1/k_La$. Linek's model further indicates that to achieve an error of $< 3\%$, the probe response time needs to be $< 1/(5k_La)$. Therefore, as long as these limits are not exceeded, it can be assumed the measured k_La values are accurate. In practice, this is rarely the case and corrections should be made (Van't Riet, 1979).

During their study of oxygen transfer in agitated systems, Hassan and Robinson (1977) used the unsteady-state method to measure k_La. Dissolved oxygen was adsorbed or desorbed from the liquid by sparging with air and nitrogen gas, respectively. The rate of change in the dissolved oxygen concentration was measured using a standard dissolved oxygen probe.

The steady state method has been considered one of the most reliable ways to measure k_La (Shuler and Kargi, 2002). However, it can be difficult to put into practice, as it requires the precise measurement of the oxygen concentration in all gas exit streams as well as within the system. Assuming steady state conditions within the cell culture, a mass balance on oxygen can be used to calculate the oxygen uptake rate (OUR). The mass transfer coefficient can then be computed as it is proportional to the OUR and inversely proportional to the difference of the oxygen concentration at saturation and within the system. This method can be successfully used at the industrial scale as long as the measurement techniques are accurate (Doran, 1995).

The dynamic method is similar to the unsteady state method for determining k_La. Performed in fermentors or bioreactors with active cells, it utilizes the same gassing out method where oxygen is removed from the system by stopping the air supply or sparging with nitrogen. As the air is returned to the system, the concentration of dissolved oxygen is monitored using a DO probe, and the slope of the ascending curve can then be used to calculate k_La in the same manner as in the unsteady state method. This method has an advantage over the unsteady state method as it estimates k_La under actual culture conditions.

Nienow et al. (1996) utilized the dynamic method in their study of oxygen transfer in large bioreactors. In the bioreactors, the dissolved oxygen was maintained between 15 and 30% saturation to ensure acceptable cell growth. Beginning at 30% saturation, the air supply was stopped and the dissolved oxygen was allowed to fall until it reached 15% saturation. Air was then returned to the system and the rate of increase in dissolved oxygen was recorded. Assuming a well-mixed liquid phase and plug flow of the air, the k_La values were determined (Nienow et al., 1996).

The sulfite method for measuring k_La is based on the reaction of absorbed O_2 with Na_2SO_3. Using copper or cobalt ions as a catalyst, the sulfur in sulfite (SO_3^{-2}) is oxidized to sulfate

(SO_4^{-2}) in a zero-order reaction. The rate of sulfate formation is monitored, as it is proportional

to the rate of oxygen consumption. This method often overestimates k_La and must therefore be

converted to the actual k_La of the system (Van't Riet, 1979).

Kensy et al. (2005) used the sulfite method for determining k_La in their study of oxygen

transfer in microtiter plates. As the sulfite method relies on the change of sulfite to the more

acidic sulfate, Kensy et al. (2005) decided to avoid the use of probes and utilize a newly

developed optical system. By monitoring the color change of bromothyol blue, a pH sensitive

dye, they were able to relate their results to the oxygen transfer rate, which then enabled them

to calculate k_La.

2.3   Shear Sensitivity

Industrial production of protein therapeutics relies on the smart design of traditional

stirred-tank reactors to ensure optimal culture conditions (Chu, 2001). The bioreactor has aided

in combating what are considered the key barriers to large-scale culture, which include shear

sensitivity and oxygen limitation. Mixing in bioreactors is required in order to disperse bubbles

and facilitate oxygen transfer (Doran, 1995). However, the development of shear forces, which

act to break apart air bubbles, can also cause disruption to the cells. Cell disruption can

negatively affect cell growth. This disruption can lead to cell death, retardation of growth,

decreases in production and changes in cell morphology. Several mechanisms are thought to

contribute to cell damage, including: interaction between cells and turbulent eddies, collisions

of cells or of cells with the impellers and the bursting of bubbles at the fluid surface. In order to

provide cells with an optimal physiological environment, the design of the reactor must insure

against shear damages from agitation and aeration upon scale-up (Chu and Robinson, 2001).

Although protected by a cell wall, microbial cultures can also be disrupted by shear

forces (Merchuk, 1991). The level of shear that cells can withstand will differ between cultures

depending on their resistance to mechanical forces and their nutrient requirements. Changes in the morphology of microbial cultures have been observed in numerous cases. One of the first documentations on the effects of agitation on the morphology of microbial cells was given by Camposano et al. (1958). Their study involved the production of kojic acid from *Aspergillus flavius*. At higher agitation rates, it was found that the formed mycelium were short and branched, leading to the production of mainly starch instead of kojic acid. This study illustrates the relationship between morphology and metabolite production, which leads to the concept of the affect morphological changes, can have on cell production. Morphological changes resulting from increased agitation rates were also reported by Wase and Ratwate (1985) in a study they performed with *E. coli*, in which the mean cellular volume increased with an increase in stirrer speed. The rate of shear stress is not reliant on agitation speeds alone, but is also affected by aeration and the presence of bubbles in the system. A study by Silva et al. (1987) showed cultures of *Dunaliella* were sensitive to specific bubbling rates. The evidence suggests that despite the presence of a cell wall, precautions should still be taken to reduce shear effects in microbial cultures (Merchuk, 1991).

Mammalian cells are known to be fragile and very sensitive to the shear stresses of bioreactors. As in microbial culture, metabolite production in animal cultures is affected by morphology (Merchuk, 1991). Changes in morphology caused by shear stresses can lead to decreases in cell growth and production. However, lower rates of shear can actually increase metabolite production in certain cells. Frangos et al. (1986) developed an apparatus to study the response of human umbilical vein endothelial cells at different ranges of shear stress. It was found that the onset of flow in the system produced a sharp increase in the production rate of prostacyclin. However, as the flow continued to increase, the rise eventually decayed to a lower steady state value. Their work confirmed that in certain ranges, shear rates may actually

increase metabolite production, but far more often the shear will lead to irreversible damage to the cells.

In another shear-related study, Petersen (1988) used a specially designed bob-and-cup viscometer to subject hybridoma cells to shear after having been cultivated in a bioreactor. The results were similar to cell death trends caused by excessive agitation in spinner flasks. They concluded viscous shear to be the main cause of cell damage. Another study, performed by Handa-Corrigan et al. (1989) was done to determine the effects of sparger aeration on suspended mammalian cultures. It was determined that cell damage was associated with bubble bursting and velocity fluctuation in the liquid film. The reviewed literature makes clear that shear can have detrimental effects on the growth and morphology of mammalian cells due to high agitation rates and bubbles.

For effective heat and mass transfer within a bioreactor, turbulent conditions must be made by the presence of mixing impellers (Doran, 1995). The impeller design as well as the rheological properties of the fluid will affect the shear conditions in the reactor. Metzner and Otto (1957) suggested that the average shear rate in a stirred vessel is linearly proportional to a constant, dependent on impeller design, and the stirrer speed. While this idea was supported by their study, it cannot be assumed that the shear rate is uniform throughout the vessel. This is particularly true of industrial cultures, which can contain volumes greater than 10,000 L. Another difficulty is maintaining constant mixing time upon scale-up.

In order to maintain mixing times, the impeller rates and power to volume input must be increased, which in turn increases shear within the culture. To counter shear effects due to impeller speeds, new impellers have been developed to provide gentler mixing. The marine-blade impeller is often the impeller of choice when working with mammalian cultures, and large-diameter impellers are able to provide superior bulk mixing while operating at slow speed

(Doran, 1995). However, smaller high-speed impellers are preferred for breaking up gas bubbles to promote oxygen transfer. When designing a bioreactor system, the impeller design and mixing rates must be optimized in order to limit the amount of shear stress on the cells.

The effect of sparging on cell cultures was examined in depth by Nienow et al. (1996). Even at low aeration rates, cell numbers were reduced when compared to their unsparged studies, and although mechanical damage was occurring, it was unclear as to how it happened. Bubble columns were used to analyze the effect of rising bubbles alone. As the introducing of the air at greater depths did not appear to cause more damage, it was assumed that this effect was negligible. Further work concluded that the damage due to bursting bubbles at the medium-air interface was the greatest cause of shear in aerated reactors. Progress has been made in mathematical modeling of the fluid flow around a bubble as it bursts, giving results similar to those obtained by speed cinephotography. The models make it possible to calculate the generated stresses associated with different sizes of bursting bubbles. Workers found experimentally that smaller bubbles caused more damage to cells than larger ones at the same volumetric flow rate. Nienow et al. (1996) concluded that bursting bubbles in a reactor have the most damaging effect on the viability of cells.

Review of available literature suggests that the influence of shear from agitation and sparging on cell viability and productivity should affect the design and scale-up of bioreactors. A successful reactor design will provide enough shear to facilitate heat and mass transfer without having it being damaging to the cells.

2.4   Predictive Modeling of $k_L a$

One of the main problems associated with the scale-up of cell cultures in bioreactors is the prediction of the physiological conditions in the larger vessels. As mentioned earlier, oxygen availability is critical to the life of the cells. Cellular respiration and production depend on

maintaining critical oxygen levels. To address this dilemma, a considerable amount of data and

research has been produced over the past few decades. By determining the factors that directly

influence oxygen solubility and dispersal, models for the prediction of $k_L a$ have been developed.

Literature on mass transfer coefficients reveals three methods commonly used to

correlate $k_L a$ (Yawalkar et al., 2002). The first method, and seemingly most common, is based

on energy input criterion. This method relates $k_L a$ to power input (P_g) and the superficial gas

velocity (v_g):

$$k_L a = f\left(P_g / V, v_g\right) \tag{7}$$

Some energy input models use Q/V in place of v_g.

$$k_L a = f\left(P_g / V, Q/V\right) \tag{8}$$

The second method relies on the use of dimensionless numbers such as the Froude number (Fr),

the gas flow number (Fl_G) and the ratio of the impeller and tank diameters (D/T), where:

$$k_L a = f\left(Fr, Fl_G, D/T, etc.\right) \tag{9}$$

The third method was developed by Yawalkar et al. (2002a), and is based on gas hold-up in stir-

tank reactors. This method uses the dispersion parameter, N/N_{cd}, where N_{cd} represents the

minimum impeller speed required for all the liquid to be in contact with the sparged gas.

Yawalkar et al. (2002b) base their work on the function shown in Equation 10.

$$k_L a = f\left(N/N_{cd}, v_g\right) \tag{10}$$

2.4.1   Energy Input Correlation

Bartholomew (1960) wrote, "Oxygen mass transfer rates and yield depend upon scale

and intensity of turbulence, which are a function of power absorbed." His assertion stemmed

from data obtained by Cooper et al. (1944), which demonstrated that $k_L a$ was a function of power per unit volume:

$$k_L a = \left(\frac{P_g}{V} \right)^{0.95} \qquad (11)$$

This model was verified by studies performed at small and large scales using flat paddle impellers. However, although it worked for the geometry used by Cooper et al.(1944), it was later found that the exponent of 0.95 did not hold upon an increase in tank size of vessels of different geometries. This deviation held true particularly with vessels using different agitators. Thus Bartholomew discredited Cooper's model as a satisfactory method for the prediction of $k_L a$.

Several physical factors must be considered when vessel volume is increased to scale up production. Oxygen mass transfer is a function of the volume of air flow, as well as power per unit volume (Bartholomew, 1960). Van't Riet (1979) stated that the most important factors affecting $k_L a$ are power consumption, gas superficial velocity and the properties of the liquid phase. Consequently, Cooper's equation was modified to account for air flow (Wang et al., 1979):

$$k_L a = f\left[\left(\frac{P_g}{V} \right)^{\alpha} v_g^{\beta} \right] \qquad (12)$$

In which v_g is the superficial gas velocity. Equation 12 then becomes

$$k_L a = K'\left(\frac{P_g}{V} \right)^{\alpha} v_g^{\beta} \qquad (1)$$

where K' and exponents α and β are functions of scale, representing the effects of flow and turbulence on both bubble dispersion and the mass-transfer boundary layer (Doran, 1995).

Van't Riet (1979) also mentioned a commonly used equation, which omitted power input (P_g) in exchange for impeller speed (N) and diameter (D_i):

$$k_L a = K' N^{a_1} D_i^{a_2} v_g^{b} \tag{13}$$

Over the years, several values for coefficients K', α and β used in Equation 1 have been suggested. A summary of the most common ones as reported in Gill et al. (2008) is shown in Table 3.

Table 3. Most commonly reported $k_L a$ correlations for stirred vessels in which, P_g/V is measured in W/s and v_g is measured in m/s. Flow rates tested ranged from 0.2-2 vvm of air in water with ions, meaning increased electrolyte concentrations (Gill et al., 2008).

References	Vessel diameter (m)	Type	Di/Dt	Proposed correlation and type of fluid
Gill et al. (2008)	0.06	Rushton turbine	0.33	Air-water with ions: $$k_L a = 0.224 \left(\frac{P_g}{V} \right)^{0.35} v_g^{0.52}$$
Van't Riet (1979)	Various	Various	Various	Air-water with ions: $$k_L a = 0.002 \left(\frac{P_g}{V} \right)^{0.7} v_g^{0.2}$$
Vilaca et al. (2000)	0.21	Rushton turbine	0.40	Air-water-sulfite solution $$k_L a = 0.676 \left(\frac{P_g}{V} \right)^{0.94} v_g^{0.65}$$
Linek et al. (2004)	0.29	Rushton turbine	0.33	Air-water: $$k_L a = 0.01 \left(\frac{P_g}{V} \right)^{0.699} v_g^{0.581}$$
Smith et al. (1977)	0.61-1.83	Disc turbine	0.5-0.33	Air-water: $$k_L a = 0.01 \left(\frac{P_g}{V} \right)^{0.475} v_g^{0.4}$$
Zhu et al. (2001)	0.39	Disc turbine	0.33	Air-water: $$k_L a = 0.031 \left(\frac{P_g}{V} \right)^{0.4} v_g^{0.5}$$

Gill et al. (2008) studied $k_L a$ in miniature (100 mL) and laboratory-scale (1.5 L working volume)

fermentors. Their coefficients shown in Table 3 are specifically for miniature fermentors using

Rushton turbine impellers. They had determined that the exponents and constants found in

previous literature did not accurately predict $k_L a$ in the miniature vessels. Van't Riet (1979) used

large reactor data obtained by Calderbank (1958) and Smith et al. (1977) to develop his

correlation for an air-water solution. Vilaca et al. (2000) used the sulfite method to collect $k_L a$

data that was then fit to Equation 1, noting that it failed to take into account the rheological

behavior of the fluids studied. Linek et al. (2004) used data collected by Alves et al. (2004) to

test the changes in $k_L a$ with increasing electrolyte concentrations. Smith et al. (1977) studied $k_L a$

in large tanks with different impellers, mostly disc-turbine, as did Zhu et al. (2001).

Nienow et al., in their 1977 article for the Second European Conference on Mixing,

discussed defining gas flow rate in terms of vessel volumes per time, commonly per minute

(vvm), in order to maintain optimal concentration gradients. If v_g were to be held constant

during scale-up, there would be an increase in gas residence time with increasing scale. The

increased residence time could in turn produce a reduction of concentration gradients and

inhibit the driving force of mass transfer. However, by keeping vvm constant, the air velocity is

allowed to increase with scale, which will theoretically maintain the constancy of gas residence

time.

Similar arguments for using vvm as opposed to v_g were made by Chapman et al. (1983)

and Schlüter and Deckwer (1992). Schlüter and Deckwer (1992) showed large deviations from

the correlations when using v_g. This phenomenon was also seen by Cents et al. (2005), whose

data showed an average relative deviation of 32%. Schlüter and Deckwer (1992) believed this

deviation was due to not accounting fully for the tank volume. They suggested using the space

velocity of the gas (ϕ_g) as opposed to the superficial gas velocity.

$$\phi_g = \frac{Q}{V} \tag{14}$$

By dividing a volumetric flow rate by volume, the resulting units are inverse time, or vvm. Thus

the gas space velocity can be replaced by vvm. The use of an aeration term, based on the

volumetric flow rate over volume, was originally developed by Zlokarnik in his 1978 publication.

Zlokarnik found $k_L a$ to have the following functional dependence:

$$k_L a = f\left(\rho, v, \sigma, \delta, S_i, \frac{P_g}{Q}, \frac{Q}{V}, g\right) \tag{15}$$

where ρ is density, v is liquid kinematic viscosity, σ is surface tension, δ is the diffusivity of the

gas in the liquid, and S_i represents the material parameters, which describe coalescence

behavior of solutions. Zlokarnik's use of Q/V was noticed by Moresi and Patete (1988), and was

used to develop the following equation:

$$k_L a = K'\left(\frac{P_g}{V}\right)^a \left(\frac{Q}{V}\right)^b \tag{16}$$

Moresi and Patete (1988) found this model (Equation 16) effective in predicting $k_L a$ values for

their system of fermentors (8-1000 L), which were equipped with one to two Rushton impellers

and two to four baffles. They found $k_L a$ to be more dependent on Q/V than on P_g/V. When

Moresi and Patete then compared Equation 17 to a similar model based on v_g, it was

determined that $k_L a$ is more influenced by Q/V than v_g.

Figure 3 from Schlüter and Deckwer (1992) shows the measured $k_L a$ values of three

geometrically similar reactors running with equivalent superficial velocity, v_g. They noted that

the data fails to fall on the same curve. However, when constant v_g is replaced by a constant vvs

(Q/V), the data fit on the same curve showing a better correlation (Figure 4).
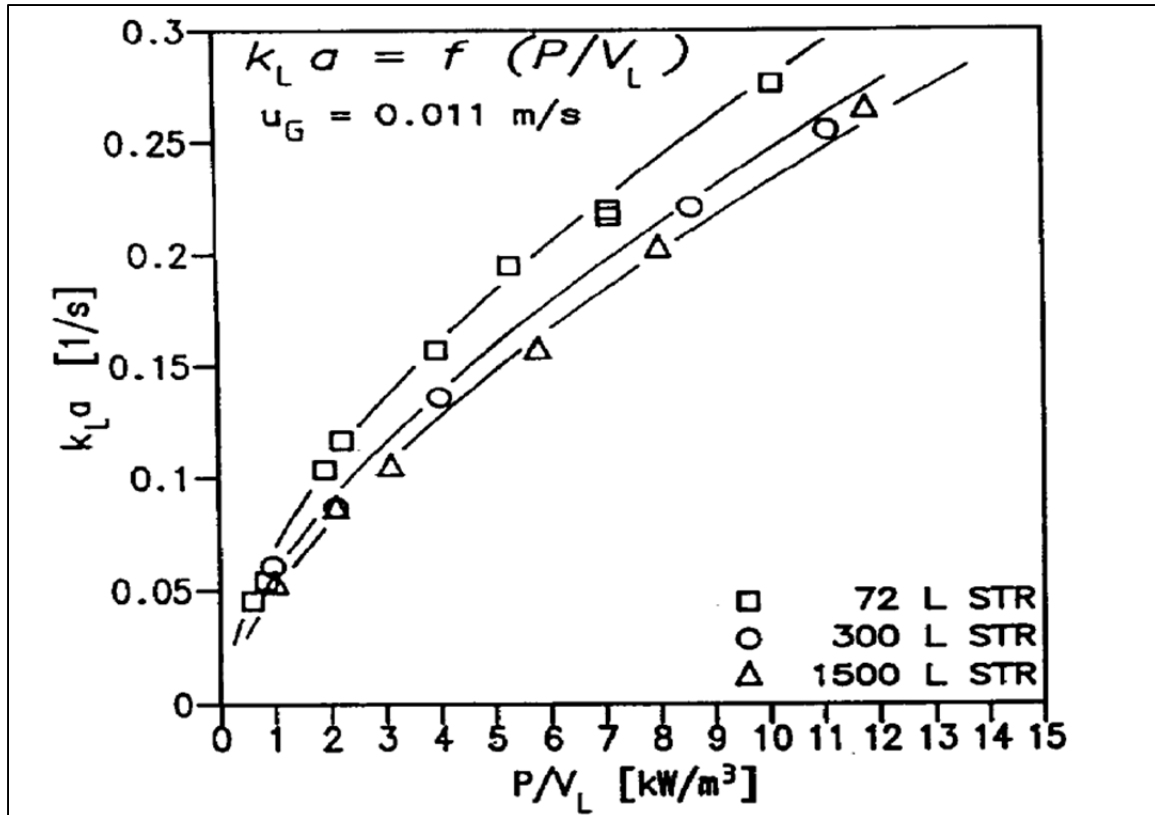
Figure 3. $K_L a$ as a function of power input at constant superficial gas velocity, v_g (Schlüter and Deckwer, 1992).

Cents et al. (2005) determined coefficients for Equation 17, which replaces superficial air velocity with gas space velocity (Schlüter and Deckwer, 1992), to correlate their $k_L a$ data.

$$k_L a = 1.5 \cdot 10^{-3} \left(\frac{P_g}{V} \right)^{0.67} \left(\phi_g \right)^{0.4} \qquad (17)$$

The exponents determined by Cents et al. (2005) are in reasonable agreement with those determined by Schlüter and Deckwer (1992), which were 0.62 and 0.23, respectively. Cents et al. (2005) noted that the average relative deviation of the model decreased by over 50% when using ϕ_g as opposed to v_g. The results from Cents et al. (2005) agree with those found by Moresi and Patete (1988), showing $k_L a$ to be more dependent on the volume of air flow than the velocity.
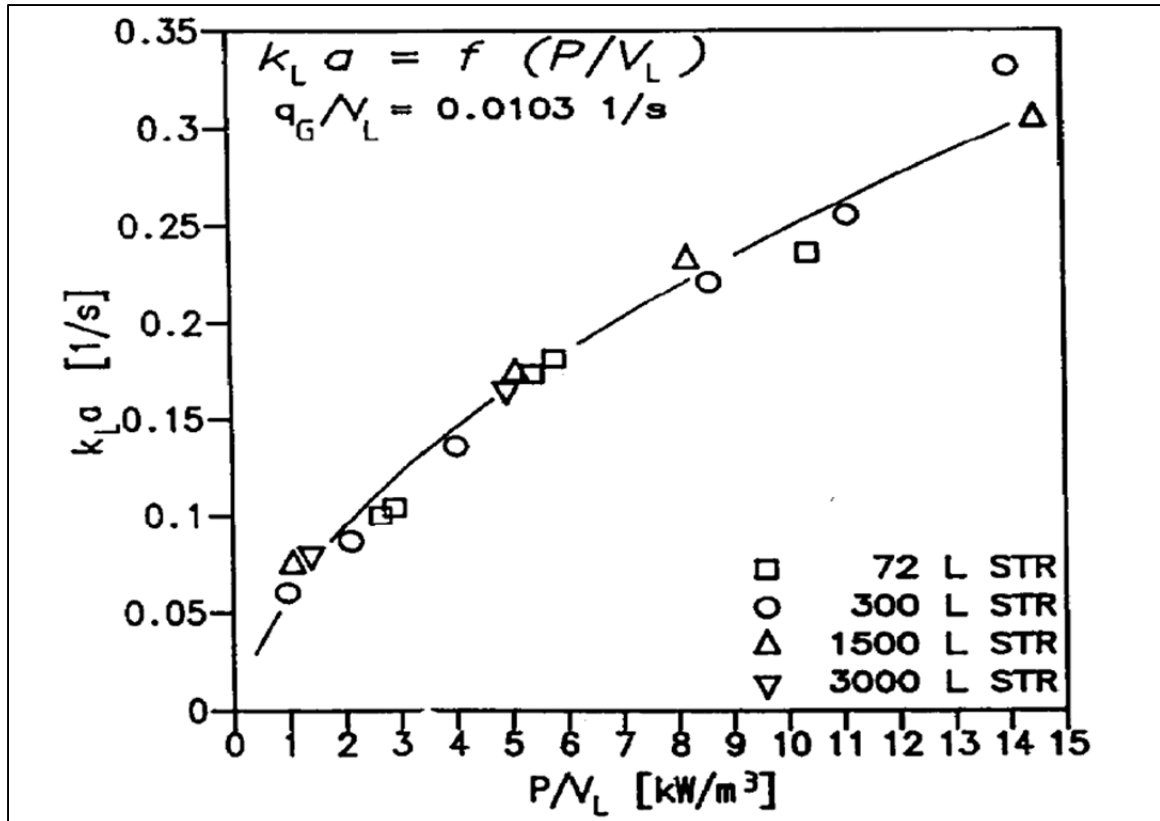
Figure 4. K_La versus Pg/V at constant Q/V or vvs (Schlüter and Deckwer, 1992).

Energy input models using either v_g or ϕ_g have mainly been used for experimental studies in fermentors using Rushton impellers and baffles. For either parameter to be used in a predictive model for this study, new coefficients would need to be determined to account for the unique geometries used in single-use bioreactors.

2.4.2   Gas Dispersion

Yawalkar et al. (2002b) determined that k_La could be correlated over a range of parameters based on the relative dispersion term N/N_{cd}. Nienow et al. (1977) defined N_{cd} (the minimum impeller speed at which all the liquid is in contact with the sparged gas) after studying a vast amount of experimental data, which incorporated several system configurations and operating conditions:

$$N_{cd} = \frac{4(Q_G)^{0.5}(D_t)^{0.25}}{D_i^2}$$ (18)

in which Q_G is the volumetric gas flow rate (m³/s). Using this equation, Yawalkar et al. (2002b)

studied data from different works and developed correlations based on the dispersion

parameter, N/N_{cd} (Table 4).

Table 4. Correlations obtained by Yawalkar et al. (2002b) for $k_L a$ data from different studies based on the relative dispersion parameter, N/N_{cd}.

Researchers	Correlation based on N/N_{cd}	R^2	Standard error	Number of data analyzed
Van't Riet (1979)	$k_L a = 2.76(N/N_{cd})^{1.14}(v_g)^{0.97}$	1	-	7
Smith and Warmoeskerken (1985)	$k_L a = 12.63(N/N_{cd})^{1.54}(v_g)^{1.27}$	0.99	0.02	15
Smith (1991)	$k_L a = 6.48(N/N_{cd})^{1.44}(v_g)^{1.12}$	0.99	0.02	32
Zhu et al. (2001)	$k_L a = 3.31(N/N_{cd})^{1.14}(v_g)^{0.97}$	1	-	15

The theory behind their correlation is based on the dependence of $k_L a$ on turbulence

intensity. Turbulence directly affects the dispersion of gas within a system. Hence, Yawalkar et

al.(2002b) references an article by Deshpande (1988), which suggests turbulence is

approximately proportional to impeller speed (*N*). Therefore, the ratio N/N_{cd} represents the

dispersion of gas and thus the volumetric gas-liquid mass transfer coefficient in the reactor.

The $k_L a$ data they obtained from the different studies was then correlated in the form of

$k_L a = f(N/N_{cd}, vvm, D_t, D_i/D_t)$. However, Yawalkar et al. (2002b) found that $k_L a$'s dependence on

D_i/D_t at a given N/N_{cd}, vvm and D_t was insignificant (Equation 19).

$$k_L a = 0.0558 \left(\frac{N}{N_{cd}} \right)^{1.464} (vvm)(D_t)^{1.05} \tag{19}$$

The exponent of D_t was then approximated to one, and the final equation was given the form:

$$k_L a = 3.35 \left(\frac{N}{N_{cd}} \right)^{1.464} (v_g) \tag{20}$$

However, the mathematical transition made by Yawalkar et al. (2002b) from Equation 19 to Equation 20 was left unexplained, and when attempted could not be replicated. It appears as though Yawalkar et al. assumed v_g to be equivalent to $(vvm)(D_t)$ in units of length per time. In order to convert from a per minute to a per second basis, they multiplied the lead coefficient by 60 instead of dividing by 60. Yawalkar et al. then observed that at a given superficial gas velocity, $k_L a$ was independent of geometric configuration with respect to the size and type of the reactor, impeller and sparger. Thus, Equation 20 implies that at a given superficial gas velocity and N/N_{cd}, $k_L a$ will be the same regardless of system configuration.

Results of the previous works studied by Yawalkar et al. (2002b), and their own studies showed experimental values to lie within 22% of the developed correlation. Thus, it appears that the relative dispersion parameter is an effective method for estimating $k_L a$. The gas dispersion method could therefore be useful in estimating mass transfer in the single-use systems, as, unlike the models based on energy input and dimensionless numbers, this model is independent of geometry.

2.4.3   Dimensionless Groups

Models predicting the mass transfer coefficient based on dimensionless groups often use the Froude number (Fr) and the gas flow number (Fl_G).

$$Fr = \frac{N^2 D_i}{g} \tag{21}$$

$$Fl_G = \frac{Q}{ND_i^3} \tag{22}$$

Plotting Fr versus Fl$_G$ defines the flow regimes in gas-liquid STRs. Smith and Warmoeskerken (1985) and Smith (1991) used this method to study regimes such as vortex clinging cavities, large cavities, flooded regions and gas recirculation, which they believe to have direct effects on mixing and mass transfer.

Smith and Warmoeskerken (1985) studied k$_L$a and gas-hold up in two groups of data. The first group was a clinging cavity system, also known as a before large cavity (BLC) regime. The second was a regime of higher gas loading, otherwise known as an after large cavity (ALC) system (Figure 5). Smith and Warmoeskerken stated, "Cavities have a streamlining action and thereby lower the drag coefficient and thus the power demand of the impeller" (1985). Thus impeller flow fields should be studied to define cavity configurations.
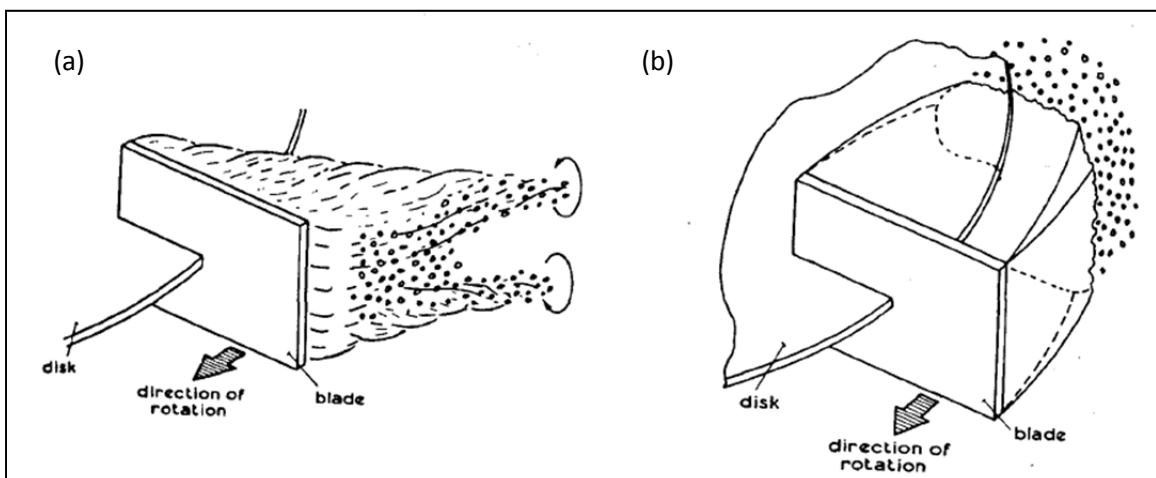
Figure 5. (a) Clinging cavity (BLC) and (b) after large cavity formations (Smith and Warmoeskerken, 1985).

Smith and Warmoeskerken consequently performed studies to predict the formation of cavities in stirred-tank systems. Using a six-bladed Rushton impeller, they developed Equation 23, which predicts the transition from clinging to large cavity structures.

$$Fl_G = 3.8 \times 10^{-3} \left(\frac{Re^2}{Fr} \right)^{0.067} \left(\frac{D_t}{D_i} \right)^{0.5} \tag{23}$$

This equation, in which the slope of the line corresponds to Fl_g (Q_G/ND_i^3), is plotted in Figure 6 by setting Equation 22 equal to Equation 23. In Figure 6, the y-axis Q_g/D^2 is regarded as a superficial gas velocity based on the cross sectional area of the impeller. The x-axis in Figure 6 contains the ND term, which represents tip velocity and is the constant of Equation 23. From their results, Smith and Warmoeskerken (1985) concluded that cavity size would increase with increasing gas flow rates. Their findings appear to support their theory of mass transfer being affected by flow regime within the system.
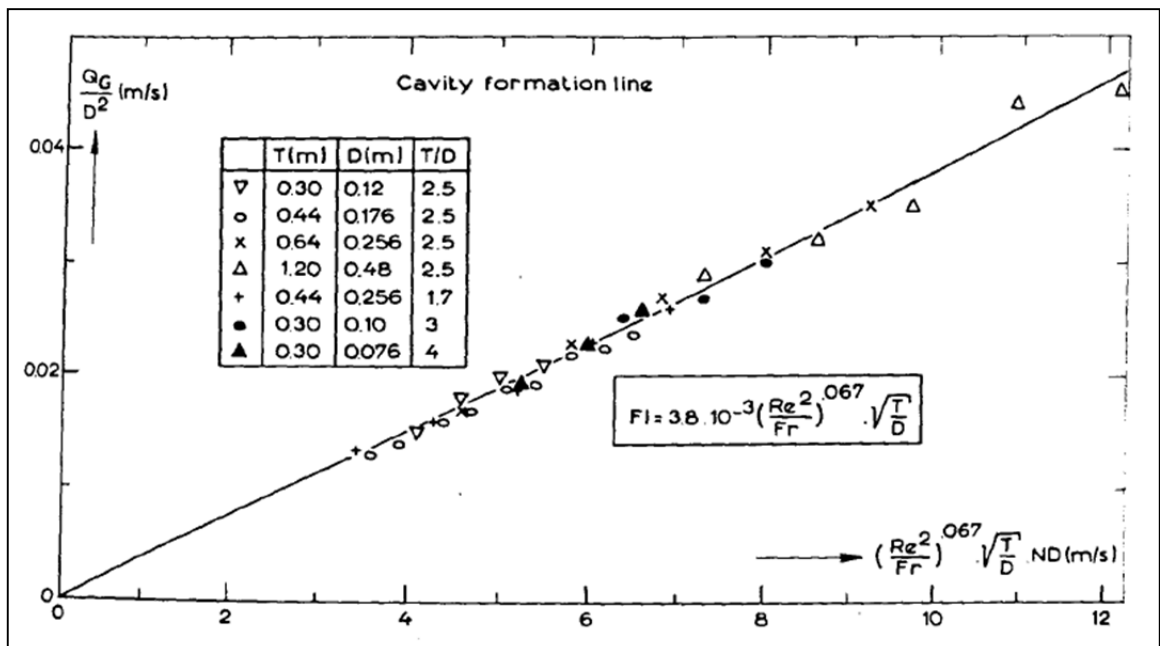
Figure 6. The cavity formation line developed by Smith and Warmoeskerken (1985).

Based on their results, Smith and Warmoeskerken (1985) developed two predictive

equations for determining $k_L a$ in systems with low (Equation 24) or high (Equation 25) gas

loading regimes.

(BLC)
$$k_L a = 1.1 \times 10^{-7} Fl_G{}^{0.6} \operatorname{Re}^{1.1} N \qquad (24)$$

(ALC)
$$k_L a = 1.6 \times 10^{-7} Fl_G{}^{0.42} \operatorname{Re}^{1.02} N \qquad (25)$$

While these equations can be related to similar air-water systems using Rushton or other radial

impellers, they cannot be utilized in systems with axial-pumping impellers until new coefficients

are determined.

Smith (1991) wanted to demonstrate that dimensionless equations can be used to

determine hydrodynamic conditions on which to base predictions of performance data. He also

recognized the importance of the differences between conditions used to establish the

correlation and those found in the operating vessel. Such differences can define the value and

limitations of the proposed equation. Smith (1991) agreed with Smith and Warmoeskerken's

(1985) observation that gas liquid systems develop flow regimes about the impeller, which

affect the directional pumping and turbulence of a reactor system. By studying the void fraction

in standard aerated tanks (H/D_t= 1, Rushton impeller), Smith found, in agreement with Hassan

and Robinson (1977), that gas fraction linearly correlates with volumetric gas rate. Giving the

correlating equation the form

$$\varepsilon_G = K'\left(\operatorname{Re} \cdot Fr \cdot Fl_G\right)^{0.35} \qquad (26)$$

in which ε_G represents gas void fraction. In order to accommodate industrial vessels, the ratio of

D_i/D_t was incorporated to Equation 26:

$$\varepsilon_G = 0.85\left(\text{Re}\cdot Fr \cdot Fl_G\right)^{0.35}\left(\frac{D_i}{D_t}\right)^{1.25}$$ (27)

Smith then expresses the complexity of calculating $k_L a$ as compared to the gas fraction. Since

$k_L a$ is not a dimensionless number, Smith multiplied $k_L a/N$ by the square root of the Froude

Number. He then developed the following equation:

$$k_L a = 1.25 \times 10^{-4}\left(\frac{D_i}{D_t}\right)^{2.8} Fr^{0.6} \, \text{Re}^{0.7} \, Fl_G{}^{0.45}\left(\frac{D_i}{g}\right)^{-0.5}$$ (28)

His correlation was calculated from data collected from a well-mixed liquid with a plug flow gas

phase, and relied heavily on the effects of gas fraction on mass transfer. As in most energy

input studies, Smith used a Rushton impeller. In the discussion section, Smith mentioned that

the exponents on the correlating equation were not very sensitive and that he failed to reduce

the equation to one independent of diameter. He also felt that surface tension, or a similar

physical property, should be included. This, however, would cause a change in the

interdependence of density and viscosity implied in his equation.

Smith's (1991) equation has a commonality among the correlating variables that

appears misleading. For example, both *Re* and *Fr* relate to power input to the system. It also

seems redundant to multiply by the square root of the Froude number if it is already present in

the equation. For a similar equation to work in a single-use bioreactor, studies would need to

be performed to determine the changes in flow regimes in the presence of an axial impeller.

However, as it seems to complicate the equation originally developed by Smith and

Warmoeskerken (1985), this study will only compare experimental results with Equations 24 and

25.

2.5   Single-Use Technology

Integration of disposable technology in the biopharmaceutical industry is growing with the increased need to deliver high quality products within strict timelines (Forgione and Van Trier, 2006). This growth is driven by the desire to reduce processing times, increase productivity and reduce cost. Stainless steel units require cleaning as well as space even when they are not being used (DiBlasi et al., 2006). In addition to the time it takes to sterilize a steel unit, large volumes of water for injection (WFI) and steam need to be used. Single-use systems on the other hand, come sterilized, negating the capital required for sterilization systems. With the industry appearing to move towards disposable reactors, the bioreactors studied in this work are single-use systems. There are currently two main types of single-use bioreactor systems, wave reactors and sterile bag inserts.

The first single-use bioreactors, known as wave reactors, were developed in the 1970s (DiBlasi et al., 2006). These pillow-shaped bags are placed on a platform, and a rocking motion creates waves, which provide mixing. While useful at the laboratory scale, the large units can be awkward and space consuming. All the components of the wave reactors are disposable except for the controller and drive platform. The bag chamber, vent filters, probes, as well as other tubing and fittings that come in contact with the product are designed to be single-use. Although these systems are efficient and easy to use, they lack the common geometry seen in the stirred tank reactors, which are the systems of choice in industry (Nienow, 2006).

The second single-use bioreactor is usually referred to as a "liner style" and functions as a typical stirred tank bioreactor and was first used in 2006 by ThermoFisher Scientific (Selker and Paldus, 2008). A disposable bag (Figure 7b) is typically comprised of mostly polyethylene is used as a liner in a cylindrical steel tank (Figure 7a). The bag has an integrated impeller for mixing as well as sampling ports and sparger system (Figure 7b). The steel tank is conventionally

open at the top, and view ports can be added to optically monitor the culture. These systems

have been commercialized by various manufacturers (see e.g., Published US Patent Applications

2005/0272146 and 2005/0239199).
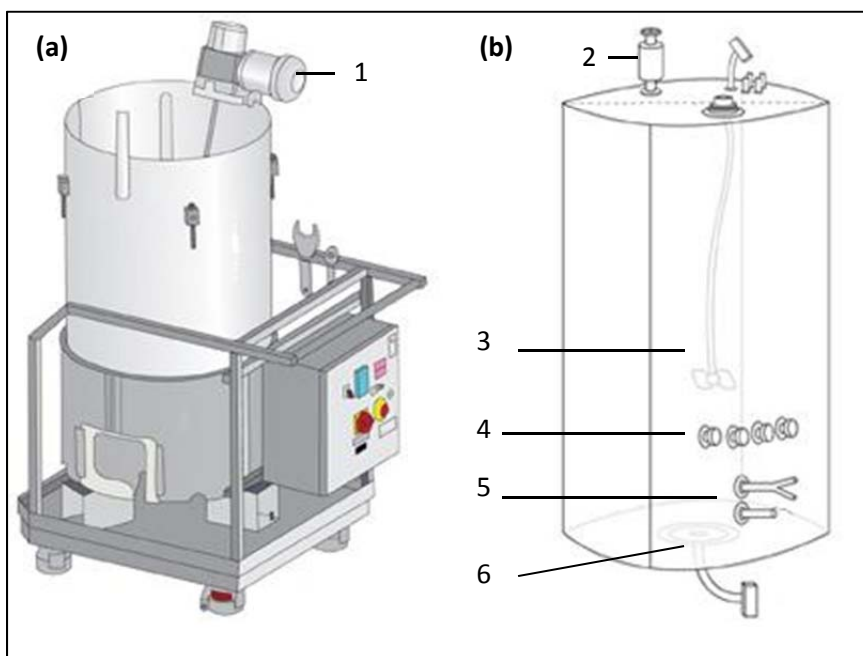
Figure 7. Steel tank (a) and disposable bag insert (b). Where: (1) Impeller motor and drive shaft, (2) Air filter, (3) Integrated impeller, (4) Probe ports located 6.5" from base, (5) RTD port and sample tubes, (6) Sparger port. Image courtesy of Thermo Fisher website: <http://www.thermoscientific.jp/hyclone-bpc/catalog/single-use-bioreactor.html>.

CHAPTER 3

MATERIALS AND METHODS

3.1 Comparison Studies

In this study, experiments were carried out to determine the operating ranges of different laboratory scale reactors (3 L working volume), and how they changed upon scale-up to industrial culture (2000 L). Parameters of mixing time, $k_L a$, shear sensitivity, and computational fluid dynamics will be used to determine the effectiveness of each reactor. These same parameters will be studied upon scale-up to larger cultures.

3.1.1 Modifications to 3 L Bioreactor

In order to obtain comparable data in the glass bioreactor, it was first modified to mimic the geometry found in the single-use systems (Figure 8). An adaptor that allowed for a 19.6° angle on the impeller shaft was machined from aluminum. The design for the 3-blade pitched elephant-ear impeller used in the disposable reactors was scaled down. The part was then manufactured on a Dimension 3D Printer system. To adjust the reactor to the working H/D_t ratio of 1.5 found in the single-use reactors, a 3.6" insert was built out of plastic. A latex and clay mold, were then used to transform the sharp edges of the insert to the smooth curve found in the bags. The same type of frit sparger used in the large reactors was molded to the insert using a silicone-based caulk. Tubing (0.125" OD) was needed to feed air to the sparger. It was assumed that the influence of the tubing on mixing was negligible.
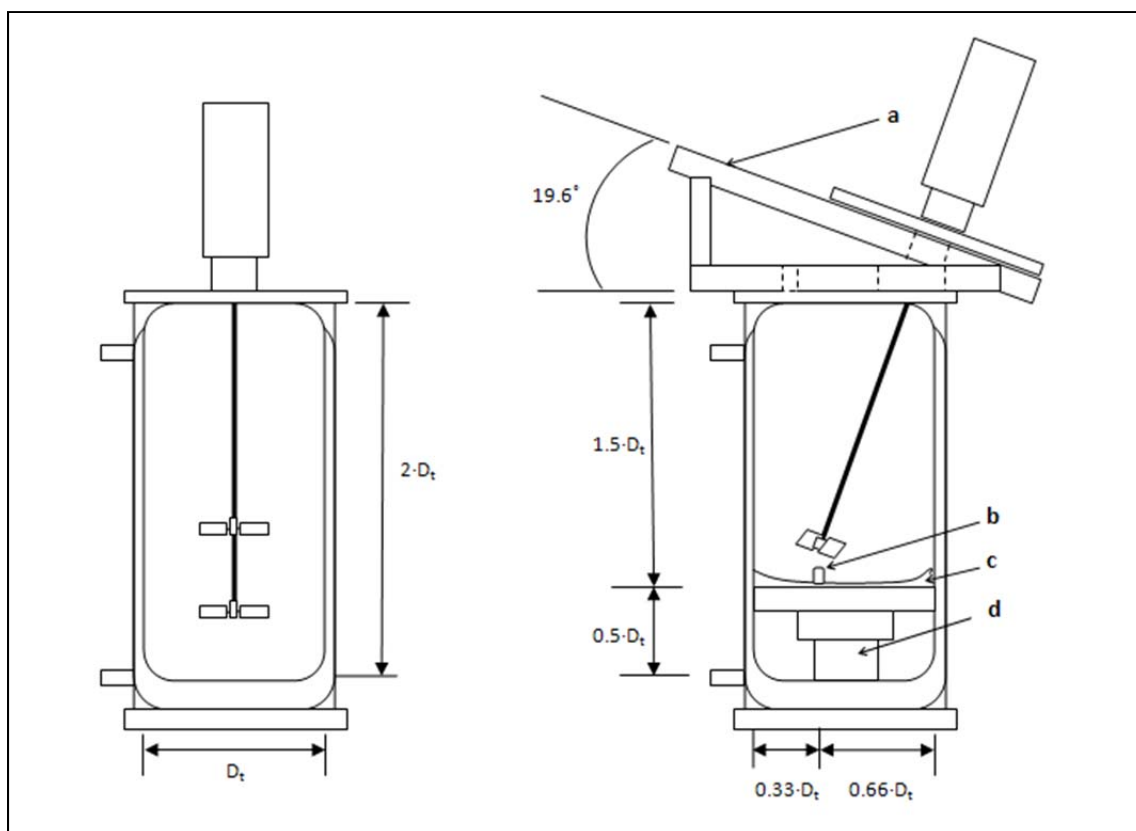
Figure 8. Schematic of 3 L bioreactor with modifications. (a) Aluminum adaptor (b) Frit sparger (c) Latex and clay mold (d) Plastic insert.

3.1.2 Determining Oxygen Mass Transfer

For simplicity, the unsteady-state method of determining k_La was utilized for performing these studies. Reactors were filled to the working volume (3, 50, 100, 250, 500, 1000, 2000 L) with distilled water and allowed to reach 37°C. In the 3 L modified reactor, a Mettler Toledo DO probe (Mettler-Toledo Inc., OH) was used, and data values were collected using Biotron LiFlus GX data logging software (Biotron, Korea). For each of the larger vessels, a Broadley James DO probe (Broadley James Corporation, CA) was used and controlled with a PendoTech controller (PendoTech, NJ). Probes were calibrated at the beginning of each test day. For the k_La runs, air was first removed from the system by sparging with N_2 gas. Once the dissolved oxygen level in the reactor was below 15% saturation, the N_2 valve was closed and air was returned to the system at predetermined flow rates (0.02, 0.03, 0.04vvm). The change in dissolved oxygen was

monitored from 15-75% saturation. The resulting data was used to calculate k_La as seen from

the following equations (Shuler and Kargi, 2002):

$$\frac{dC_L}{dt} = k_L a\left(C * - C_L\right) \tag{29}$$

$$\frac{-d\left(C * - C_L\right)}{dt/\left(C * - C_L\right)} = k_L a \tag{30}$$

$$-k_L a = \ln\left(C * - C_L\right) \tag{31}$$

The slope of the plot of $\ln(C*-C_L)$ versus time was approximately equal to k_La. To eliminate bias,

data lying within 20-80% of the total measured values were used when graphing and

interpreting the slope of $\ln(C*-C_L)$.

In order to more accurately determine oxygen transfer within the reactor, three probe

positions were tested on the 3 L reactor. Since the reactor was glass, it was impossible to insert

the probe at the base of the reactor behind the impeller, as the probes are located in the single-

use systems. In the 3 L vessel, the probe was inserted from the top approximately 0.33D from

the edge of the tank, and offset clockwise from the impeller as seen in Figure 9.

3.1.3   Mixing Time Calculations and Experiments

Mixing times in the three-liter vessel were determined by three different methods: pH

tracer, conductance, and color change. Mixing time in all three methods was assumed to be the

time it took for the solution to reach 95% homogeneity (Equation 32). The pH tracer method

was used to closely follow the work of Cabaret et al. (2007), in which a color indicator helped

identify mixing patterns. Thus, the pH and color change methods were performed

simultaneously. A standard Finesse TrupH probe (Finesse, CA) was used for the study, and was

positioned at approximately 0.5H and 0.33D from the outer edge of the tank, above the

impeller. The reactor was filled with three liters of distilled water and 0.013g of Bromocresol

purple dye. For each run, the pH level was adjusted to 7.2-7.4. After 10 seconds of data

collection (obtained at one collection point per second), 3.5 mL of 1M HCl was added which

caused the pH to drop below 5.2. As Bromoresol purple is pH sensitive, the water appeared

purple when the pH was above 7, and yellow below 5.2 pH. The pH was then adjusted back to

7.2-7.4 using 1M NaOH. Each run was recorded (Figure 10) using a Canon PowerShot S5 IS

digital camera (Canon, NY). The footage was later analyzed and timed visually. Data for the pH

method was collected using LiFlus GX software (Biotron, Korea) and was analyzed using

Microsoft Excel (Microsoft, WA) to determine mixing time.
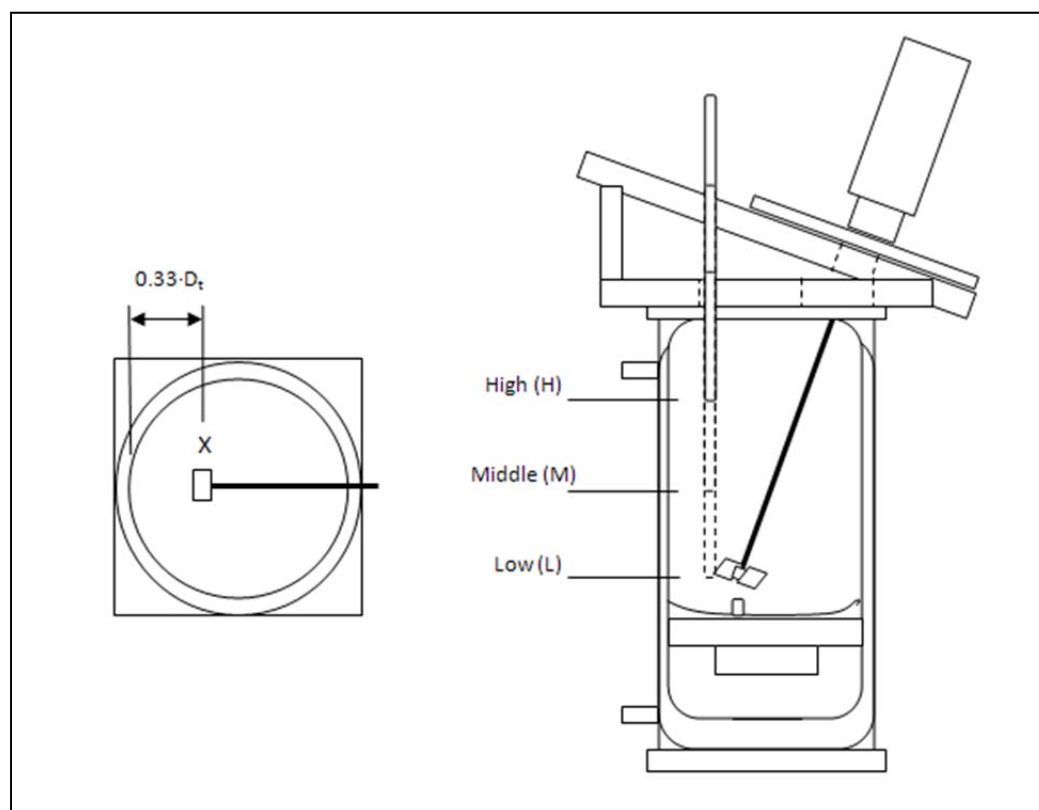
Figure 9. *Left* Top view of probe location (X) in 3 L reactor. *Right* Tested probe depths.

The conductance method was tested using a EUTECH Instruments' αlpha CON500

conductivity transmitter and probe (ThermoFisher Scientific, MA). Data was collected using

Tracer DAQ software. The conductance probe was positioned in the same location as the pH

probe in the pH and color change methods. For each run, the reactor was filled with three liters

of distilled water. After 10 seconds of data collection, 8 mL of 9M HCl was added. This would

cause a change of roughly 3-4V. Data for each run was collected at a rate of 10Hz for

approximately 40 seconds. After data collection was completed for the run, the tank was

drained and refilled with distilled water. Data was analyzed using Microsoft Excel to determine

mixing time.
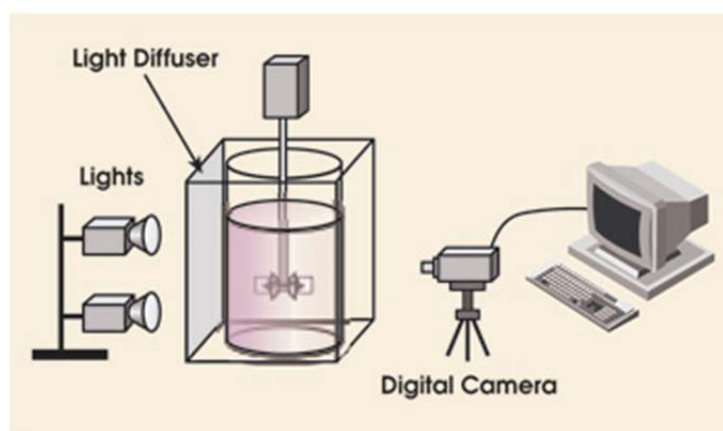
Figure 10. Set up of lights, diffuser, and camera for mixing time studies (Hogan, 2009).

Mixing times in the large-scale bioreactors were measured using the same conductance

method and equipment used in the 3 L reactor. However, in an attempt to map mixing patterns

at the larger scale, three conductance probes were used and positioned at the top, middle and

bottom of each tank. To avoid using large amounts of acid, a salt solution (5M NaCl) was used

instead. For each run the salt solution, at 10 mL per liter of vessel volume, was quickly poured

into the vessel directly above the impeller (Vrabel et al., 1999), and mixing time was then

determined as the amount of time it takes for the conductance probes to reach 95%

homogeneity (Vrabel et al., 1999). Equation 32 describes the homogeneity criterion (Hadjiev et

al., 2006; Oniscu et al., 2002):

$$I = \frac{pH_\infty - 0.5\Delta pH}{pH_\infty} \times 100 = 95\% \qquad (32)$$

3.1.4 Dissolved Oxygen Probe Response Time

To measure dissolved oxygen, galvanic probes were used. Galvanic probes consist of a gas-permeable membrane and electrolyte fluid. To correct for lag in the probe response time, two constants were determined and used, to account for the time required for the oxygen to dissolve through the membrane and through the fluid (Davis et al., unpublished data). Beckwith et al. (1993) used Newton's equation for a spring mass damper system (Equation 33) to derive an equation for a jacketed temperature probe (Equation 34).

$$\frac{1}{g_c}\left[m\left(\frac{d^2 s}{dt^2}\right)\right] + \varsigma_d\left(\frac{ds}{dt}\right) + ks = F(t) \qquad (33)$$

Substituting time constant: $\tau = 2m/\varsigma_d g_c$

$$\tau_1 \tau_2 \frac{d^2 C_m}{dt^2} + (\tau_1 + \tau_2)\frac{dC_m}{dt} + C_m = C \qquad (34)$$

In this equation, the time constants, τ_1 and τ_2, represent the time it takes for the heat to cross the jacket and the probe. For a galvanic dissolved oxygen sensor, these constants can be used to represent the time required for the oxygen to pass through the gas-permeable membrane and dissolve through the electrolyte fluid. This second-order model accounts for both sources of lag time, and is therefore considered to be theoretically more accurate than a traditional first-order model (Davis et al., unpublished data).

The second-order model was used to correct for lag in probe response times after the time constants were determined. The time constants were calculated using an artificial step function. The probe was subjected to a dissolved oxygen step response. The probe was placed

in nitrogen-saturated water. After reaching equilibrium, the probe was transferred to air-saturated water and the response was recorded using LiFlux GX software (Figure 11). This method was repeated three times.
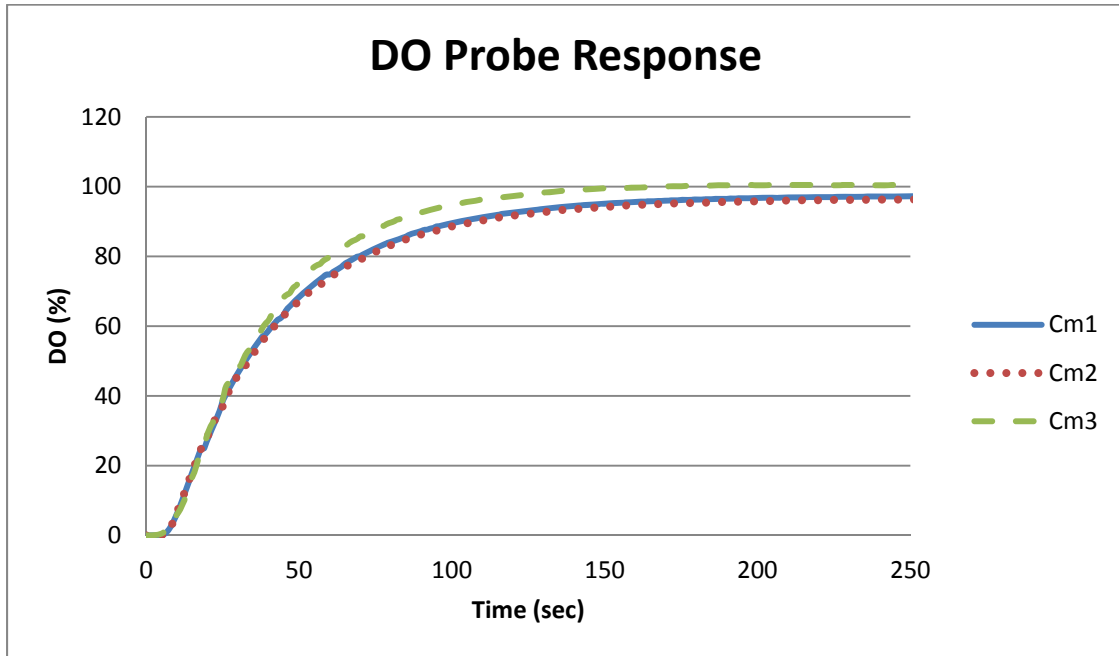
Figure 11. Response times for Mettler Toledo probe, where Cm represents measured DO concentration.

The responses of the dissolved oxygen probes were then fitted to a general step response solution (Equation 35).

$$\frac{C_L - C_m}{C_L - C_O} = \left(\frac{\varsigma}{\varsigma - 1}\right) \cdot e^{-t/\varsigma \cdot \tau_2} - \left(\frac{1}{\varsigma - 1}\right) \cdot e^{-t/\tau_2} \qquad (35)$$

This was achieved using Excel Solver to determine time constants, which would produce the least amount of error between the calculated and measured DO concentrations. For the second-order approximations, the time constants τ_1 and τ_2 for a Mettler Toledo DO probe were determined to be 3.3790 and 34.2805 seconds, respectively. The derivatives in Equation 34

were then approximated as outlined by Chapra and Canale (2006), and the correction was applied to the data (Figure 12).

$$f'(x_i) = \frac{f(x_{i+1}) - f(x_{i-1})}{2h} \tag{36}$$

$$f''(x_i) = \frac{f(x_{i+1}) - 2 \cdot f(x_i) + f(x_{i-1})}{h^2} \tag{37}$$
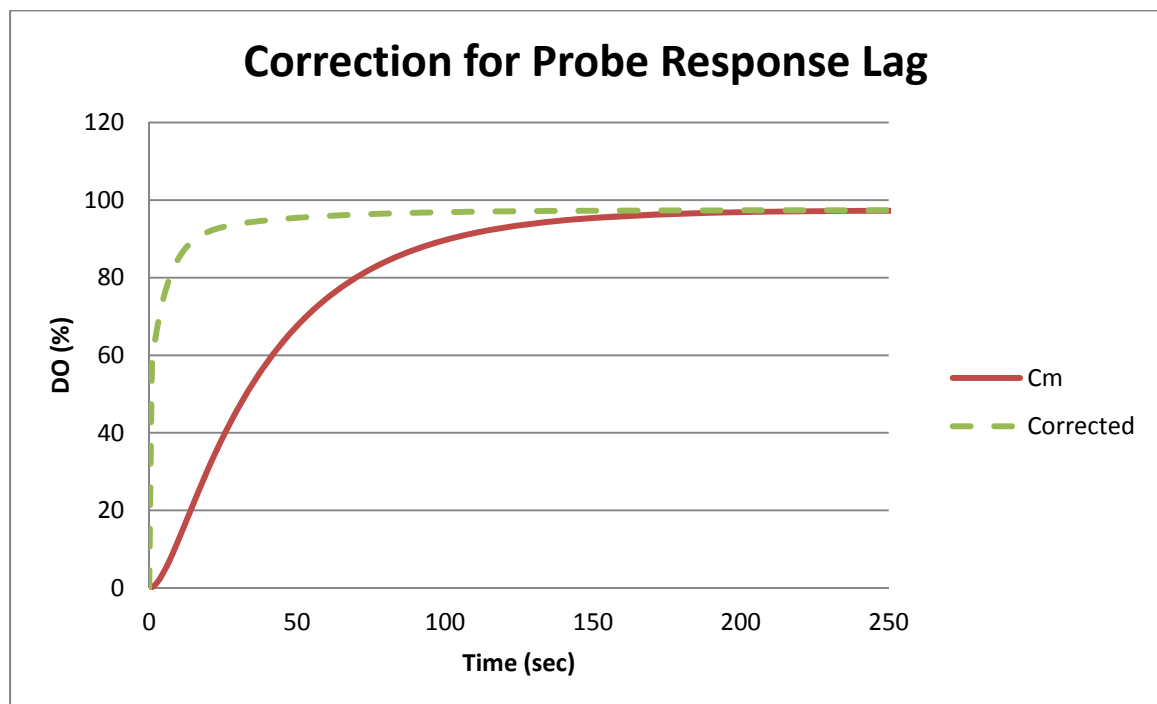
Figure 12. Graph of the measured DO concentrations (Cm), and the concentrations with the correction for probe response time (Equation 34).

3.2   Statistical Analysis

Advanced statistical analysis was used to analyze the data from the $k_L a$ and mixing studies. For each study, factors of variance were determined and a corresponding statistical model was developed. Each model was factorial in design, with the random error term (ε_{ijkl}) assumed to be identically distributed, mutually independent, and approximately normal in

distribution with mean value equal to zero and standard deviation σ^2. Table 5 lists the factors

involved in analysis of the k_La data collected for scale-up comparisons. Equation 38 is the

corresponding model for the factors listed in Table 5.

Table 5. A description of the factors involved in scale-up k_La studies.

Factor	Number of Levels	Random or Fixed	Treatment Structure
Vessel Volume	7	Fixed	Crossed w/Constant and Aeration
Scale-up Constant	2	Fixed	Crossed w/Volume and Aeration
Aeration	3	Fixed	Crossed w/Volume and Constant
Observations	3	-	-

$$Y_{ijkl} = \mu_s + V_i + C_j + A_k + (VC)_{ij} + (VA)_{ik} + (CA)_{jk} + (VCA)_{ijk} + \varepsilon_{ijkl} \quad (38)$$

where:

Y_{ijkl} = the value of the lth observation that got k^{th} level of factor A and the jth level of factor C and
the ith level of factor V

μ_s = the overall or grand mean

V_i = the effect due to the ith level of factor V (Vessel Volume)

C_j = the effect due to the jth level of factor C (Scale-up Constant)

A_k = the effect due to the kth level of factor A (Aeration rate)

$(VC)_{ij}$ = the effect due to the interaction of the ith level of factor V and the jth level of factor C

$(VA)_{ik}$ = the effect due to the interaction of the ith level of factor V and the kth level of factor A

$(CA)_{jk}$ = the effect due to the interaction of the jth level of factor C and the kth level of factor A

$(VCA)_{ijk}$ = the effect due to the interaction of the ith level of factor V, the jth level of factor C and
the kth level of factor A

ε_{ijk} = the residual or random error term

     Table 6 lists the factors involved in analysis of mixing time data collected for scale-up

comparisons. Equation 39 is the corresponding model for the factors listed in Table 6.

Table 6. A description of the factor levels involved in scale-up mixing time studies.

Factor	Number of Levels	Random or Fixed	Treatment Structure
Vessel Volume	7	Fixed	Crossed w/Constant and Probe
Scale-up Constant	2	Fixed	Crossed w/Volume and Probe
Probe Location	3	Fixed	Crossed w/Volume and Constant
Observations	2	-	-

$$Y_{ijkl} = \mu_s + V_i + C_j + P_k + (VC)_{ij} + (VP)_{ik} + (CP)_{jk} + (VCP)_{ijk} + \varepsilon_{ijkl} \quad (39)$$

where:

Y_{ijkl} = the value of the lth observation that got k^{th} level of factor A and the jth level of factor C and the ith level of factor V

μ_s = the overall or grand mean

V_i = the effect due to the ith level of factor V (Vessel Volume)

C_j = the effect due to the jth level of factor C (Scale-up Constant)

P_k = the effect due to the kth level of factor P (Probe Location)

$(VC)_{ij}$ = the effect due to the interaction of the ith level of factor V and the jth level of factor C

$(VP)_{ik}$ = the effect due to the interaction of the ith level of factor V and the kth level of factor P

$(CP)_{jk}$ = the effect due to the interaction of the jth level of factor C and the kth level of factor P

$(VCP)_{ijk}$ = the effect due to the interaction of the ith level of factor V, the jth level of factor C and the kth level of factor P

ε_{ijk} = the residual or random error term

A statistical analysis software package, SAS (SAS Institute, NC), was used to analyze the data. The PROC GLM method was used to extract residuals from each comparison set, and to generate the Least Sum of Squares. Histograms, normal overlays, normal quantile plots, box plots and formal tests for normality were used to determine if the data was approximately normal and homoscedastic. If the data was found to not comply with the standard rules of normality and homoscedasticity, transformations were tested to optimize the data. If outliers were removed, their removal was accounted for in the software. The Ryan-Einot-Gabriel-Welsch Multiple Range Test (REGWQ) was also utilized to interpret the data and to aid in visualization of significant differences in the factor levels.

3.3   Computational Fluid Dynamics

Models derived from computational fluid dynamics (CFD) were run by Dr. Robert Spall of

the Mechanical and Aerospace Engineering Department. Conditions for a 250 L single-use

bioreactor at determined agitation and aeration rates were represented in CFD. Mixing models

for reactors with volumes ranging from 3 to 2000 L were created to determine mixing times and

flow patterns. These models were used to study fluid flow within the reactors and for

comparison with experimental results for mixing times.

Governing equations, as outlined in the ANSYS Fluent User's Manual 12.0 (2009), were

solved using CFD solver FLUENT 12.0.3 (ANSYS, PA). A no-slip boundary condition was used on

all solid surfaces. The equations were solved in a rotating reference, which incorporated a

multiple reference frame to account of the angle of the impeller/shaft. Tetrahedral volume

meshes were generated using Gambit (Gambit Software, CA). These meshes were then

converted to polyhedral meshes in Fluent to improve convergence characteristics. Figure 13

and Figure 14 show meshes of the 250 L bioreactor and corresponding impeller surface

respectively.

Calculations for predicting mixing times were based on the converged transport

equation used for the convection and diffusion of a passive scalar. The scalar was given an

initial value of 100 within the zone immediately surrounding the impeller. Seven other points in

the reactor, also used to calculate the convergence of the velocity field, were tracked over time.

Thus, the mixing time was defined as the amount of time needed for the values of each scalar to

deviate by no more than 5% of the final steady-state concentration.
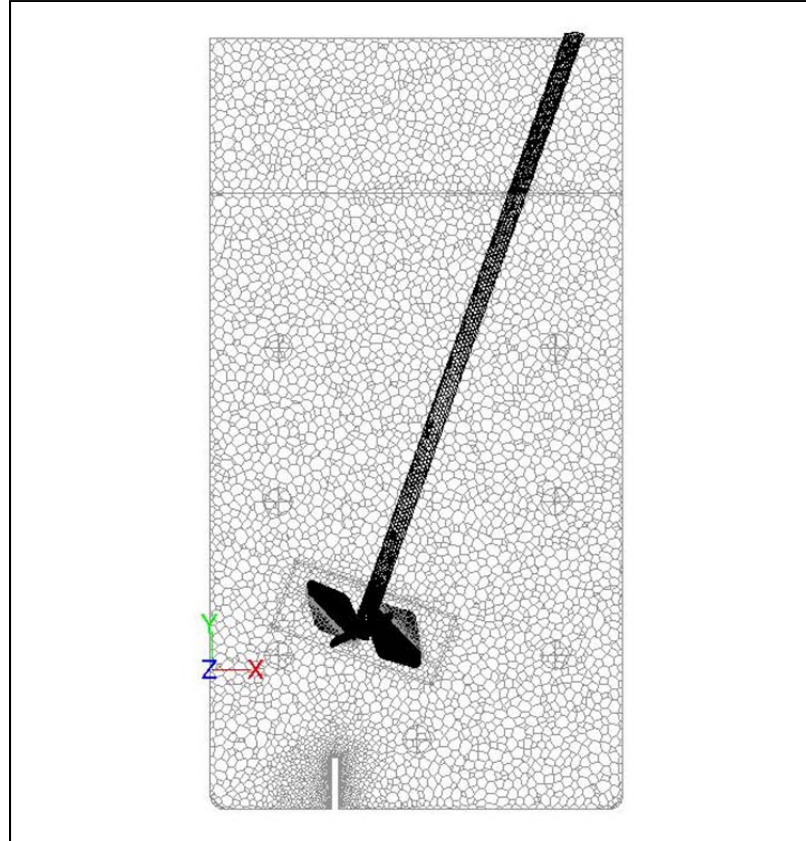
Figure 13. Representative polyhedral mesh for a 250 L SUB displayed on z=0 plane (Spall et al., 2010).
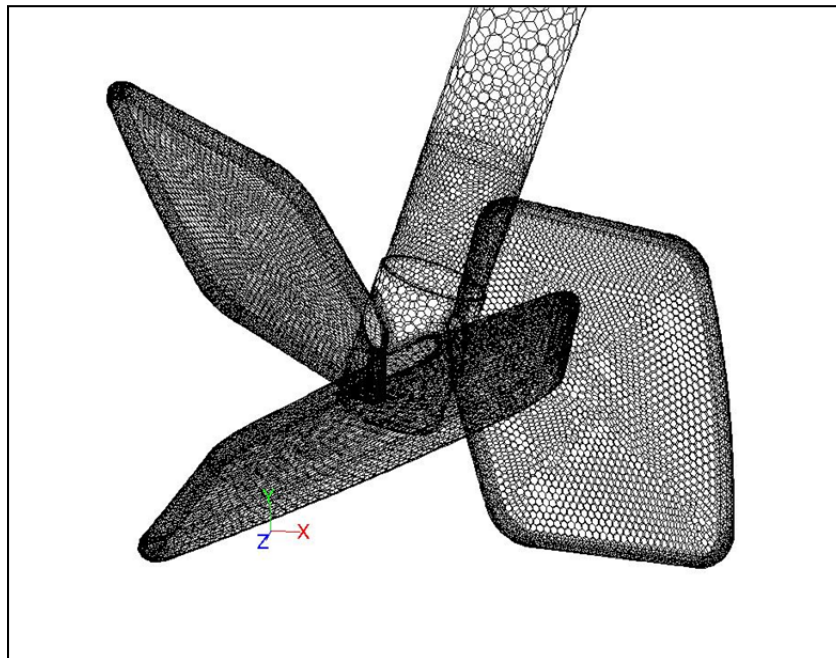
Figure 14.The impeller surface mesh for 250L SUB (Spall et al., 2010).

3.4   Scale-Up Studies

The goal of this study was to address the scale-up of single-use bioreactors by providing quantitative data at the laboratory level (3 L) up to a large scale process (2000 L) and to perform the derivation of empirical equations and calculate CFD models which will aid users in industry. As oxygen availability is often a limiting factor upon scale up, most methods attempt to maintain constant $k_L a$ values during scale-up (Ju and Chase, 1992). In this study, tests were run to determine the change in $k_L a$ upon scale-up when the following parameters were held constant: impeller tip speed (N), volumetric gas flow rate (Q/V) and mean power input to volume (P_g/V). The resulting data helped determine what steps need to be taken to preserve constant $k_L a$ at larger volumes.

The comparison studies performed at the laboratory scale for mixing time and $k_L a$ were also carried out at the larger scales in order to determine the changes in physiological conditions upon scale-up.

Table 7 shows the test parameters for the scale-up studies maintaining constant P_g/V, shear and Q/V. The following equations used to calculate power consumption are found in Doran (1995):

$$P = N_p \rho N^3 D_i^{5} \qquad (40)$$

The impeller power number N_p, is equal to 0.64 from Wheetman and Coyle (1989), and P is the ungassed power consumption of the impeller system. The ungassed power is then used to calculate the gassed power input P_g.

$$P_g = P \cdot 0.1 \left(\frac{Q}{NV} \right)^{-1/4} \left(\frac{N^2 D_i^{4}}{g W V^{2/3}} \right)^{-1/5} \qquad (41)$$

Table 7. Test matrix for scale-up studies. (*) denotes parameters which were tested under a previous scale-up constant.

		3 L	50 L	100 L	250 L	500 L	1000 L	2000 L
Constant P_g/V	(rpm)	338	169	145	118	100	87	75
No gas	(reps)	3	3	3	3	3	3	3
Air (0.03 vvm)	(reps)	3	3	3	3	3	3	3
Constant Shear	(rpm)	500	186	150	109	87	68	55
No gas	(reps)	3	3	3	3	3	3	3
Air (0.03 vvm)	(reps)	3	3	3	3	3	3	3
Constant Q/V	(rpm)	338	169	145	118	100	87	75
No gas	(reps)	*	*	*	*	*	*	*
Air (0.02 vvm)	(reps)	3	3	3	3	3	3	3
Air (0.03 vvm)	(reps)	*	*	*	*	*	*	*
Air (0.04 vvm)	(reps)	3	3	3	3	3	3	3

In order to test the validity of geometric similarity between reactors, measurements were taken of each impeller. Any irregularities in the scale-up of the impeller could account for differences seen in the mixing times and k_La values achieved. Table 8 lists the measurements of each impeller.

Table 8. Dimensions of the impellers, in inches, used in single-use bioreactors. V_d represents the volume dispersed by the impeller and V_t is the volume of the vessel.

Vessel Volume (L)	Area (in)	Height (in)	Outer radius (in)	Inner radius (in)	Vd (L)	Vd/Vt
3	0.59	0.68	0.86	0.25	0.02	0.0079
50	3.25	1.53	2.19	0.50	0.36	0.0071
100	5.73	1.96	2.94	0.50	0.85	0.0085
250	11.45	2.72	4.00	0.50	2.20	0.0088
500	16.35	3.43	4.94	0.59	4.25	0.0085
1000	26.70	4.40	6.13	0.61	8.41	0.0084
2000	42.63	5.60	7.50	0.60	16.12	0.0081

V_d represents the volume of liquid directly disrupted by the impeller (Figure 15), and was calculated using the washer method for solids of revolution (Equation 42).

$$V_d = \pi \int_0^H \left(R^2 - r^2 \right) dy \qquad (42)$$
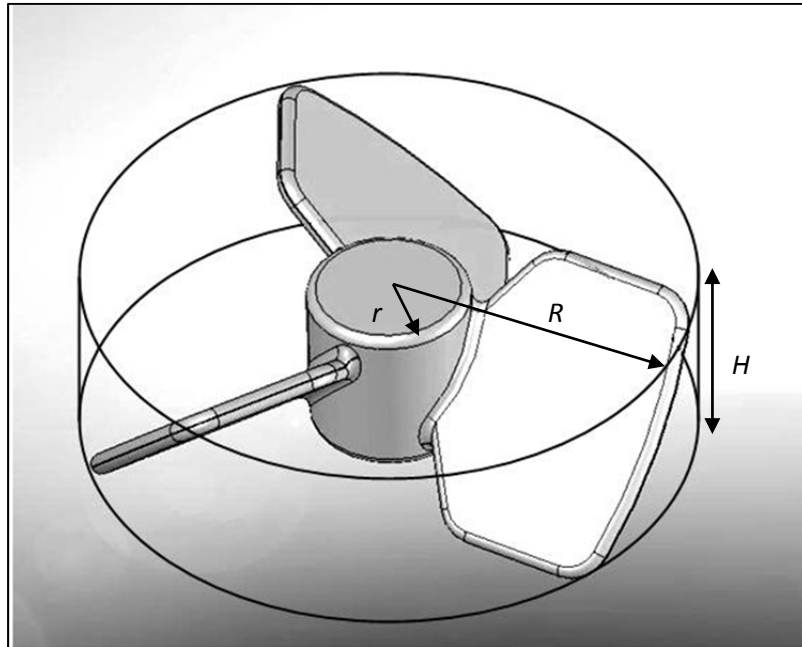
Figure 15. Image of the volume of disruption (V_d) caused by the impeller.

CHAPTER 4

RESULTS AND DISCUSSION

4.1   Results for Mixing Studies

4.1.1   Method Verification Studies

Mixing time results from uncorrected and corrected data, with respect to probe

response time, were analyzed in SAS to determine statistical significance (Tables 9-12). After

applying a square-root transformation to normalize the data, the results for the Least Sum of

Squares as well as the REGWQ Test were used to interpret the outcome. Results showed that

the probe correction, in either method, did not make a significant difference in mixing time.

Thus, the following results are for the original data only.

Table 9. Results for pH mixing studies obtained using the GLM procedure. Results had an R^2
value of 0.434. Sources with a Pr value < 0.05 have a significant effect on $k_L a$.

Source	DF	Type I SS	Mean Square	F Value	Pr> F
Agitation	1	0.154	0.154	8.46	0.0066
Aeration	3	0.074	0.025	1.35	0.2764
Correction	1	0.006	0.006	0.35	0.5608

Table 10. REGWQ test grouping for mean mixing times (sec) obtained with (Y) and without (N)
correction for pH data. Means with the same letter are not significantly different.

Grouping	Mean	N	Correction
A	2.175	24	N
A	2.152	24	Y

Table 11. Results for conductance mixing studies obtained using the GLM procedure. Results
had an R^2 value of 0.96. Sources with a Pr value < 0.05 have a significant effect on $k_L a$.

Source	DF	Type I SS	Mean Square	F Value	Pr> F
Agitation	1	1.444	1.44	173.82	<.0001
Aeration	3	0.097	0.032	3.89	0.0178
Correction	1	0.016	0.016	1.97	0.1702

Table 12. REGWQ test grouping for mean mixing times obtained with (Y) and without (N) correction for conductance data. Means with the same letter are not significantly different.

Grouping	Mean	N	Correction
A	2.164	24	N
A	2.128	24	Y

Graphs of mixing time (Figures 16-18) data display a pattern of decreased mixing times with increased agitation rates.

The study for comparing methods for determining mixing time was factorial in design. The three treatment factors were: method of determination (Tables 13-15, Figures 16-18), agitation rate and aeration rate. Upon initial observation, the data did not fit within the rules of homoscedasticity and normality. Several transformations were tested, but all showed two outliers present which skewed the data. To meet the standards of homoscedasticity and normality, the two outliers were removed. The outliers were from data points taken during the color changer method at 338 rpm and 0.00 vvm. Using Proc GLM and a square root transformation, the table of Least Sum of Squares revealed that the method and agitation rate were the only significant factors affecting mixing time (Table 16).

REGWQ Test showed that mixing times were significantly different when comparing the pH and Conductance methods (Tables 17 and 18). Mixing time was less under 500 rpm than 338 rpm. Mixing times were similar under all aeration rates (Table 19).

Video from studies using the color method revealed flow patterns found in the 3 L reactor. Figure 19 and 20 show the progression of the color change after the acid was inserted. The change from purple to yellow first occurs in the bottom of the tank. The last region to become yellow is the upper –right quadrant.
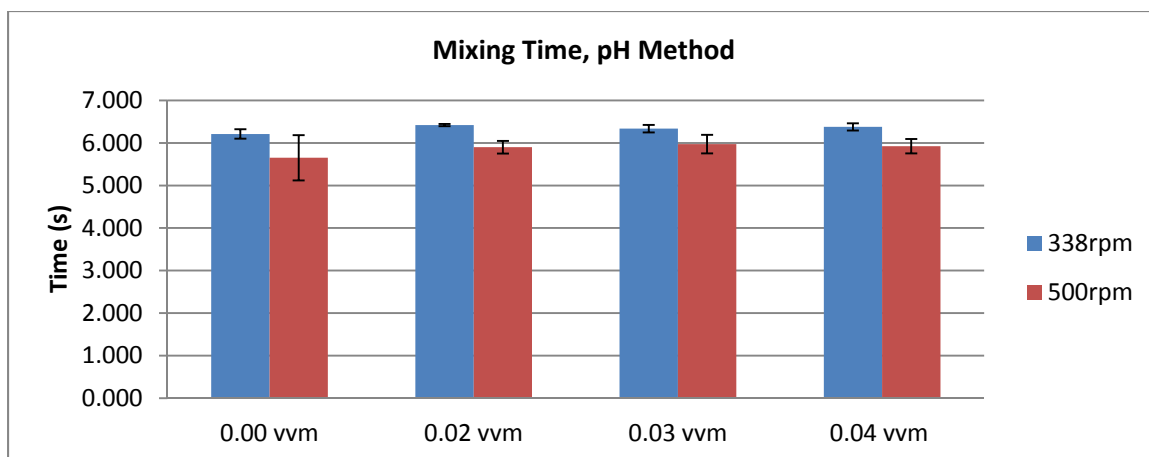
Figure 16.Mixing time results using the pH tracer method in the 3 L reactor.
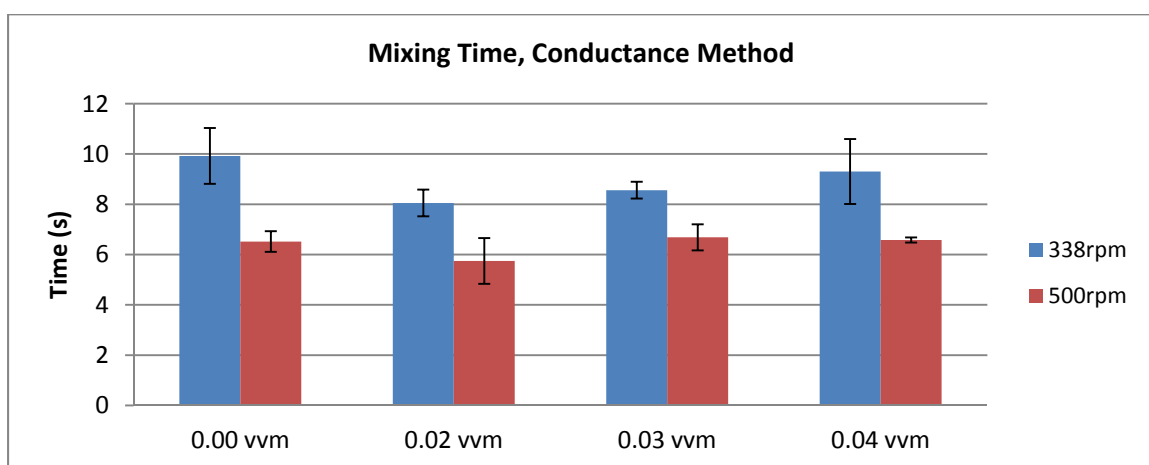
Figure 17.Mixing time results using the conductance tracer method in the 3 L reactor.
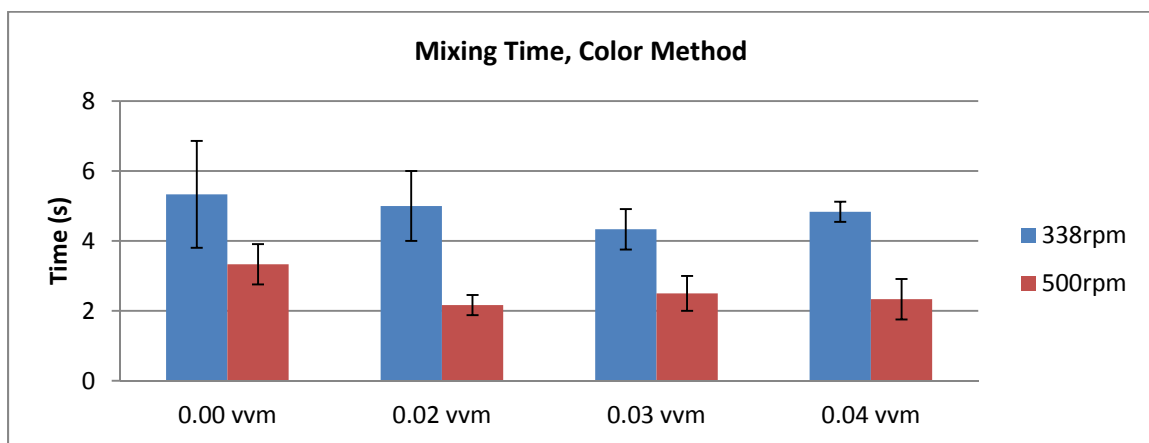
Figure 18.Mixing time results using the color tracer method in the 3 L.

Table 13. Average mixing times (s) using the pH method.

	0.00 vvm		0.02 vvm		0.03 vvm		0.04 vvm	
	Ave	Stdev	Ave	Stdev	Ave	Stdev	Ave	Stdev
338 rpm	6.21	0.11	6.42	0.03	6.34	0.09	6.38	0.09
500 rpm	5.65	0.53	5.90	0.15	5.97	0.22	5.92	0.17

Table 14. Average mixing times (s) using the conductance method.

	0.00 vvm		0.02 vvm		0.03 vvm		0.04 vvm	
	Ave	Stdev	Ave	Stdev	Ave	Stdev	Ave	Stdev
338 rpm	9.92	1.11	8.05	0.53	8.56	0.33	9.30	1.29
500 rpm	6.52	0.41	5.75	0.91	6.68	0.52	6.58	0.10

Table 15. Average mixing times (s) using the color method in the 3 L.

	0.00 vvm		0.02 vvm		0.03 vvm		0.04 vvm	
	Ave	StDev	Ave	StDev	Ave	StDev	Ave	StDev
338 rpm	5.33	1.53	5.00	1.00	4.33	0.58	4.83	0.29
500 rpm	3.33	0.58	2.17	0.29	2.50	0.50	2.33	0.58

Table 16. Results for mixing studies in the 3 L obtained using the GLM procedure. R^2 value of 0.86. Sources with a Pr value < 0.05 have a significant effect on mixing time.

Source	DF	Type III SS	Mean Square	F Value	Pr> F
Method	2	9.147	4.573	255.34	<0.001
Agitation	1	2.713	2.713	151.46	<0.001
Method*Agitation	2	0.822	0.411	22.94	<0.001
Aeration	3	0.167	0.056	3.10	0.035
Method*Aeration	6	0.237	0.039	2.20	0.059
Agitation*Aeration	3	0.045	0.015	0.83	0.484
Method*Agitation*Aeration	6	0.091	0.015	0.85	0.539

Table 17. REGWQ test for mean mixing time values for pH, conductance and color methods in 3 L. Means with the same letter are not significantly different.

Grouping	Mean	N	Method
A	2.756	24	Conductance
B	2.469	24	pH
C	1.898	24	Color

Table 18. REGWQ test for mean mixing time values for agitation rates of 338 and 500rpm in 3 L. Means with the same letter are not significantly different.

Grouping	Mean	N	RPM
A	2.568	36	338
B	2.180	36	500

Table 19. REGWQ test for mean mixing time values for aeration rates of 0, 0.02, 0.03 and 0.04vvm in 3 L. Means with the same letter are not significantly different.

Grouping	Mean	N	Aeration
A	2.12465	16	0
A	2.10632	18	0.04
A	2.03769	18	0.02
A	2.02598	18	0.03
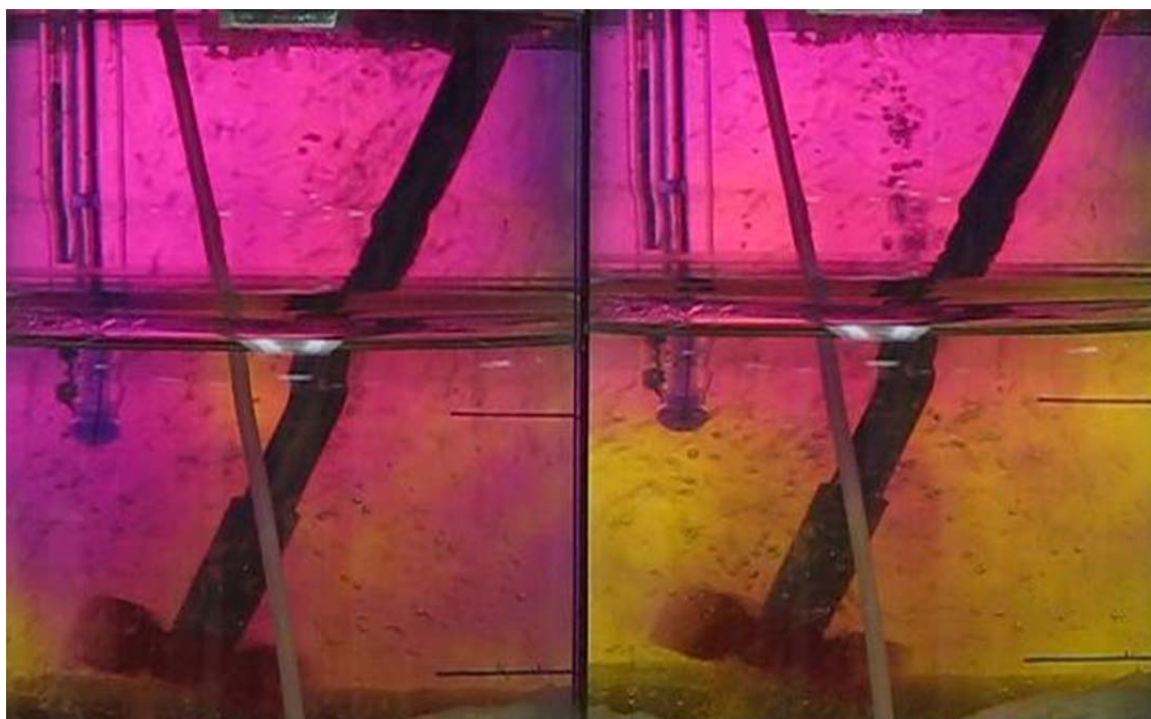
Figure 19. Images of the 3 L reactor after HCl was added during the color tracer method for mixing time determination. Time progression is from left to right. Reactor conditions are at 500 rpm and 0.04 vvm.
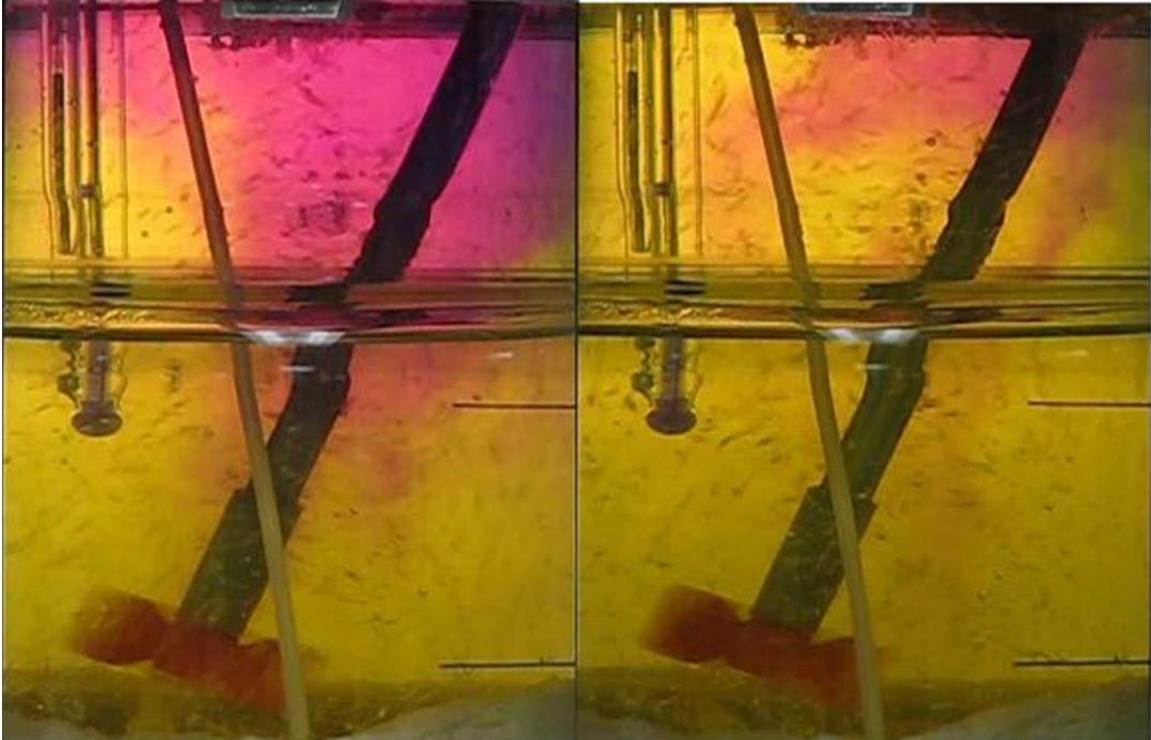
Figure 20. Images of the 3 L reactor using the color tracer method. Time progression is from left to right. Reactor conditions are at 500rpm and 0.04 vvm.

4.1.2   Large-Scale Studies

In order to decrease the amount of testing parameters, it was decided to confirm if aeration rate was a statistically significant factor affecting mixing time in the larger reactors. Aeration rates of 0.00, 0.02, 0.03 and 0.04 vvm were tested at agitation rates of 145 (Constant P_g/V) and 150 (Constant N) rpm in the 100 L SUB. Results were analyzed in SAS based on the parameters of aeration rate, constant maintained, and probe location. Without any transformation, the rules of normality and homoscedasticity were met, and the model fit the data with an R^2 value of 0.69.

Using Proc GLM, the Least Sum of Squares revealed the probe location was the only significant factor effecting mixing times in the 100 L SUB (Table 20). Therefore, the mixing time studies for the rest of the SUB vessels were tested with an aeration rate of 0.03 vvm.

Table 20. Results for mixing studies in the 100 L obtained using the GLM procedure. Sources with a Pr value < 0.05 have a significant effect on mixing time.

Source	DF	Type I SS	Mean Square	F Value	Pr> F
Constant	1	33.208	33.208	0.93	0.3452
Aeration	3	10.085	3.362	0.09	0.9623
Constant*Aeration	3	24.075	8.025	0.23	0.8777
Probe Location	2	1163.335	581.667	16.34	<.0001
Constant*Probe	2	45.376	22.688	0.64	0.5387
Aeration*Probe	6	82.887	13.815	0.39	0.8784
Aeration*Probe*Constant	6	277.958	46.326	1.3	0.2997

The data for all mixing studies were evaluated in SAS, observing parameters of vessel volume, scale-up constant and probe location (Table 21). The data did not require a transformation and fit rules for normality and homoscedasticity. The model fit the data with an R^2 value of approximately 0.94. The Least Sum of Squares revealed all three parameters to be statistically significant, with significant interactions between volume and constant, volume and probe location, and the three-way interaction of all parameters.

Table 21. Results for mixing studies in all bioreactors obtained using the GLM procedure. Sources with a Pr values < 0.05 have a significant effect on mixing time.

Source	DF	Type I SS	Mean Square	F Value	Pr> F
Volume	6	2492.018	490.336	19.67	<.0001
Constant	1	32.468	32.468	1.3	0.2612
Volume*Constant	6	1586.121	264.354	10.61	<.0001
Probe	2	5126.144	2563.072	102.84	<.0001
Volume*Probe	9	1813.798	201.533	8.09	<.0001
Constant*Probe	2	207.265	103.63	4.16	0.0237
Volume*Constant*Probe	9	1569.391	174.377	7	<.0001

In order to better visualize the statistical differences of each parameter, the data was analyzed using the REGWQ test method. The results of this test showed the three smallest reactors (3, 50 and 100 L) to have the fastest mixing times (Table 22). The 3 L reactor was significantly faster than all other reactors. The larger reactors had slower mixing times, and although there were variations between each, these differences were not statistically

significant, except in the 250 L vessel. N values are lower for the 1000 and 3 L bioreactors

because there were only two probes in the 1000 L (top and bottom), and only one probe in the 3

L (middle).

Unlike in the k_La studies, the scale-up constant did not have a significant effect on

mixing times in the SUBs (Table 23). The top probe results were statistically slower than the

times given by the probes in the middle and bottom of the vessels (Table 24). Average mixing

times calculated using the conductance tracer method are given in Table 25.

Table 22. REGWQ test for mean mixing time values for vessel volumes of 3, 50, 100, 250, 500, 1000 and 2000 L. Results with the same grouping letter are not significantly different.

Grouping			Mean	N	Volume
A			35.17	12	250
A	B		30.403	12	500
A	B		30.198	8	1000
A	B		28.92	12	2000
	B	C	26.119	12	50
		C	21.235	12	100
		D	7.758	4	3

Table 23. REGWQ test for mean mixing time values for scale-up constants of P_g/V and Shear. Means with the same grouping letter are not significantly different.

Grouping	Mean	N	Constant
A	28.099	36	Shear
A	26.756	36	P_g/V

Table 24. REGWQ test for mean mixing time (s) values for probe locations of top, middle and bottom of the vessel. Means with the same grouping letter are not significantly different.

Grouping		Mean	N	Constant
A		40.015	24	Top
	B	22.313	24	Middle
	B	19.954	24	Bottom

Table 25. Average mixing times (s) determined using the conductance tracer method.

	Scale-up Constant	
	P/V	Shear
Volume (L)	Mixing Time (s), (rpm)	Mixing Time (s), (rpm)
3	8.75±0.8%, (338)	6.765±11%, (500)
50	26.99±46%, (169)	25.25±53%, (186)
100	22.32±47%, (145)	20.15±42%, (150)
250	34.82±36%, (118)	35.52±26%, (109)
500	21.34±20%, (100)	39.46±21%, (87)
1000	38.40±52%, (87)	22.00±55%, (68)
2000	26.55±61%, (75)	31.29±71%, (55)

4.2 Results for K_La Studies

4.2.1 Method Verification Studies

Results from uncorrected and corrected data, with respect to probe response time, were analyzed in SAS to determine statistical differences. After applying a square-root transformation to normalize the data and removing two outliers,[1] the results for the Least Sum of Squares as well as REGWQ were used to interpret the data (Table 26 and 27).

Table 26. Results for kLa studies obtained using the GLM procedure. Results had an R^2 value of 0.979. Sources with a Pr value < 0.05 have a significant effect on kLa.

Source	DF	Type I SS	Mean Square	F Value	Pr> F
Agitation	1	12.28	12.28	474.47	<.0001
Aeration	2	48.08	24.04	928.63	<.0001
Probe Location	2	2.80	1.40	54.07	<.0001
Correction	1	0.77	0.77	29.72	<.0001

Table 27.REGWQ test grouping for mean k_La values obtained with (Y) and without (N) correction. Means with the same letter are not significantly different.

Grouping	Mean	N	Correction
A	3.35926	54	Y
B	3.18957	52	N

---

[1] Outliers from data set 338 rpm, 0.03 vvm, no correction

Both the Sum of Squares and the REGWQ imply the k_La values obtained from the corrected data are significantly different. It was then assumed that the corrected data was most accurate, and the following results are for the corrected data only.

Figure 21 shows the data collected during k_La studies show a trend of increasing k_La with increasing aeration and agitation rates. Figure 22 reveals the effect of probe position on k_La.

The study for determining k_La was assumed to be factorial in design. The three treatment factors were: agitation rate, aeration rate and probe location. Upon initial observation, the data did not fit within the rules of heteroscedasticity and normality. A square root transformation was therefore used to pull in some moderate outliers, resulting in an R^2 value of 0.96. Using Proc GLM, the table of Least Sum of Squares revealed that agitation rate, aeration rate and probe location effected k_La (Table 28).
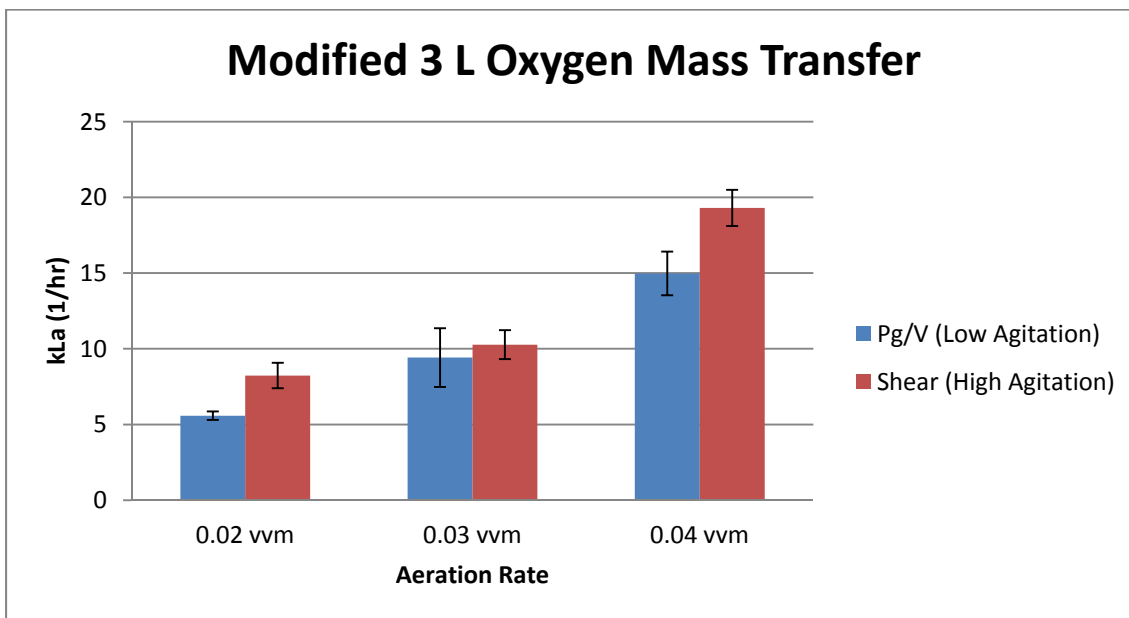

Figure 21. Graph of the effects of aeration and agitation on k_La.
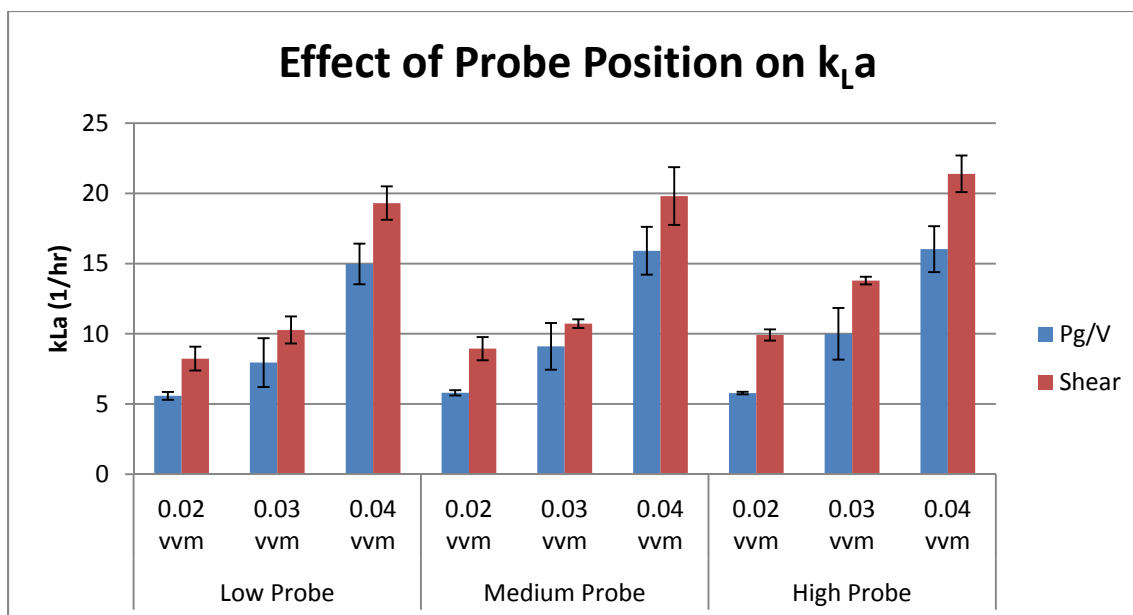
Figure 22. Graph of the effect of probe placement on $k_L a$ in the 3 L reactor.

Table 28. Results for corrected $k_L a$ studies obtained using the GLM procedure. Results had an R^2 value of 0.96. Sources with a Pr value < 0.05 have a significant effect on $k_L a$.

Source	DF	Type I SS	Mean Square	F Value	Pr> F
Agitation	1	3.92	3.92	128.18	<.0001
Aeration	2	21.94	10.97	358.99	<.0001
Agitation*Aeration	2	0.05	0.02	0.74	0.4836
Probe	2	0.75	0.37	12.23	<.0001
Agitation*Probe	2	0.10	0.05	1.58	0.22
Aeration*Probe	4	0.25	0.06	2.01	0.1134
Agitation*Aeration*Probe	4	0.06	0.02	0.51	0.7319

Groupings using the REGWQ test were used to reveal statistical differences in the data. The average $k_L a$ value obtained in studies running at 500rpm was significantly higher than that obtained at 338 rpm (Table 29). Similarly, $k_L a$ values were notably higher under 0.04 vvm than at 0.03 and 0.02 vvm (Table 30). The $k_L a$ values at 0.03 vvm were significantly higher than those achieved at 0.02 vvm. Results for probe location revealed that $k_L a$ increases as the probe location is raised from the bottom of the tank (Table 31). Table 32 shows the average $k_L a$ values obtained at each probe location. Table 33 gives the average $k_L a$ values for the 3 L vessel.

Table 29. REGWQ test grouping for mean corrected k_La values obtained for 338 and 500 rpm. Means with the same letter are not significantly different.

Grouping	Mean	N	RPM
A	3.62858	27	500
B	3.08994	27	338

Table 30. REGWQ test grouping for mean corrected k_La values obtained for 0.02, 0.03 and 0.04 vvm. Means with the same letter are not significantly different.

Grouping	Mean	N	VVM
A	4.21941	18	0.04
B	3.16272	18	0.03
C	2.69561	18	0.02

Table 31. REGWQ test grouping for mean corrected k_La values obtained for probe positions 0.25H, 0.50H and 0.75H. Means with the same letter are not significantly different.

Grouping	Mean	N	RPM
A	3.50685	18	High
B	3.35203	18	Mid
C	3.21890	18	Low

Table 32.Mean values for test repetitions of k_La (1/hr) methods in 3 L.

		Low Probe		Middle Probe		High Probe	
		Average	StDev	Average	StDev	Average	StDev
338rpm	0.02 vvm	5.89	1.27	6.31	1.25	6.16	0.19
	0.03 vvm	7.91	2.28	8.12	0.63	9.68	0.29
	0.04 vvm	16.55	2.07	18.02	2.65	19.22	3.91
500rpm	0.02 vvm	8.86	1.30	9.55	0.89	10.67	0.60
	0.03 vvm	11.03	1.41	12.31	0.31	15.46	0.90
	0.04 vvm	22.88	2.37	24.40	2.56	24.65	1.49

Table 33. Average k_La (1/hr) values for 3 L.

	0.02vvm		0.03vvm		0.04vvm	
	Average	StDev	Average	StDev	Average	StDev
338rpm	6.12	0.215	8.57	0.966	17.93	1.335
500rpm	9.69	0.914	12.93	2.282	23.98	0.958

4.2.2   Large-Scale Studies

Data collected for the large-scale reactors were corrected for probe response time before being analyzed in SAS. Time constants τ_1 and τ_2 for the Broadley James DO probe were 12.8551 and 12.8546 seconds, respectively.

To normalize the data and have it fit the rules of homoscedasticity, a negative inverse transformation was applied and two outliers were removed.[2] Results of PROC GLM Least Sum of Squares revealed all factor levels to significantly affect $k_L a$ values (Table 34).

Table 34. Results for corrected $k_L a$ studies obtained using the GLM procedure. R^2 value of 0.99.
Results with Pr> 0.05 have a statistically significant effect on $k_L a$.

Source	DF	Type III SS	Mean Square	F Value	Pr> F
Volume	7	0.087	0.012	517.6	<.0001
Scale-up Constant	1	0.001	0.002	67.27	<.0001
Volume*Constant	7	0.011	0.002	63.3	<.0001
Aeration	2	0.105	0.052	2182.87	<.0001
Volume*Aeration	14	0.015	0.001	45.79	<.0001
Constant*Aeration	2	0.000	0.000	4.77	0.0106
Volume*Constant*Aeration	14	0.003	0.000	9.3	<.0001

Table 35-37 show results from the REGWQ test for vessel volume, scale-up constant and aeration, respectively. A duplicate study was run in the 250 L reactor in order to determine the reproducibility of the results. The 250 L reactor was chosen for the duplicate study as it is of medium volume and was available for extended use. The REGWQ test for the factor Volume shows that the $k_L a$ values achieved in the 3 L were significantly higher than those attained in the other vessels. Conversely, the $k_L a$ values for the 50 L were significantly lower. The high values in the 3 L were likely attained due to errors in applying proper air flow. The small sparge volumes required in the 3 L were below the standard capability of the Biotron's flow meter. Thus the aeration rates had to be roughly measured, and accurate repeatability was low. The lower

---

[2] Outliers were from 3 L data set, 338 rpm and 0.03 vvm

values in the 50 L are likely a result of its smaller than average dispersion volume. The duplicate

studies performed in the 250 L reactor were revealed to be statistically different. However, the

difference was slight and could be the result of having different probe calibrations. Studies

maintaining constant P_g/V achieved higher k_La values than those runs, which held shear

constant, and as with the 3 L studies, k_La increased with increased aeration rates.

From the scale-up studies it was found that k_La could be maintained upon an increase in

volume by maintaining P_g/V or shear constant.

Table 35. REGWQ test grouping for mean corrected k_La values obtained for tested vessel volumes. Means with the same letter are not significantly different. Volume 250.2 represents the duplicate runs in the 250 L.

Grouping			Mean	N	Volume
A			-0.104	16	3
	B		-0.125	18	1000
		C	-0.132	18	250
		C D	-0.134	18	2000
		C D	-0.136	18	500
		D	-0.137	18	250.2
		D	-0.139	18	100
		E	-0.199	18	50

Table 36. REGWQ test grouping for mean corrected k_La values obtained for scale-up constants. Means with the same letter are not significantly different.

Grouping		Mean	N	Constant
A		-0.136	70	P_g/V
	B	-0.142	72	Shear

Table 37. REGWQ test grouping for mean corrected k_La values obtained for aeration rates of 0.02, 0.03 and 0.04vvm. Means with the same letter are not significantly different.

Grouping			Mean	N	Aeration
A			-0.108	48	0.04
	B		-0.135	46	0.03
		C	-0.174	48	0.02

A plot of the data in Microsoft Excel reveals the k_La values for the 3 L to be significantly higher than the other volumes (Figure 23). This drastic difference is most likely due to the difference in probe position in the 3 L reactor compared with the larger vessels. The probe in the 3 L reactor was positioned much closer to the sparger and impeller. Thus, the probe was exposed to a higher gas concentration, even before thorough mixing, and is therefore expected to see higher k_La values. On the other hand, k_La values in the 50 L are shown to be considerably lower than the values obtained from all the other reactors. The plot also confirms the increase in k_La with increasing aeration rate, and that higher k_La values are achieved when P_g/V is held constant rather than shear upon scale-up.
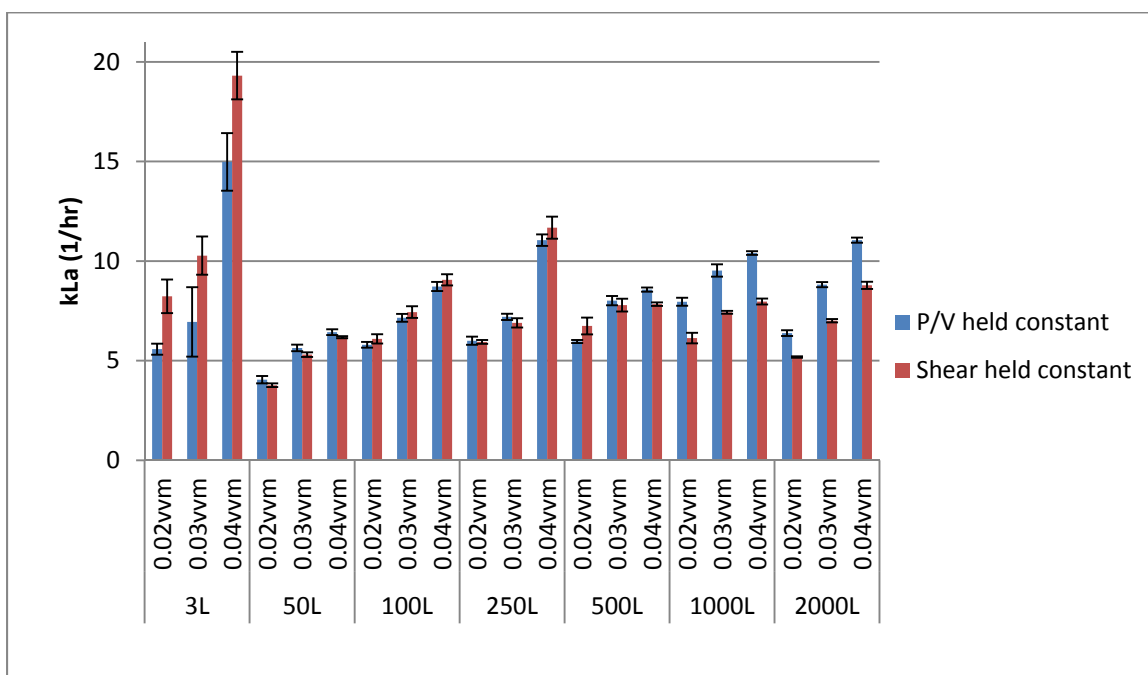

Figure 23. Graphical plot of average k_La values obtained during scale-up studies. Results shown are for aeration rates of 0.02, 0.03 and 0.04vvm.

4.3   Computational Fluid Dynamics

4.3.1   Mass Transfer and Aeration Results

Results calculated in CFD were found to be significantly lower than k_La values obtained in experimental studies. The k_La model of the 250 L SUB at 118 rpm, with a frit aeration rate of 0.01 vvm and an open pipe flow of 0.008 vvm, and a bubble diameter of 9mm was calculated to be 2.2/hr. Therefore it was concluded that the models were unable to accurately predict the physics and are not capable of estimating mass transfer within the SUBs.

Figure 24 is a depiction of the predicted pathlines of air as calculated using CFD. Unexpectedly, the image shows the air hitting the impeller before being pushed back down to the bottom of the vessel. Literature on this phenomenon has been varied. Figure 24 appears to reveal a lack of air in the area behind the impeller shaft, an event which was also observed during experimental studies in the 3 L modified glass vessel.
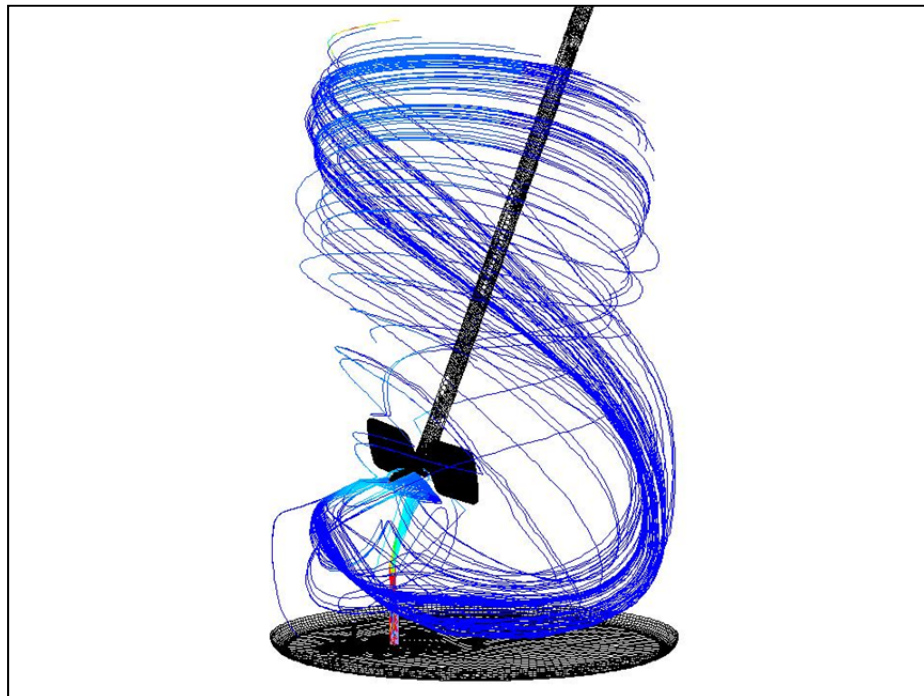

Figure 24.Pathlines of air released from large sparger for 250 L SUB at 118 rpm (Spall et al., 2010).

4.3.2   Mixing Results

Velocity fields calculated using CFD found the fluid directly surrounding the impeller to have the highest velocity. This result is not unexpected in a stirred-tank reactor, and can be seen in Figure 25. Spall's CFD models showed the formation of large cavities on the impeller were present at the tested mixing rates. As cavity tests were not run during experimental studies, further work would need to be performed to verify his findings. Fluid rotation in the tank is centered about the impeller, but at the tested rotation rates did not significantly affect the shape of the free surface, suggesting the angle of the impeller shaft was sufficient in breaking up the rotational flow, which could have led to poor mixing.
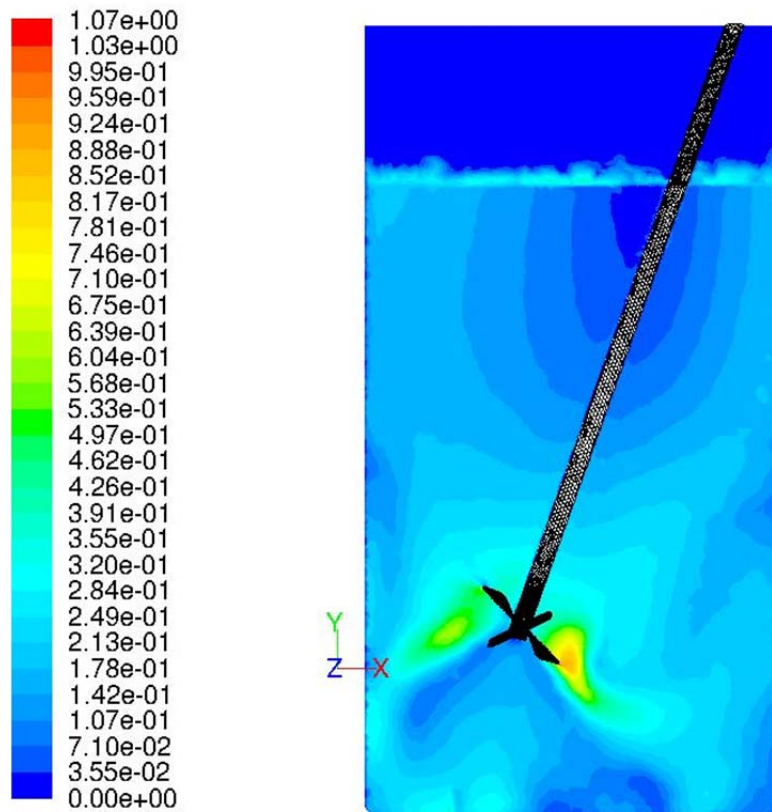

Figure 25. Contours of velocity magnitude for 250 L SUB at 118rpm (Legend units in m/s; Spall et al., 2010).

Results for mixing times calculated by CFD are shown in Table 38. Figures 26 and 27 compare the experimental and calculated results. It appears that the calculated mixing times are very similar to experimental results up to the 250 L vessel. Differences in calculated and experimental mixing times for the 500, 1000 and 2000 L vessels are shown to be substantially different in Figure 26. However, calculated results at constant shear agitation rates are only considerably different in the 2000 L reactor.

Table 38. Computed mixing times at various impeller speeds (Spall et al., 2010).

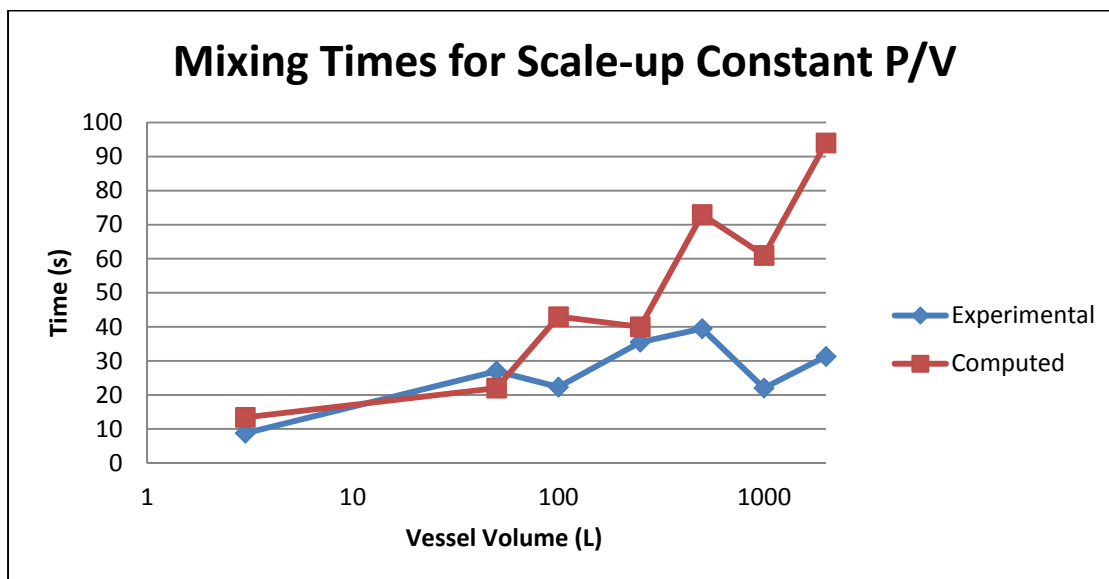| Volume (L)	Low Speed Mixing Time (s)	Mid Speed Mixing Time (s)	High Speed Mixing Time (s)
3	13.4 (338)	10.3 (400)	8.7 (500)
50	51 (100)	22 (169)	18 (213)
100	43 (100)	25 (149)	21 (183)
250	40 (100)	30 (118)	21 (149)
500	73 (70)	31 (101)	23 (128)
1000	61 (70)	44 (97)	38 (110)
2000	91 (60)	76 (74.5)	48 (94)

Figure 26. Graph of the differences in calculated and experimental mixing times for constant P_g/V studies.
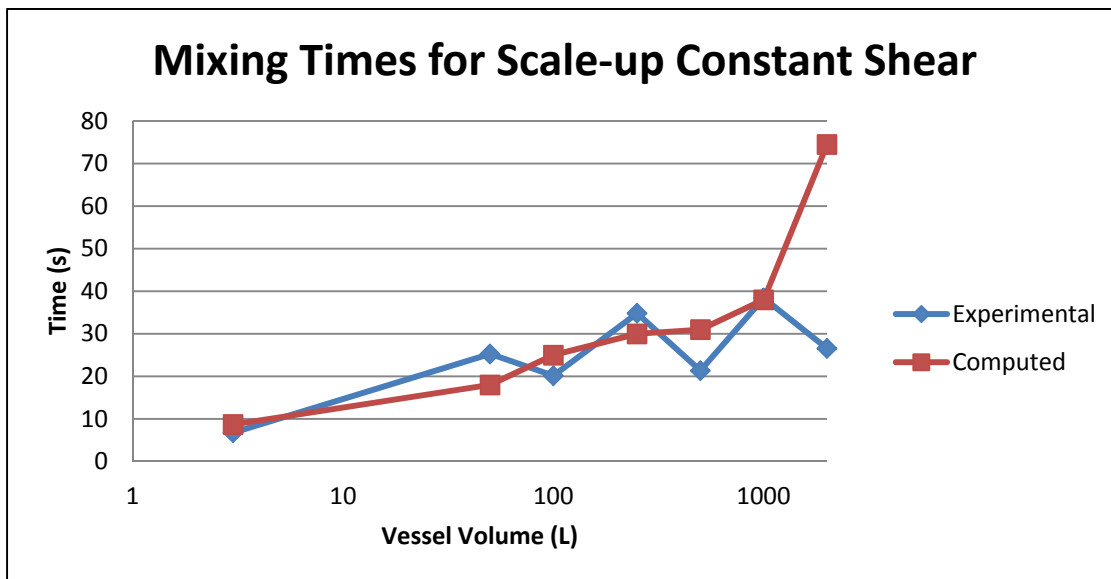
Figure 27. Graph of the differences in calculated and experimental values for constant shear studies.

4.4   Uncertainty Analysis

In order to understand the accuracy of the experimental results, an uncertainty analysis was performed on the k_La results. The Broadly James DO sensor probes claim to accurately read dissolved oxygen within 2-5% of the full scale. Since no experiments were performed to confirm the claim, it was assumed the sensor had a maximum uncertainty of 5% DO. The data acquisition device used to collect DO values is reported to be accurate within 6 seconds, which over the average run means an uncertainty of 1.7%.

For the approximations of the first and second order partial differential equations, a repeated measurement from the same probe in the same experiment was used. Thus, a precision uncertainty analysis is required. Precision uncertainty is calculated by multiplying the confidence interval by a Gaussian correlation of its standard deviation, and divided by the number of samples squared. This is shown in Equation 43:

$$U = z_{c/2}\left(\frac{\sigma}{\sqrt{n}}\right) \tag{43}$$

where $z_{c/2}$ is the z-distribution for a confidence c on a standard normal curve, σ is the standard

deviation, and n is the number of samples (Beckwith et al., 1993).

To approximate the uncertainty of the partial derivatives the standard deviation was

calculated based on Beckwith et al.'s definition of 'maximum error' as ±3.29σ. Based on this

definition the standard deviations of the probe readings is 2.04% DO (Beckwith et al., 1993).

Additionally, the average error between the step function and the corrected step response was

found to be 4.05% (Davis et al., unpublished data). The need for such corrections to the probe

response time suggests the $k_L a$ rates calculated from the raw measurements are under-

estimating the true potential of the oxygen mass transfer within the system.

CHAPTER 5

MODELING OXYGEN MASS TRANSFER

5.1   Conceptual Studies of Model Development

Suggested models for k_La determination are generally based on two factors: gas dispersion or mixing and oxygen availability. Past researchers have applied a dispersion term to their models, which is meant to incorporate vessel and impeller geometry as well as agitation rates. The energy input models use P_g/V, assuming energy input directly relates to mixing efficiency. Yawalkar et al. (2002b) used their relative gas dispersion term (N/N_{cd}), which they determined to be proportional to turbulence intensity. Those who used dimensionless numbers relied on Reynold's Number and agitation rates (N) to model mixing conditions in the reactors. As seen in Equation 18, N_{cd} is directly proportional to Q, which in turn makes k_La inversely proportional to Q. Thus k_La should decrease upon increasing Q, which is contrary to the experimental results. Due to this contradiction, P_g/V is a better candidate than the N/N_{cd} term for use in this study.

Oxygen mass transfer also relies on oxygen availability, which implies the need of an aeration term to be used in the predictive equation. Most historic models have used superficial velocity (v_g) to account for aeration in the vessel. In order to visualize the concept of k_La being directly proportional to v_g, as is seen in both the energy input models and the gas dispersion models, imagine two vessels of equal volume. The first is an infinitely wide and shallow vessel, while the second is correspondingly narrow and deep (Figure 28).
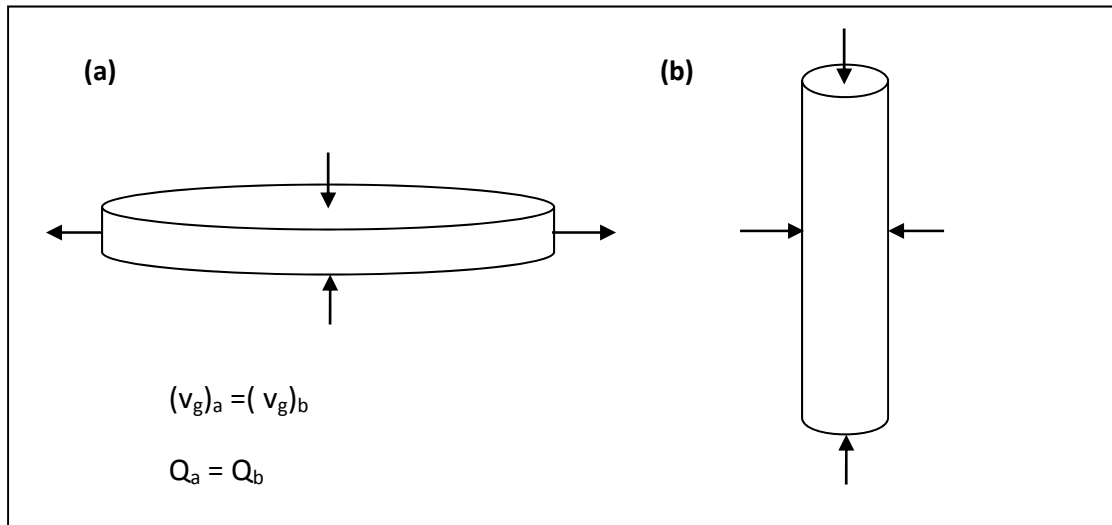
Figure 28. Depiction of an (a) infinitely wide and an (b) infinitely narrow vessel.

Assume the vessels are well mixed and are aerated at a gas flow rate (Q) of 0.01 vvm. Therefore if:

$$v_g = \frac{Q}{A} \qquad (44)$$

v_g would approach zero as $(D_t)_a$ increases and conversely would approach infinity as $(D_t)_b$ decreases. If one were then to assume that k_La is proportional to v_g then k_La would change accordingly. Yet if these tanks are of equal volume, are well mixed and are being aerated at the same rate, their mass transfer rates should also be equal.

Physical factors must also be considered when scaling up equipment volume. The volume of a batch will increase as a cubic function, whereas the escape velocity of air is a function of the square of the diameter (Bartholomew, 1960). By maintaining a constant air volume per batch volume ratio (vvs), the air flow rate will increase linearly while superficial air velocity increases exponentially, as shown in Figures 29 and 30, respectively. The gas flow number Fl_G used in the dimensionless equation also increases exponentially (Figure 31).

Since the gas flow number also fails to increase at a linear rate upon scale-up, it was not chosen as a method for measuring aeration in this study. The gas flow number appears to mistakenly include the diameter of the impeller (Equation 22), yet the air flow should not be affected by the diameter of the impeller as much as it would be related to the diameter of the vessel. This contradiction was another reason Fl_G is not seen as the ideal measurement of aeration for predicting k_La.
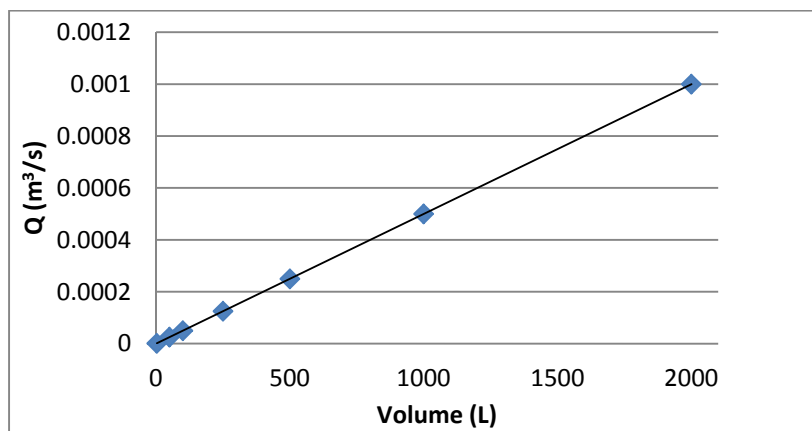

Figure 29. Air flow rate (Q) is shown to increase linearly upon scale-up. Values were calculated from maintaining flow rates of 0.03vvm.
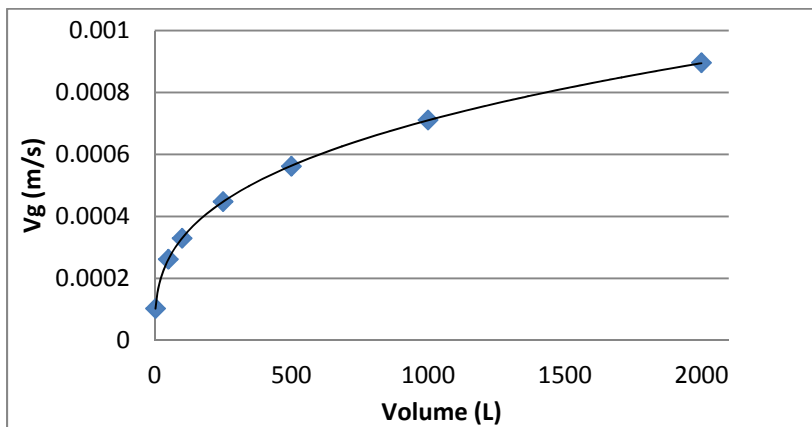

Figure 30. Air velocity (v_g) is shown to increase at an exponential rate upon scale-up. Values were calculated for maintaining flow rates of 0.03vvm.
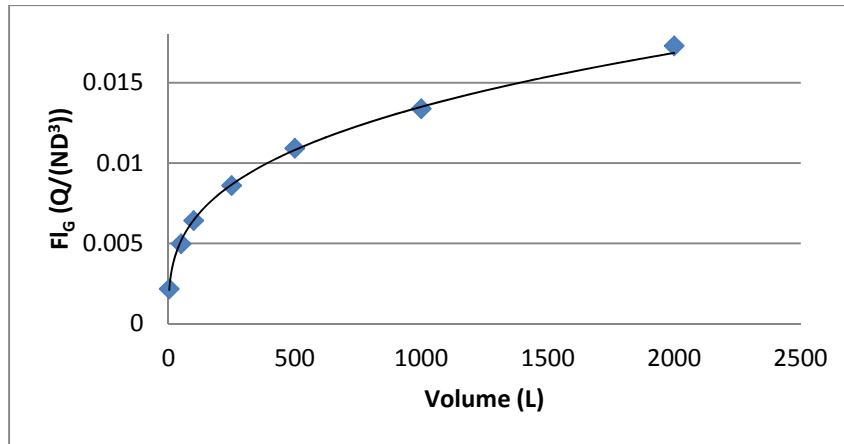
Figure 31. Gas flow number (Fl_G) is shown to increase at an exponential rate upon scale-up. Values were calculated for maintaining flow rates of 0.03 vvm.

5.2 Comparing Historic Models

After experimental results were obtained and evaluated, the data was fit to commonly used models based on energy input (Equation 1 and Equation 16), gas dispersion (Equation 44) and dimensionless numbers (Equation 45).

$$k_L a = K' \left(\frac{P_g}{V} \right)^\alpha v_g^{\;\beta} \tag{1}$$

$$k_L a = K' \left(\frac{P_g}{V} \right)^\alpha \left(\frac{Q}{V} \right)^\beta \tag{16}$$

$$k_L a = K' \left(\frac{N}{N_{cd}} \right)^\alpha \left(v_g \right)^\beta \tag{41}$$

$$k_L a = K' \left(Fl_G \right)^\alpha \left(\mathrm{Re} \right)^\beta \left(N \right) \tag{42}$$

As each model contains multiple independent variables, MathCad version 15.0 software (© 2010 Parametric Technology Corporation, MA) was used for curve fitting and coefficient determination. The constants K', α and β were determined for each model under constant P_g/V

and again under constant shear at 0.03 vvm of air flow. Figure 32 is an example of the codes used for determining unknowns K', α and β.

The constants calculated by MathCad were usually more than a degree of magnitude less than values found by past researchers (Smith et al., 1977; Smith and Warmoeskerken, 1985; Yawalkar et al., 2002). As past studies used fermentors with much higher agitation and aeration rates, the coefficients found for these studies were acceptable. Applying the obtained coefficients results in the following equations for three of the historic models: energy input (Equation 43), gas dispersion (Equation 44) and dimensionless numbers (Equation 45):

$$k_L a = 4.347 \times 10^{-3} \left(\frac{P_g}{V} \right)^{0.438} \left(v_g \right)^{0.185} \tag{43}$$

$$k_L a = 9.915 \times 10^{-3} \left(\frac{N}{N_{cd}} \right)^{0.025} \left(v_g \right)^{0.200} \tag{44}$$

$$k_L a = 3.725 \times 10^{-3} \left(Fl_G \right)^{0.839} \left(\mathrm{Re} \right)^{0.251} \left(N \right) \tag{45}$$

With the new constants, the models appeared to fit the data fairly well with average errors of 23.0, 21.1, and 16.4%, respectively. While each of these methods sufficiently predicts $k_L a$, the Moresi and Patete model (Equation 16) was determined to be the most conceptually sound and is explored in the following section.
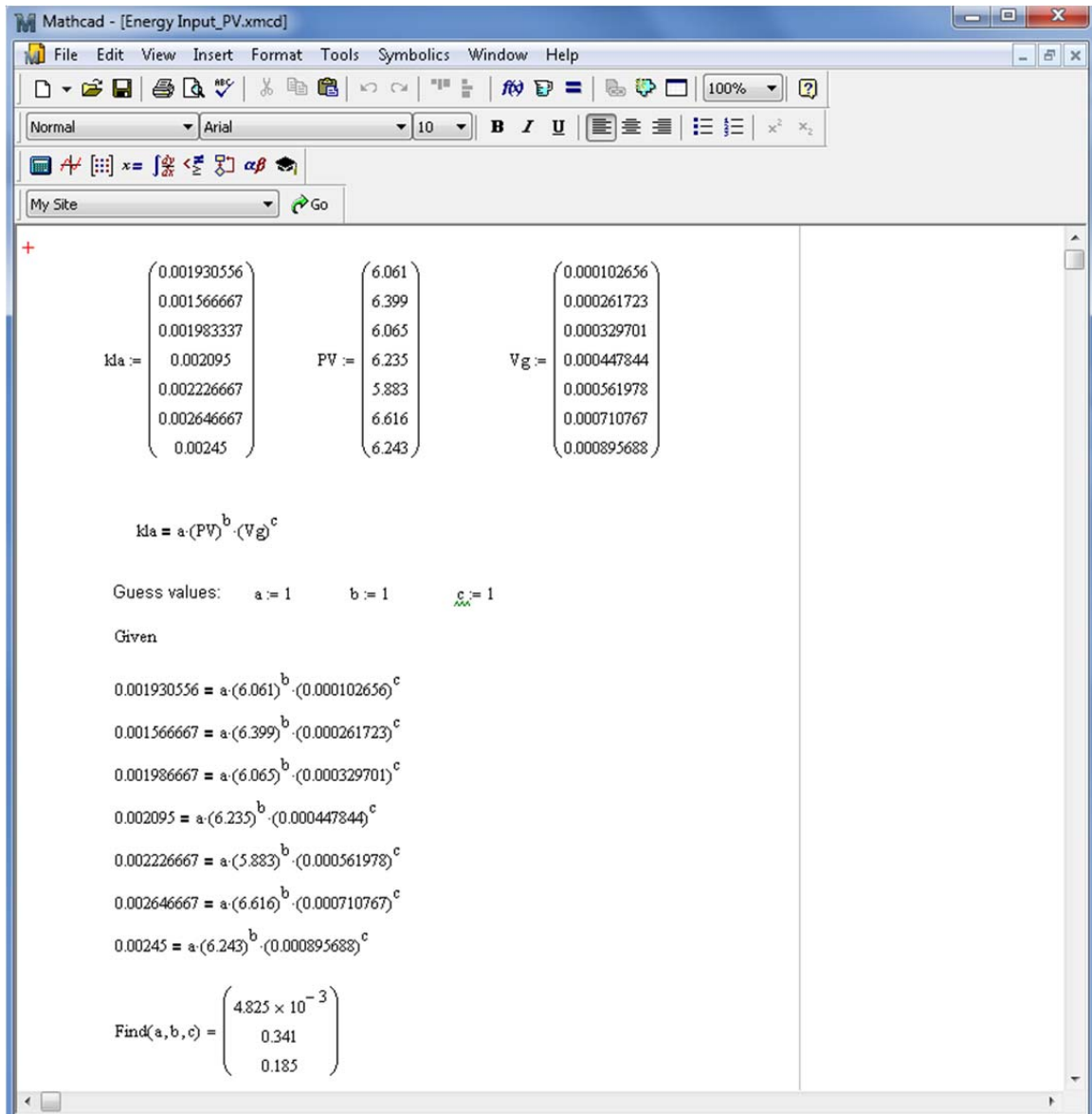
Figure 32. Example MathCad code to determine unknowns K', α and β (a, b, c respectively) using data obtained under constant P_g/V at 0.03 vvm of air.

5.3   Developing the Moresi and Patete Model

After reviewing the past literature and conceptual models, the model by Moresi and Patete (1988)was used to correlate the experimental data, using a mixing term of power to volume and an aeration term of volume of air per volume of liquid (Equation 46).

$$k_L a = K' \left(\frac{P_g}{V} \right)^{\alpha} (vvs)^{\beta} \tag{46}$$

Constants K', α, and β of Equation 50 were determined using MathCad version 15.0 software.

The values of K', α, and β were determined to be 1.182, 0.297, and 0.896, respectively.

$$k_L a = 1.182 \left(\frac{P_g}{V} \right)^{0.297} (vvs)^{0.896} \tag{47}$$

When analyzed in Microsoft Excel, these constants resulted in a model with an average error of

19.7%, which is within the range of error found in the three previously tested historic models.

Figures 33-36 show detailed views of the model and how it corresponds to the experimental

data. The experimental data collected under constant P_g/V is shown in blue and the data

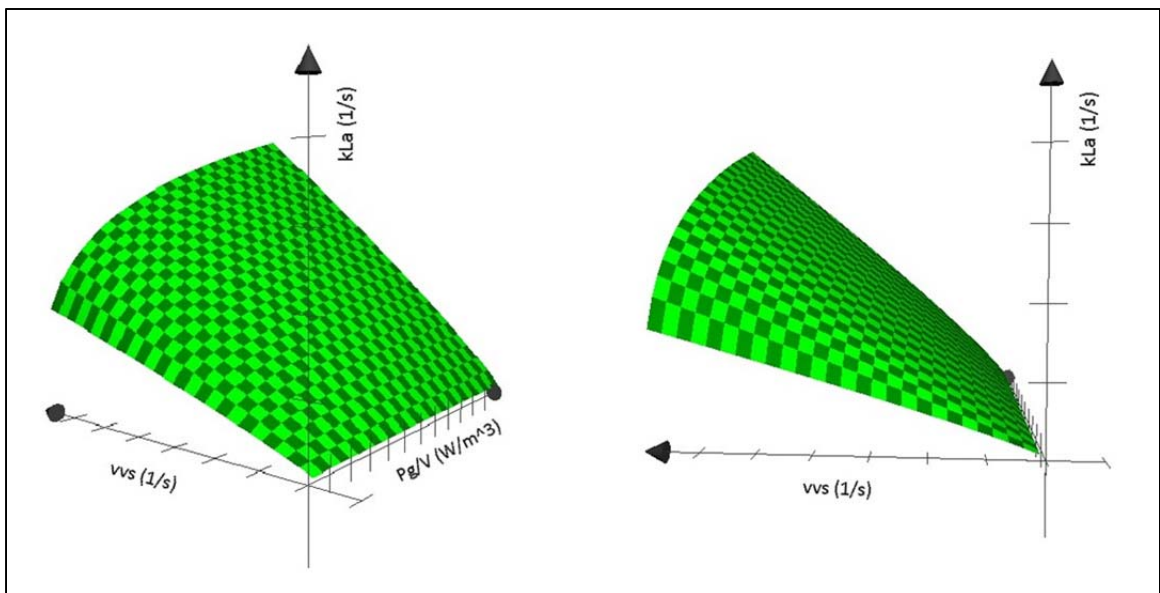collected under constant shear is shown in red. The green surface represents Equation 47.

Figure 33. Surface plots of Equation 47, which estimates the value of kLa (0.000-0.002 s^{-1}) given Pg/V (0-25 W/m^3) and vvs (0.00-0.0007 sec^{-1}).
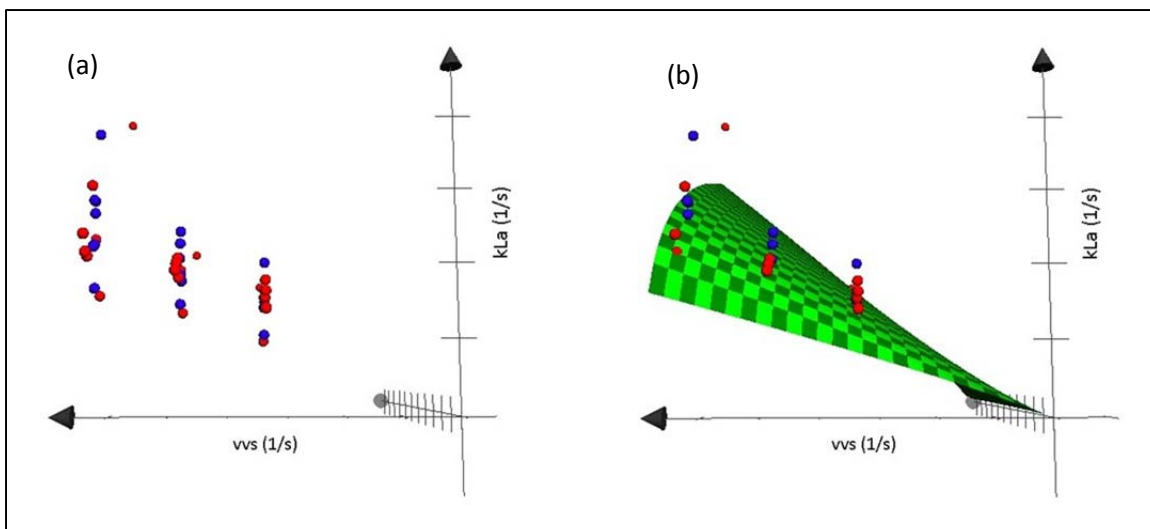
Figure 34. (a) Scatter plot of experimental data (b) Correlating model plot for Equation 47.
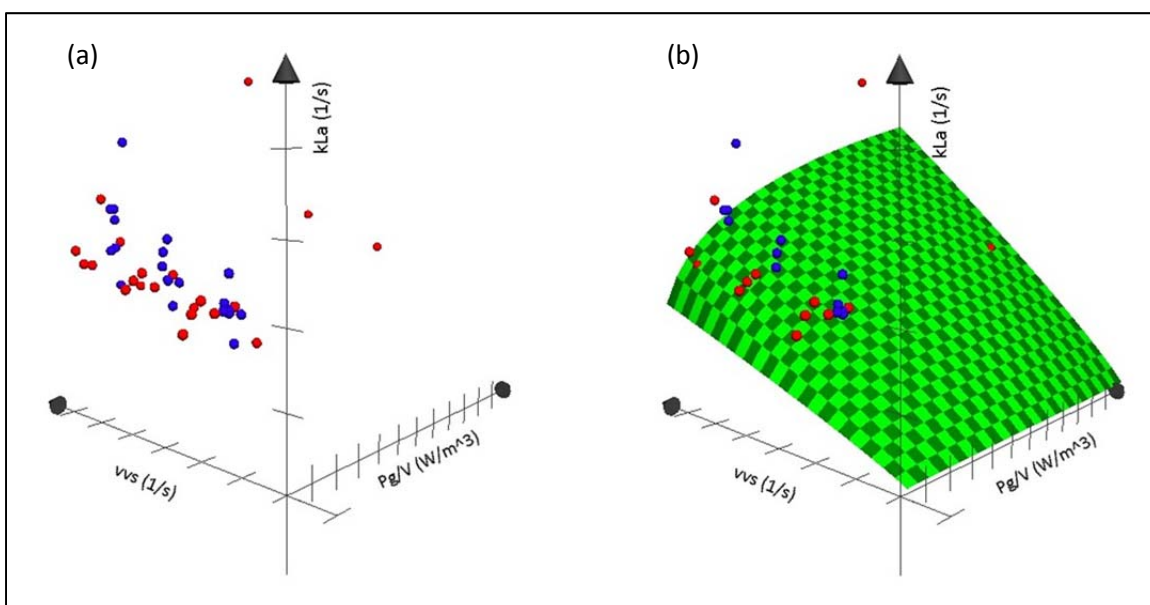

Figure 35. (a) Scatter plot of experimental data (b) Correlating model plot for Equation 47.
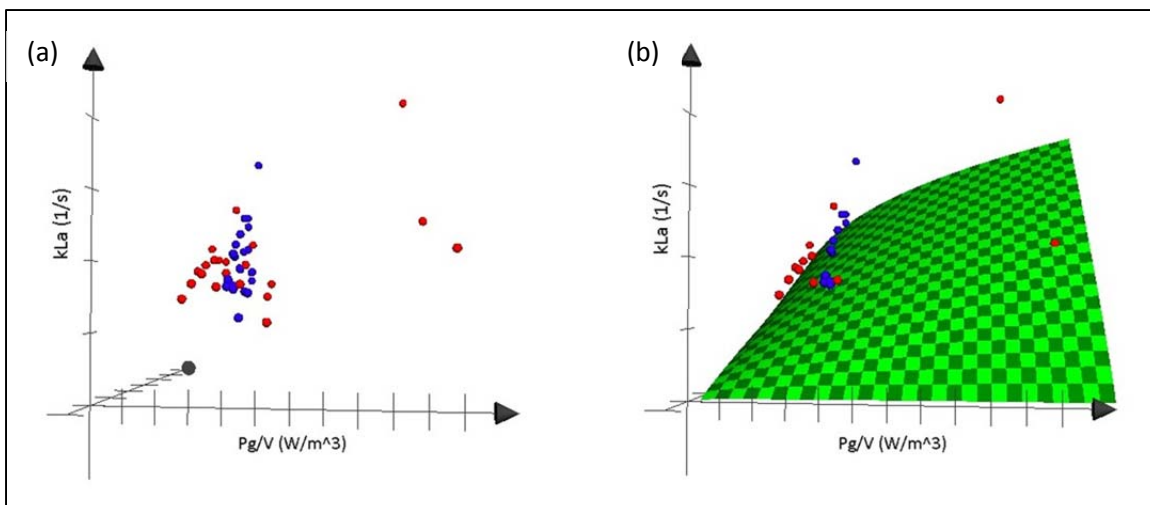
Figure 36. (a) Scatter plot of experimental data (b) Correlating model plot for Equation 47.

On a two-dimensional scale, it is easy to see the large deviations between the model and experimental data for the 3 and 50 L bioreactors (Figures 37 and 38). If the 3 L and 50 L data sets were to be removed, the average error would drop to 9%. However, Figure 39 reveals the model to still be a good fit despite its errors.

Figure 37. Two-dimensional graphical comparison of the experimental model derived from Equation 47 and experimental data obtained using scale-up constant P_g/V.

Figure 38. Two-dimensional graphical comparison of the experimental model derived from Equation 47 and experimental data obtained using scale-up constant shear.
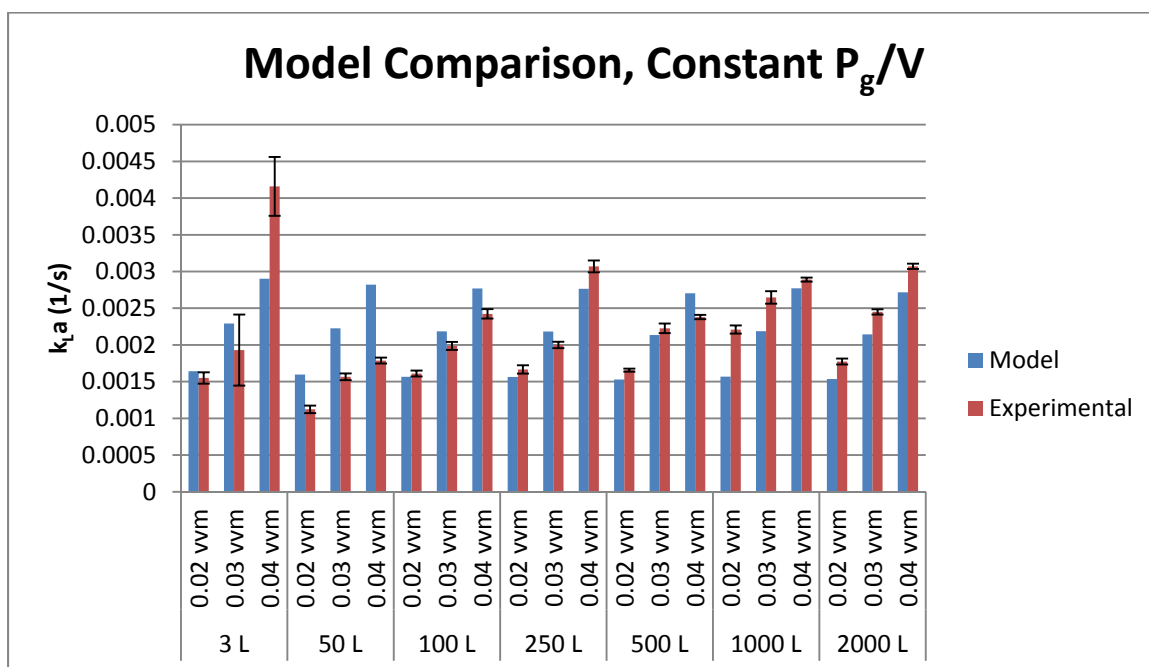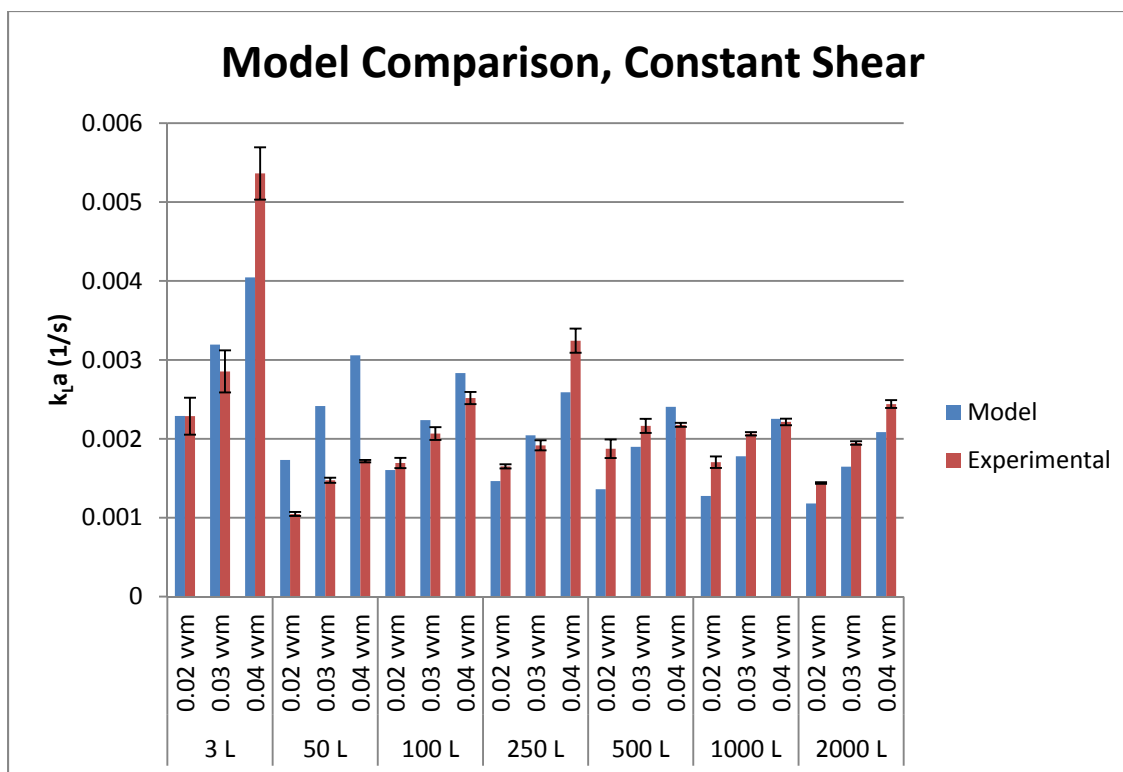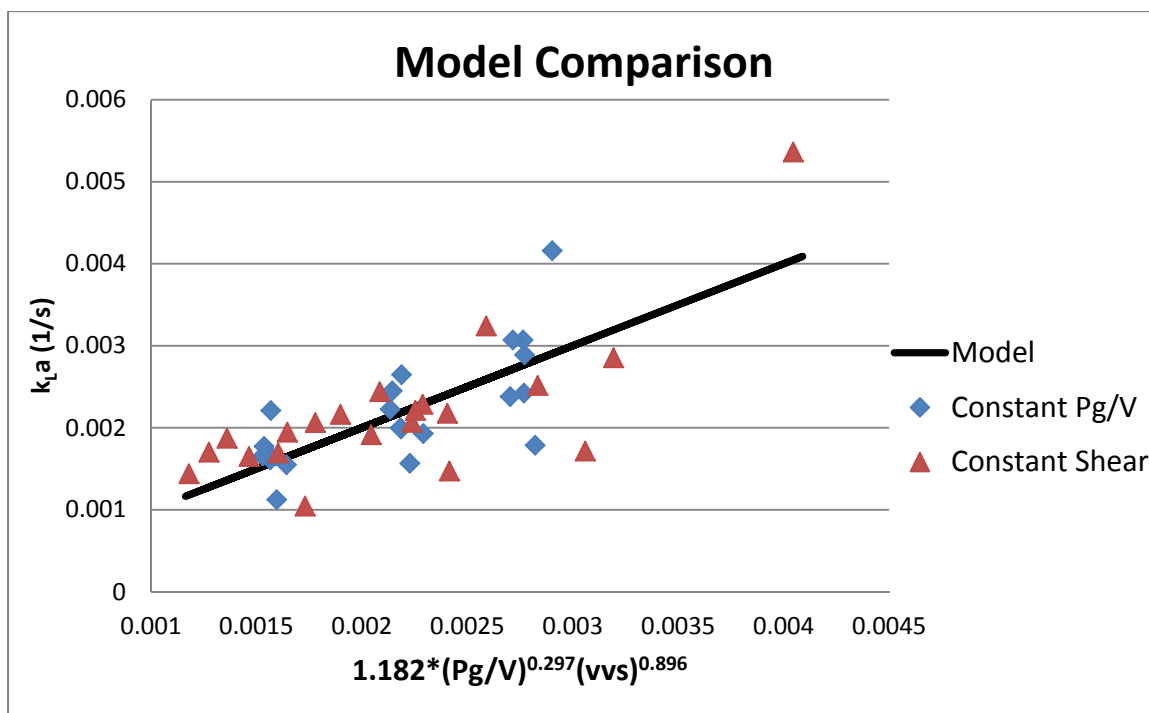

Figure 39. Experimental values compared to the model derived from Equation 47.

Although the model was a good fit, the large errors in the 3 and 50 L data were examined further. In Chapter 3 Table 8, dispersion ratios were calculated for each impeller. Some impellers, specifically the 50 L impeller, were found to have significantly lower or higher dispersion ratios than other vessel volumes. To determine if this finding would account for the deviations, the power term was adjusted as follows:

$$P_g = P \cdot 0.1 \left(\frac{Q}{NV} \right)^{-1/4} \left(\frac{N^2 D^4}{g W V^{2/3}} \right)^{-1/5} \left(\frac{\text{Vessel}\left(V_d / V_t\right)}{\text{Average}\left(V_d / V_t\right)} \right) \qquad (48)$$

Equation 51 multiplies the power term by a correction factor, which compares the vessel dispersion ratio with the average dispersion ratio. Thus, the predicted $k_L a$ values will be lower for vessels with below average dispersion volumes due to smaller impellers. Similarly, vessels with above average dispersion volumes will have higher predicted $k_L a$ values. Tables 39 and 40 compare the calculated P_g/V for each vessel with the new corrected values.

Table 39. Comparison of P_g/V values with and without correction using constant P_g/V. The correction factor is equal to the quotient of the vessel dispersion ratio and the average dispersion ratio.

Vessel Size (L)	Correction Factor	P_g/V			Corrected P_g/V		
		0.02 vvm	0.03 vvm	0.04 vvm	0.02 vvm	0.03 vvm	0.04 vvm
3	0.965	7.407	6.693	6.229	7.149	6.460	6.011
50	0.867	6.731	6.082	5.660	5.838	5.275	4.909
100	1.038	6.317	5.708	5.312	6.559	5.927	5.516
250	1.075	6.287	5.681	5.286	6.758	6.107	5.683
500	1.038	5.829	5.267	4.902	6.053	5.470	5.090
1000	1.026	6.340	5.729	5.331	6.506	5.879	5.471
2000	0.990	5.923	5.352	4.981	5.861	5.296	4.929

Table 40. Comparison of P_g/V values with and without correction using constant shear. The correction factor is equal to the quotient of the vessel dispersion ratio and the average dispersion ratio.

Vessel Size (L)	Correction Factor	P_g/V			Corrected P_g/V		
		0.02 vvm	0.03 vvm	0.04 vvm	0.02 vvm	0.03 vvm	0.04 vvm
3	0.965	22.641	20.458	19.038	21.850	19.744	18.374
50	0.867	8.837	7.986	7.431	7.665	6.926	6.446
100	1.038	6.833	6.174	5.746	7.095	6.411	5.966
250	1.075	5.042	4.556	4.239	5.420	4.897	4.558
500	1.038	3.931	3.552	3.306	4.082	3.688	3.432
1000	1.026	3.157	2.853	2.655	3.240	2.927	2.724
2000	0.990	2.432	2.198	2.045	2.407	2.175	2.024

New constants for Equation 50were determined using MathCad (version 15.0) software. When using the corrected P_g/V values in MathCad, K', α, and β were found to be 1.049, 0.332, and 0.888, respectively.

$$k_L a = 1.049 \left(\frac{P_g}{V} \right)^{0.332} (vvs)^{0.888} \tag{49}$$

When analyzed in Excel, these values resulted in an average error of 19.1%. Thus, the correction method does not appear significant at these power ranges. Both models showed $k_L a$ to be much more dependent on aeration than on power input. As the power ranges tested in this study were so small, the changes due to the correction seem insignificant. Figures 40 and 41 give a two-dimensional view of the model derived from Equation 49, with corrected P_g/V values.
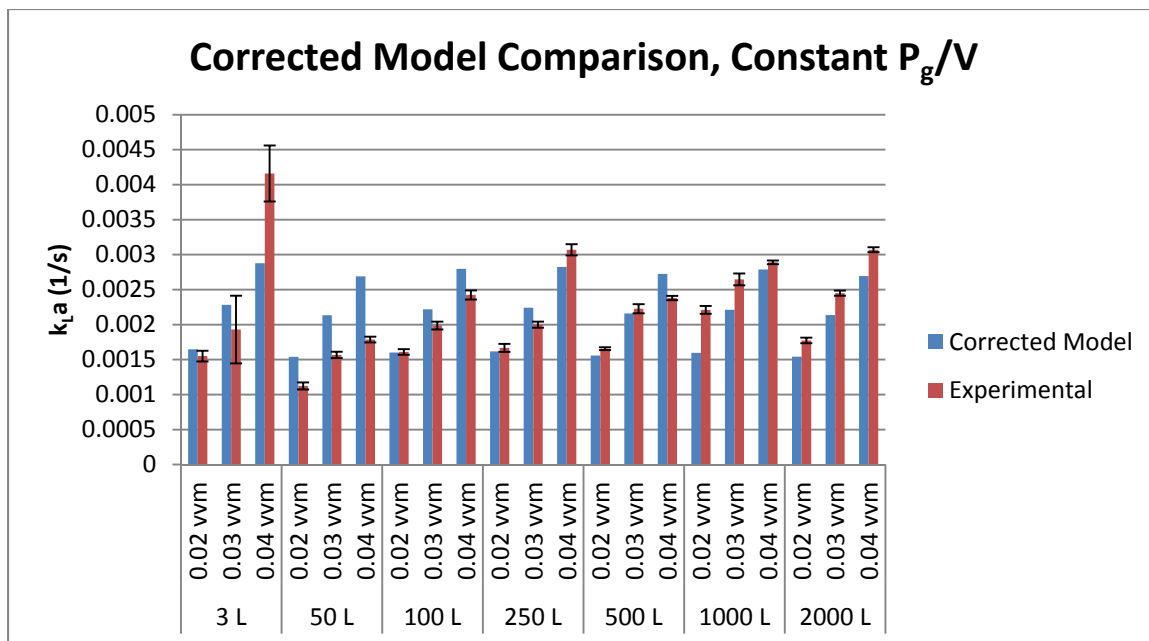
Figure 40. Graphical comparison of the corrected model derived from Equation 49, and experimental data obtained using scale-up constant P_g/V.
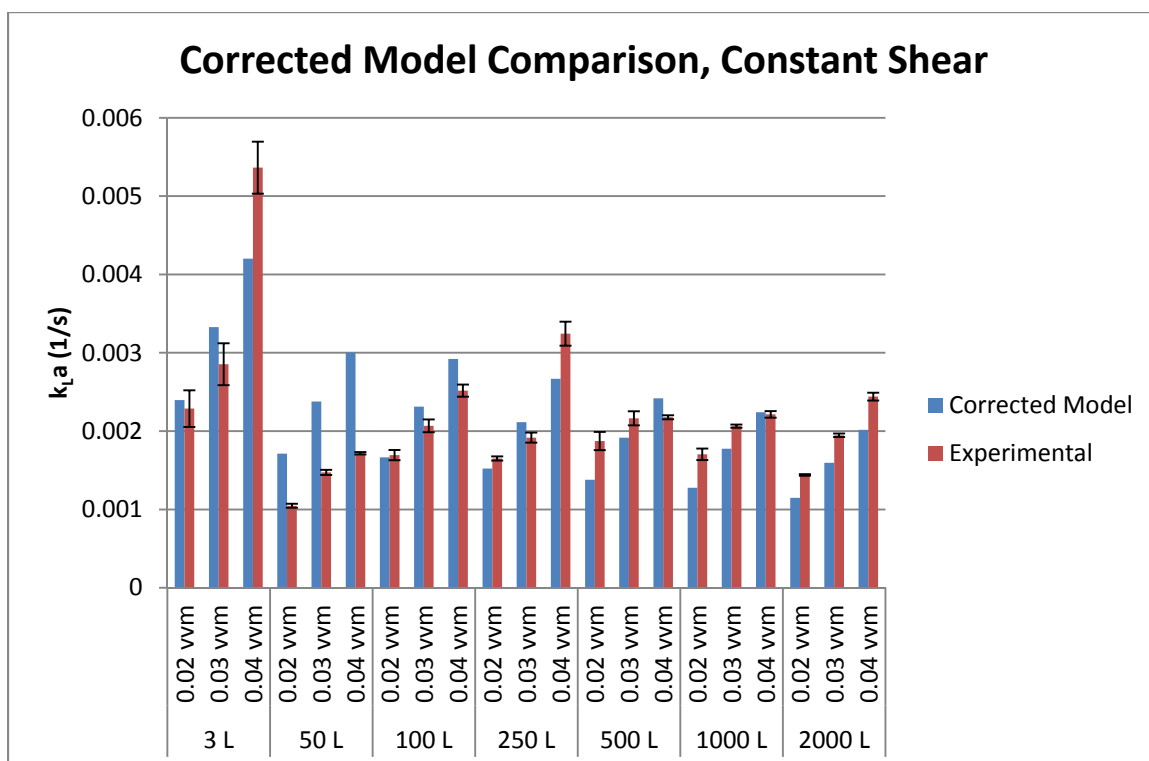

Figure 41. Graphical comparison of the corrected model derived from Equation 49, and experimental data obtained using scale-up constant shear.

In both developed models, the greatest deviations occurred with data collected from the 3 and 50 L reactors. The error in the 3 L data is most likely due to human error in calibrating air flow. The 3 L reactor was so small that air flow rates of 0.02 vvm, which is equal to 60 mL/min, which became difficult to apply accurately. Deviations in the 50 L reactor could also be the result of a smaller volume of dispersion to volume of liquid ratio despite the attempt to correct this difference with Equation 51. The errors in the 50 L data could also be due to its proximity to the outlying 3 L data. The high 3 L values could significantly distort the model and cause the lower 50 L values to appear less accurate. Because the three liter reactor was not built exactly like the production models of 50 to 2000 liters and used a different dissolved oxygen probe and data acquisition system, it was decided to examine the data excluding the data collected from the 3-liter system. The new coefficients K', α, and β determined after removing the 3 L data were 0.474, 0.085, and 0.730, respectively.

$$k_L a = 0.474 \left(\frac{P_g}{V} \right)^{0.085} \left(vvs \right)^{0.730} \tag{50}$$

When compared to the experimental data, excluding the 3 L outliers, the average error rate was 15.8%. Figure 42 is a graphical representation of Equation 50. Figures 43 and 44 compare the experimental data with the predicted values derived from Equation 50.
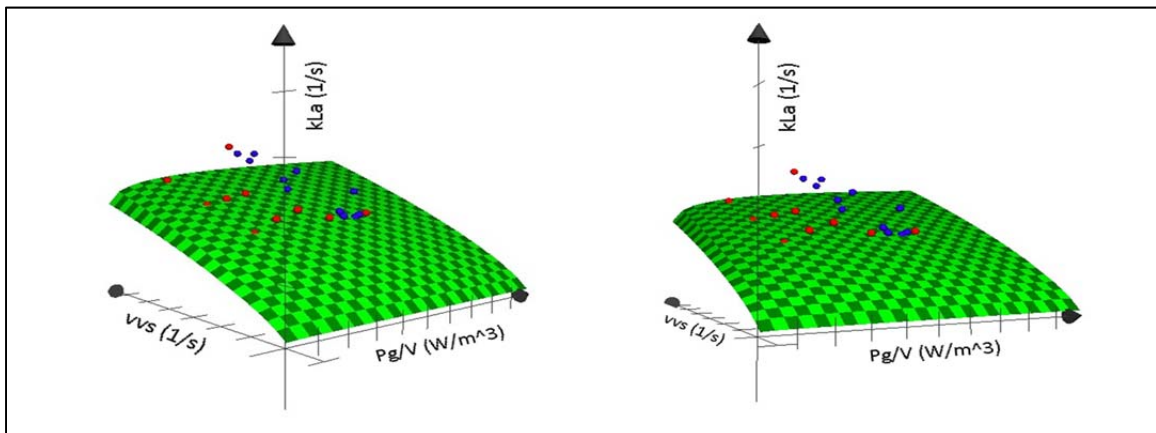

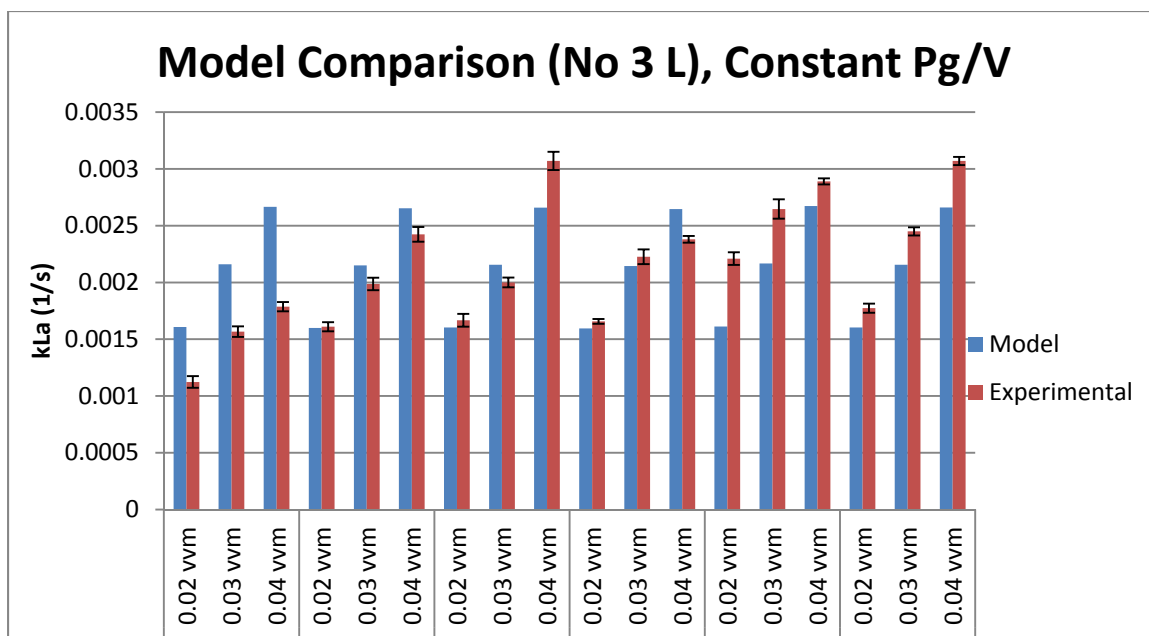Figure 42. Graphical representation of Equation 50, which excludes the outlying 3 L data.

Figure 43. Graphical comparison of the corrected model derived from Equation 50, and experimental data obtained using scale-up constant P_g/V.
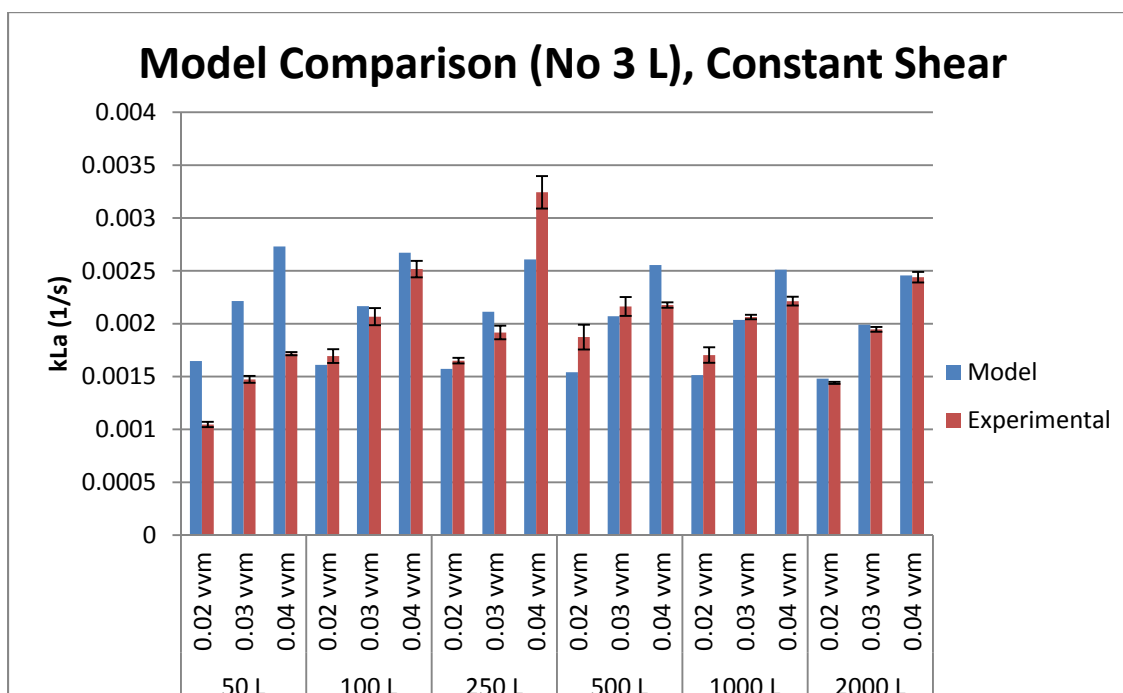

Figure 44. Graphical comparison of the corrected model derived from Equation 50, and experimental data obtained using scale-up constant shear.

CHAPTER 6

CONCLUSIONS

The results on probe response data showed corrected data to be significantly different than uncorrected data with respect to dissolved oxygen probes. Thus, all $k_L a$ results were corrected to account for lag response times in the dissolved oxygen probes. The conductance probes used for mixing studies did not require correction for lag response time.

Mixing studies performed in the 3 L reactor revealed the conductance tracer method to give the slowest mixing times with respect to the pH and color tracer methods. The conductance method was used to measure mixing time in the larger vessels for safety reasons. It would have been difficult to handle the large amounts of acid solution required to make the pH change in the larger vessels. Likewise, the color method would have been impossible to use in the single-use systems, which were all incased in stainless steel housings.

As expected, lower agitation rates resulted in slower mixing times. Probe position was another significant factor in mixing, with probes placed at the bottom of the tank measuring the fastest mixing times. Probes located at the top of the tank recorded the slowest mixing times. This pattern is likely the result of the downward pumping action of the elephant-ear impeller, as well as better mixing occurring near the impeller. The response times also parallel the mixing zones seen in the color tracer studies performed in the 3 L, in which the lower regions achieved homogenization before the upper regions.

The low aeration rates tested, from 0.02-0.04 vvm, did not significantly affect mixing times. However, volume was a significant factor affecting mixing time with the smallest reactor (3 L) achieving the fastest time. Surprisingly, the 250 L achieved the slowest time. This is most likely due to human error, with regard to introducing the salt solution, and likely would not be a trend if further studies were performed. It is possible the salt solution was entered at a slower

rate, or may have been prepared incorrectly, resulting in a solution of lower molarity. The fast

mixing times in the 1000 and 2000 L reactors may also have been affected by the amount of salt

solution required to achieve the needed conductance change. The 1000 L and 2000 L vessels

required 10 and 20 L of salt solution, respectively. The large amounts of solution made it

difficult to input the liquid into a concentrated area as was done in the smaller vessels. Instead,

the salt solutions were quickly dumped into the top of the reactors and were therefore

introduced into a larger area, which likely impacted the mixing conditions within the systems.

Results from k_La studies indicate that k_La will increase with increasing agitation and

aeration rates. Results also imply that the low probe position (probe aligned with impeller) used

in k_La studies measured lower k_La values than the average mass transfer value for the entire

volume. These low values are likely due to the low agitation rates, which fail to adequately

disperse the gas before it rises. Thus, sufficient aeration most likely occurs after

homogenization has occurred and the dissolved oxygen has reached the bottom of the tank.

When reviewing the results of using the two scale-up constants, constant P_g/V and

constant shear, it was found that scaling-up based on P_g/V resulted in slightly higher k_La values

in the larger vessels. Therefore, if a higher k_La is needed, scale-up could rely on a constant

P_g/V as long as the cells are not shear sensitive. The models however, do show k_La relies less on

power input and more on aeration. Increasing aeration rates to the system could therefore also

increase KLa.

When these studies were performed, there were four principle models used for

predicting k_La upon scale-up. Each model was compared to the experimental data in MathCad

to determine coefficients that would match the geometries and range of parameters used. The

power input method that used superficial air velocity was found to have an average error of

23%. The dimensionless numbers model showed an average error of 16.4%. Lastly, the model

based on gas dispersion had an average error of 21%when compared with the experimental data. After reviewing three of the four principle models; the model (Equation 46) developed by Moresi and Patete (1988) was fit to the experimental data. With an average error of 19.7%, this model is believed to satisfactorily estimate $k_L a$ in single-use systems and to be the most conceptually accurate model. The correction factor, accounting for differences in dispersion volumes, was then incorporated into the model resulting in Equation 49. The average error obtained from the corrected model was 19.1%. The large $k_L a$ values found in the 3 L data were considered outliers, and new coefficients were determined by excluding the 3 L data from the calculations. This last model was found to have an average error of 15.8%.

The results of this study were for ranges of aeration rates (0.02-0.04 vvm) and agitation rates (P_g/V range of 2-20 W/m^3) that are commonly used in single-use bioreactor systems. In order to further increase the knowledge of oxygen transfer and mixing times in disposable bioreactors gained in this work, studies should be performed which expand the agitation and aeration rates tested.

CHAPTER 7

FUTURE RESEARCH

In order to enhance the results found in this study, the test parameters need to be expanded. By expanding the power and aeration ranges studied, further insights to the physiological trends upon scale-up could be achieved. The results obtained could then be used to supplement the data used in making the mathematical correlations for predicting $k_L a$.

The results of the mixing studies appear to be erroneous due to human error in maintaining parallel protocols upon scale-up. In order to correct this problem, it would be beneficial to establish a new protocol to study mixing times which can be used easily across all vessel volumes. By obtaining more accurate results, a better understanding of the mixing conditions can be determined.

REFERENCES

Aiba S, Humphrey A, Millis N. 1973.Biochemical Engineering. 2nd edition. New York: Academic Press. 133 p.

Alam Z, Muhd NH, Razali F. 2005.Scale-up of stirred and aerated bioengineering bioreactor based on constant mass transfer coefficient. J Teknologi 43:95-110.

Alves SS, Maia CI, Vasconcelos JMT. 2004. Gas-liquid mass transfer coefficient in stirred tank interpreted through bubble contamination kinetics. Chem Eng Proc 43:823-830.

Anderson, DC, Bridges T, Gawlitzek M, Hoy C. 2000.Multiple cell culture factors can affect the glycosylation of Asn-184 in CHO-produced tissue-type plasminogen activator. Biotechnol Bioeng 70: 25-31.

Ansys Fluent Theory Manual 12.0, 2009.

Bartholomew, WH. 1960. Scale-up of submerged fermentation. Adv Appl Microbiol 2:289-300.

Beckwith TG, Marangoni RD, Lienhard JH V. 1993.Mechanical Measurements. 5th ed. Reading, MA: Addison-Wesley Publishing Company Incorporated.

Biryukov VV, Kantere VM. 1985. Optimization of batch processes of microbial synthesis. Nauka, Moscow: Nauka. 25-31 p.

Cabaret F, Bonnot S, Fradette L, Tanguy PA. 2007. Mixing time analysis using colorimetric methods and image processing. Ind Eng Chem Res 46:5032-5042.

Calderbank, PH. 1958. Physical rate process in industrial fermentation. Part I: The interfacial area in gas-liquid contacting with mechanical agitation. Trans Ins tChem Eng 36:443-463.

Camposano A, Chain EB, Gualandi G. 1958. 7th International Congress of Microbiology. Stockhom, Sweden.

Catapano G, Czermak P, Eible R, Eible D, Pörtner R. 2009. Bioreactor design and scale-up. In: Cell and tissue reaction engineering: Principles and practice. Berlin Heidelberg, Germany:173-186.

Cents AHG, de Bruijn FT, Brilman DWF, Versteeg GF. 2005. Validation of the Danckwerts-plot technique by simultaneous chemical absorption of CO_2 and physical desorption of O_2. Chem Eng Sci 60:5809-5818.

Chapra SC, Canale RP. 2006. Numerical Methods for Engineers, 5th Edition. New York City: Mcgraw Hill.

Chapman CM, Nienow AW, Cooke M, Middleton JC. 1983. Particle-gas-liquid mixing in stirred vessels. Part II: Gas-liquid mixing. Chem Eng Res Des 61:82-95.

Chu L, Robinson DK. 2001. Industrial choices for protein production by large-scale cell culture. Curr Opin Biotechnol 12:180-187.

Cooper CM, Fernstrom GA, Miller SA. 1944. Performance of agitated gas-liquid contactors. Ind Eng Chem36:504-509.

Deshpande GB. 1988. Fluid mechanics in mechanically agitated contactors. M Chem Eng Thesis. University of Bombay, Bombay, India.

Dhanasekharan K. 2006. Design and scale-up of bioreactors using computer simulations. BioProcess Int 4:34-40.

DiBlasi K, Jornitz MW, Gottschalk U, Priebe PM. 2006. Disposable biopharmaceutical processes-myth or reality. BioPharm International 02 Nov2006.<http://biopharminternational.findpharma.com/biopharm/Article/Disposable-Biopharmaceutical-ProcessesndashMyth-or/ArticleStandard/Article/detail/423540>.

Doran PM. 1995. Bioprocess engineering principles. 1st ed. San Diego: Elsevier Academic Press.

Flores E, Perez F, De La Torre M. 1997. Scale-Up of *Bacillus thuringiensis* fermentation based on oxygen transfer. J Ferment Bioeng 83:561-564.

Forgione P, Van Trier M. 2006.The end for stainless steel. BioProcess Int 4:58-62.

Frangos JA, McIntre LV, Eskin SG. 1988. Shear stress induced stimulation of mammalian cell metabolism. Biotechnol Bioeng 32:1053-1060.

Garcia-Ochoa F, Gomez E. 2009. Bioreactor scale-up and oxygen transfer rate in microbial processes: An overview. Biotechnol Adv 27:153-176.

Genetic Engineering and Biotechnology News. 2006. Disposable Bioreactors Gaining Favor 26:1. <http://www.genengnews.com/articles/chitem.aspx?aid=1807>.

Gill NK, Appleton M, Baganz F, Lye GJ. 2008. Quantification of power consumption and oxygen transfer characteristics of a stirred miniature bioreactor for predictive fermentation scale-up. Biotechnol Bioeng 30:1-12.

Gogate PR, Beenackers AACM, Pandit AB. 2000. Multiple-impeller systems with a special emphasis on bioreactors: A critical review. Biochem Eng J 6:109-144.

HadjievD, Sabiri NE, Zanati A. 2006.Mixing time in bioreactors under aerated conditions.Biochem Eng J 27:323-300.

Handa-Corrigan A, Emery AN, Spier RE. 1989. Effect of gas-liquid interfaces on the growth of suspended mammalian cells: mechanisms of cell damage by bubbles. Enzyme Microbial Technol 11:230-235.

Hassan ITM, Robinson CW. 1977. Stirred tank power requirement and gas holdup in aerated aqueous phases. A IChE J 23:48-56.

Hogan H. 2009. Measuring and improving mixing times with image analysis. Photonics.com. <http://www.photonics.com/Content/ReadArticle.aspx?ArticleID=30492>.

Hudcova V, Machon V, Nienow AW. 1989. Gas-liquid dispersion with dual Rushton turbine impellers. Biotech Bioeng 34:617-628.

Hughmark GA. 1980. Power requirements and interfacial area in gas-liquid turbine agitated systems. Ind Eng Chem Proc Des Dev 19:638-641.

Ju LK, Chase GG. 1992. Improved scale-up strategies of bioreactors. Bioprocess Eng 8:49-53.

Julien C. 1998. Scaling-Up from spinners, t-flasks & shakers: A versatile bioreactor for mammalian and microbial cells. Am Biotech Lab 16:12-13.

Kensy F, Zimmermann HF, Knabben I, Anderlei T, Trauthwein H, Dingerdissen U, Büchs J. 2005. Oxygen transfer phenomena in 48-well. Biotechnol Bioeng 89:698-708.

Langer ES. 2008. Users are sold on single-use systems. Genetic Eng and Biotechnol News 28:1-4.

Liden G. 2002. Understanding the bioreactor. Bioprocess Biosys Eng 24:273-279.

Linek V, Korda M, Fujasova M, Moucha T. 2004.Gas-liquid mass transfer coefficient in stirred tanks interpreted through models of idealized eddy structure of turbulence in the bubble vicinity. Chem Eng Process 43:1511-1517.

Maranga L, Cunha A, Clemente J, Cruz P, Carrondo MJ. 2004. Scale-up of virus-like particles production: effects of sparging, agitation and bioreactor scale on cell growth, infection kinetics and productivity. J Biotechnol 107:55-64.

Marks DM.2003. Equipment design considerations for large scale cell culture. Cytotechnology 42:21-33.

Merchuk JC. 1991. Shear effects on suspended cells. Adv Biochem Eng/Biotechnol 44:65-95.

Metzner AB, Otto RE. 1957. Agitation of non-Newtonian fluids. AlChE J 3:3-10.

Moresi M, Patete M. 1988. Prediction of $k_L a$ in conventional stirred fermenters. J Chem Tech Biotechnol. 42:197-210.

Nienow AW. 1996. On impeller circulation and mixing effectiveness in the turbulent flow regime. Chem Eng Sci 52:2557-2565.

Nienow AW. 2006. Reactor engineering in large scale animal cell culture. Cytotechnology 50:9-33.

Nienow AW, Langheinrich C, Stevenson NC, Emery AN, Clayton TM, Slater NKH.1996. Homogenization and oxygen transfer rates in large agitated and sparged animal cell bioreactors: Some implications for growth and production. Cytotechnol 22:87-94.

Nienow AW, Wisdom DJ, Middleton JC. 1977. The effect of scale and geometry on flooding, recirculation, and power in gassed stirred vessels. Proceedings of 2ndEuropean Conference on Mixing. Cambridge, UK:F1(1-16).

Oniscu C, Galaction AI, Cascaval D, Ungureanu F. 2002. Model of mixing in stirred bioreactors 2. Mixing time for non-aerated broths. Biochem Eng J 12:61-69.

Oosterhuis N, Kossen N. 1984. Dissolved oxygen concentration profiles in a production scale bioreactor. Biotechnol Bioeng 26:546-550.

Petersen JF.1988. Shear sensitivity of cultured hybridoma cells (CRL-8018) depends on mode of growth, culture age and metabolite concentration. J Biotechnol 7:229-246.

Rouf SA, Moo-Young M, Scharer JM, Douglas PL. 2000. Single versus multiple bioreactor scale-up: economy for high-value products. Biochem Eng J 6:25-31.

Schlüter V, Deckwer, WD. 1992. Gas–liquid mass transfer in stirred vessels. Chem Eng Sci 47:2357–2362.

Schmidt FR. 2005. Optimization and scale up of industrial fermentation processes. Appl Microbiol Biotechnol 68:425-435.

Selker M, Paldus B. 2008. Disposable Bioreactor System. US Patent 20080274541.

Shuler ML, Kargi F. 2002. Bioprocess engineering: Basic concepts. 2. Upper Saddle River, NJ: Prentice Hall PTR.

Silva HJ, Cortifas T, Ertola RJ. 1987. Effect of hydrodynamic stress on dunaliella growth. J Chem Technol Biotechnol 40:41-49.

Smith JM. 1991. Simple performance correlations for agitated vessels. Proceedings of 7th European Conference on Mixing. Brugge, Belgium.

Smith JM, Van't Riet K, Middleton JC. 1977. Scale-up of agitated gas-liquid reactors for mass transfer. Proceedings of 2nd European Conference on Mixing. Cambridge, UK:F4(51-66).

Smith JM, Warmoeskerken MMCG. 1985. The dispersion of gases in liquids with turbines. Proceedings of 5th European Conference on Mixing.Wurzeburg, Germany.

Sorenson KL. 2010. Comparative studies on oxygen mass transfer for the design and development of a single-use fermentor. Master's thesis, Utah State University, Logan, Utah.

Spall R, Jones N, Staheli C. 2010. Computational fluid dynamics analysis of fluid mixing in single-use bioreactors. ASME International Mechanical Engineering Congress and Exposition. Vancouver, British Columbia.

Takamatsu T, Shioya S, Okuda K. 1981. A comparison of unstructured growth models of microorganisms. J Ferment Technol 59:111-124.

Thermo Fisher Scientific KK. Single-use bioreactor. 2010. Retrieved from <http://www.thermoscientific.jp/hyclone-bpc/catalog/single-use-bioreactor.html>.

Van't Riet K. 1979. Review of measuring methods and results in nonviscous gas-liquid mass transfer in stirred vessels. Industrial Eng Process Des Equip 18:357-364.

Vilaca PR, BadinoAC, Facciotti MCR, Schmidell W. 2000. Determination of power consumption and volumetric oxygen transfer coefficient in bioreactors. Bioprocess Eng 22:261-265.

Votruba J, Sobotka M. 1992. Physiological similarity and bioreactor scale-up. Folia Microbiol 37:331-345.

Vrabel P, Van der Lans RGJM, Cui YQ, Luyben KChAM. 1999. Compartment model approach: Mixing in large scale aerated reactors with multiple impellers. Trans Inst Chem Eng 77:291-302.

Wang DI, Cooney CL, Demain AL, Dunnill P, Humphrey AE, Lilly MD. 1979. Fermentation and Enzyme Technology. New York: Wiley. 194-210 p.

Wase JD, Ratwate AM. 1985. Variation of intracellular sodium and potassium concentration with changes in agitation rate of chemostat-cultivated *Escherichiacoli.* Appl Microbiol Biotechnol 22:325-328.

Wheetman RJ, Coyle CK. 1989. The use of fluid foil impellers in viscous mixing applications. AIChE Annual Meeting, San Francisco. 5-10 p.

Yang JD, Lu C, Stasny B, Henley J, Guinto W, Gonzalez C, Gleason J, Fung M, Collopy B, Benjamino M, Gangi J, Hanson M, Ille E. 2007. Fed-batch bioreactor process scale-up from 3-L to 2,500-L scale for monoclonal antibody production from cell culture. Biotechnol Bioeng 98:141-154.

Yawalkar A, Heesink ABM, Versteeg GF, Pangarkar VG. 2002. Gas-liquid mass transfer coefficient in stirred tank reactors. Can J Chem Eng 80:840-848.

Zhu Y, Bandopadhayay PC, WU J.2001. Measurement of gas-liquid mass transfer in an agitated vessel – a comparison between different impellers. J Chem Eng Jpn 34:579-584.

Zlokarnik, M. 1978. Sorption Characteristics for Gas-Liquid Contacting in Mixing Vessels. Adv Biochem Eng 8:133-157